Comparisons of Native and Chimeric Shiga Toxins Indicate that the Binding Subunit Dictates Degree of Toxicity

by

Lisa M. Russo

Dissertation submitted to the Faculty of the
Emerging Infectious Disease (EID) Graduate Program
Uniformed Services University of the Health Sciences
In partial fulfillment of the requirements for the degree of
Doctor of Philosophy 2014

DISSERTATION APPROVAL FOR THE DEGREE OF DOCTOR OF PHILOSOPHY IN THE EMERGING INFECTIOUS DISEASE GRADUATE PROGRAM

Title of Dissertation: "Comparisons of Native and Chimeric Shiga Toxins Indicate that the Binding Subunit Dictates Degree of Toxicity"

Name of Candidate: Lisa Russo
Emerging Infectious Diseases
March 17, 2014

DISSERTATION AND ABSTRACT APPROVED:

DATE:

3/18/14

Dr. Stephen Davies
DEPARTMENT OF MICROBIOLOGY AND IMMUNOLOGY
Committee Chairperson
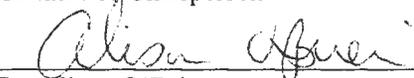
3/18/14

Dr. Alison O'Brien
DEPARTMENT OF MICROBIOLOGY AND IMMUNOLOGY
Dissertation Advisor

3/18/14
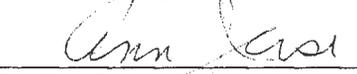
Dr. Ann Jerse
DEPARTMENT OF MICROBIOLOGY AND IMMUNOLOGY
Committee Member
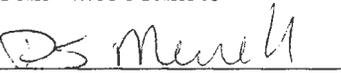
3/18/14

Dr. D. Scott Merrell
DEPARTMENT OF MICROBIOLOGY AND IMMUNOLOGY
Committee Member

3/18/14

Dr. Beverly Mock
NIH/NCI
Committee Member

ACKNOWLEDGMENTS

To my thesis advisor, Alison O'Brien – Your mentorship molded me into the scientist I am today. Thank you for the opportunity to work in a stimulating environment with the freedom to explore multiple interests. Your guidance has prepared me for wherever my career may lead.

To my thesis committee – Thank you for your advice and guidance throughout this process. I truly appreciate your enthusiasm toward my projects over the years.

To the O'Brien lab, past and present – Thank you for always being there to help out in the lab or provide thoughtful insights. Especially Angela Melton-Celsa, you were an excellent mentor and I could not have completed this dissertation without your assistance.

To my friends and family – Your encouragement and support helped me survive my journey through graduate school.

DEDICATION

I dedicate my thesis to the many individuals who fostered my scientific curiosity and prepared me for the rigors of graduate school. To my parents, who answered me *every single time* I asked "why" as a child. You encouraged me to always ask questions and explore my surroundings. To the exceptional science teachers I had the privilege of learning from over the years. You made science exciting and laid the foundation for future success. Finally, to Michael Boyle, my undergraduate research advisor. You taught me how to think like a scientist, to accept the failures as a learning experience and to appreciate the successes. I am grateful for the opportunity that I had to work with you; without your support and guidance I don't know where my journey would have led.

COPYRIGHT STATEMENT

Lisa M. Russo
Emerging Infectious Diseases Graduate Program
Department of Microbiology and Immunology
March 28, 2014

ABSTRACT

Title of Dissertation:

Comparisons of Native and Chimeric Shiga Toxins Indicate that the Binding

Subunit Dictates Degree of Toxicity

Lisa M. Russo, Doctor of Philosophy, 2014

Dissertation directed by:

Alison O'Brien, Ph.D.
Professor and Chair, Department of Microbiology and Immunology

Shiga toxin (Stx) producing *Escherichia coli* (STEC), particularly serotype
O157:H7, are important foodborne human pathogens that cause outbreaks of hemorrhagic
colitis and a severe sequela, the hemolytic uremic syndrome. Stx, the primary virulence
factor for this group of organisms, is responsible for the histopathological kidney lesions
that result after infection with STEC. An O157:H7 strain may produce Stx1a, Stx2a, or
both Stxs. The Stxs are biologically similar, though antigenically distinct, AB5 toxins
with an identical mode of action that inhibits host cell protein synthesis and leads to cell
death. The A subunit is comprised of two parts, the A_1 subunit that is responsible for the
N-glycosidase activity of the molecule and the A_2 peptide that is threaded through the
center of the homopentameric B subunit and non-covalently links the A and B subunits

together. The B subunit is responsible for binding to the host cell receptor, globotriaosylceramide (Gb3).

Although the Stxs have an identical mode of action, Stx1a is associated with increased cytotoxicity for Vero cells *in vitro* compared to Stx2a, while Stx2a is associated with increased *in vivo* toxicity compared to Stx1a. The primary goal of this dissertation was to investigate that paradox. First, we determined the oral toxicity of the Stxs in a mouse model. We assessed the oral LD_{50} for Stx2a, defined the resultant kidney histopathology, and, finally, protected and rescued mice with a monoclonal antibody against Stx2a. However, we did not observe any morbidity or mortality after intoxication with Stx1a. Second, we used chimeric toxins to analyze the contribution of the individual Stx subunits to *in vitro* cytotoxicity and *in vivo* morbidity and mortality. Our chimeras were unique in that the A_2 and B subunit were generated from one native Stx, while the A_1 subunit that contained the catalytic domain was derived from the heterologous Stx. We found that the A_2 peptide increased stability of the chimeric holotoxin. Our chimerics were the first such molecules reported to exhibit activity equivalent to the native Stx with the corresponding B subunit. Additionally, the origin of the B subunit was responsible for the degree of binding to Gb3 and toxicity. The Stx1a B subunit was associated with increased *in vitro* binding and cytotoxicity compared to the Stx2aB subunit; conversely, the Stx2a B, when compared to the Stx1aB subunit, was correlated with increased *in vivo* toxicity and enhanced amounts of active toxin recovered in feces after oral intoxication.

TABLE OF CONTENTS

LIST OF TABLES

LIST OF FIGURES

CHAPTER 1

Introduction

Historical overview

Shiga toxin (Stx) producing *E. coli* (STEC) were recognized as an emerging cause of disease in the early 1980s with the publication of three seminal papers that defined the field. First, in 1983, Karmali and colleagues reported that the stools of patients with the hemolytic uremic syndrome (HUS) contained a cytotoxin and that that cytotoxin was also made by certain *E. coli* isolates from those fecal specimens (128). Second, Riley *et al.* described two outbreaks of bloody diarrhea that occurred in Oregon and Michigan, each of which was associated with consumption of beef patties from a particular fast food restaurant (233). These investigators also noted that a novel serotype, *E. coli* O157:H7, had been isolated from the stools of 9 of 12 patients in Michigan and from a hamburger patty linked to the outbreak. Third, O'Brien and colleagues discovered that *E. coli* O157:H7 produces a cytotoxin that can be neutralized by antibodies to Stx from *Shigella dysenteriae* type 1 (Stx was discovered by Dr. Kiyoshi Shiga in 1898 (257)) and that the cytotoxin was identical to the toxin described by Karmali *et al.* (203). O'Brien *et al.* also purified that cytotoxin from *E. coli* O157:H7 (202). Later, Stx2, a second, closely related toxin that is not neutralized by anti-Stx sera was also discovered in certain isolates of *E. coli* O157:H7 (254; 275). In a retrospective review of the literature, Tarr *et al.* proposed that the occurrence of earlier cases of sporadic HUS were likely attributable to *E. coli* O157:H7 (280).

Nomenclature

The initial nomenclature for what we in the United States now call Shiga toxin was complicated by the identification of the same *E. coli* cytotoxin by different groups

who gave the toxins different names. Konowalchuk *et al.* originally described a cytotoxin made by some diarrheagenic *E. coli* strains that killed Vero cells (145). Karmali and colleagues called the cytotoxin they found associated with *E. coli* strains that caused HUS Verotoxin (128) based on the findings of Konowalchuk *et al.* (145). O'Brien *et al.* reported that the same cytotoxin was actually equivalent in structure and activity to Stx from *S. dysenteriae* type 1 (202; 203) and, therefore, named it a "Shiga-like" toxin. O'Brien *et al.* proposed that all future publications refer to the toxin as Shiga-like toxin instead of Verotoxin because the former name had historical precedence and indicated its relationship to Shiga toxin (201). The proposal was not fully supported, and both names continued throughout the literature. Later, "like" was removed from "Shiga-like", and the two toxin non-cross-neutralizable serogroups were named Stx type 1 (Stx1) and Stx type 2 (Stx2) to indicate their relationship to Stx (44). Recently, a modification of that nomenclature scheme has been developed to differentiate the prototype toxins within each family, Stx1a and Stx2a, from the numerous Stx variants that have been identified (described below) (248). For the remainder of this dissertation the prototype Stxs will be referred to as Stx1a and Stx2a.

Factors that led to development of *E. coli* O157:H7 as a pathogen responsible for food-borne outbreaks

After the discovery that *E. coli* O157:H7 infections were responsible for bloody diarrhea and HUS, the number of reported outbreaks caused by these agents increased rapidly. Whittam and colleagues then undertook phylogenic analyses of STEC isolates to determine whether this group of organisms had recently emerged from a common

3

ancestor or whether they had existed but were simply not recognized (313). These investigators concluded that STEC serotype O157 strains had recently diverged from an O55 enteropathogenic *E. coli* (EPEC) strain with a high propensity to acquire virulence factors (314). Thus, multiple evolutionary changes from the progenitor O55 EPEC strain had occurred that led to the genomic content of the current O157:H7 STEC strains. Of particular importance was the acquisition of the stx_1 gene prior to the acquisition of the stx_2 gene (73). Additionally, changes in the way food (particularly beef) was processed and distributed had taken place in the United States during the period just prior to recognition of the first O157:H7 outbreak in 1983. Specifically, the increase in the fast food culture resulted in centralized beef production (12; 21).

Source of STEC

Cattle and other ruminants are the natural reservoir for STEC (12; 13; 102). The animals are asymptomatically colonized at the recto-anal junction (196). Colonization levels are cyclical; however, at any time, approximately 60-70% of feedlots have at least one *E. coli* O157:H7- positive animal and fecal samples from up to 20-30% of cattle may test positive for the organism (68; 70). Stx does not damage the ruminant vasculature and appears not to reach the systemic circulation to cause disease. The most likely explanation for the lack of Stx toxicity in cattle is that these animals do not express the Stx receptor globotriaosylceramide (discussed later) at the site of bacterial colonization or in the kidneys (225). The absence of physical symptoms in cattle and the challenge of culturing large numbers of such animals preclude the identification and removal of infected animals before they enter meat processing facilities, the primary sites where

contamination of hamburger occurs (46). Multiple approaches to decrease STEC carriage in feed lot cattle have been undertaken, such as dietary management, competitive colonization with probiotics, and antibiotics; however, the results of these attempts have been mixed (reviewed in (46)). Cattle vaccines have demonstrated the potential to decrease *E. coli* O157:H7 colonization levels; nevertheless, the practice of vaccination against *E. coli* O157:H7 is not widespread (188; 265; 289).

Human STEC infection is primarily a foodborne disease acquired through transmission from contaminated food stuff, although environmental and person to person spread are known to occur (18; 228). Initially, ground beef was implicated in the majority of outbreaks (16; 65); however, fresh produce and unpasteurized beverages are now also prominent vehicles (41; 58; 83; 136; 181). The majority of STEC infections occur in the summer and early fall, and the incidence of STEC infections is increased in rural versus urban environments, probably due to exposure to cattle or their manure (141; 264). Upon ingestion of STEC O157:H7, the bacteria colonize the colon and release Stx. The primary disease manifestation is hemorrhagic colitis (HC), which occurs in 90% of infected individuals, and a subset of patients progress to the serous sequela, HUS (described below) (280).

STEC epidemiology

STEC are an ever expanding subset of *E. coli* strains that are defined by the presence of *stx$_1$* and/or *stx$_2$* genes (98; 125; 126; 195). Strains are identified by their serotype, i.e., the particular lipopolysaccharide (LPS) or O antigen and the flagellar or H

5

antigen expressed by the organism. The serotype O157:H7 is the most frequently reported cause of illness due to STEC in the United States (247). Indeed, the CDC estimates that the O157:H7 serotype accounts for approximately 63,000 of the 120,000 estimated STEC cases each year, and that agency reports that it is also the most frequent STEC linked to the development of HUS in infected individuals (247). Recently, non-O157 STEC serogroups have also been recognized as pathogens that can cause significant human disease (43; 67; 74; 122). Specifically, serogroups O26, O45, O103, O111, O121, and O145 are classified as the "big six" and are now, like O157:H7, considered adulterants in food. As such, if any of these six STEC serogroups or O157:H7 are detected in ground beef (for example), the product will be recalled (43). As previously mentioned, non O157 serotypes are reported less frequently than O157:H7 as agents of foodborne outbreaks and or sporadic cases of STEC illnesses; however, these non-O157:H7 serotypes are probably underreported due to the difficulty of distinguishing these organisms from normal flora *E. coli* present in stool samples (23). Conversely, serotype O157:H7 is easily identified on sorbitol-MacConkey (SMAC) agar, since it is unable to ferment sorbitol and grows as colorless colonies while the majority of other *E. coli* serotypes readily ferment sorbitol and grow as pink colonies.

Virulence factors of STEC other than Stx

STEC strains are classified as locus of enterocyte effacement (LEE)- positive or LEE- negative strains. Enterohemorrhagic *E. coli* (EHEC), a subset of STEC comprised of LEE- positive strains, contain the serotypes most often associated with human disease.

6

As mentioned above, *E. coli* O157:H7 is prominent among these EHEC as a cause of human disease. The LEE is a chromosomally-encoded pathogenicity island that contains multiple virulence factors (reviewed in (195)). Intimin, encoded by the *eae* gene, is the primary STEC adhesin and is responsible for the close association of the bacterium with the colonic epithelial cell (79). Intimin initially binds to nucleolin on the host cell until its primary receptor, Tir (translocated intimin receptor), is transported through the type three secretion system (T3SS) into the cytoplasm of the host cell (132; 263). Other *E. coli* *s*ecreted proteins (Esps) are also exported through the T3SS. As a group, the Esps are responsible for the actin cytoskeletal rearrangement and pedestal formation that is characteristic of the attaching and effacing (A/E) lesion that protrudes from the intestinal microvillus of the EHEC-infected cell. Effacement of the microvillus leads to destruction of the microvilli and subsequent loss of gastrointestinal absorptive properties; together, these events result in diarrhea in the infected host. (A model of the proposed steps in EHEC pathogenesis is depicted in Figure 1).

LEE- negative STEC strains can also cause disease. They encode adhesins other than intimin, such as the long polar fimbriae. These factors promote adherence to the host cell (without A/E lesions) and *in vivo* colonization and disease (72; 217). Additionally, some STEC isolates contain a large plasmid, pO157 that encodes potential virulence factors, α hemolysin and a type 2 secretion system; however, the roles of the products encoded on this plasmid in STEC pathogenesis are unknown (249).

7
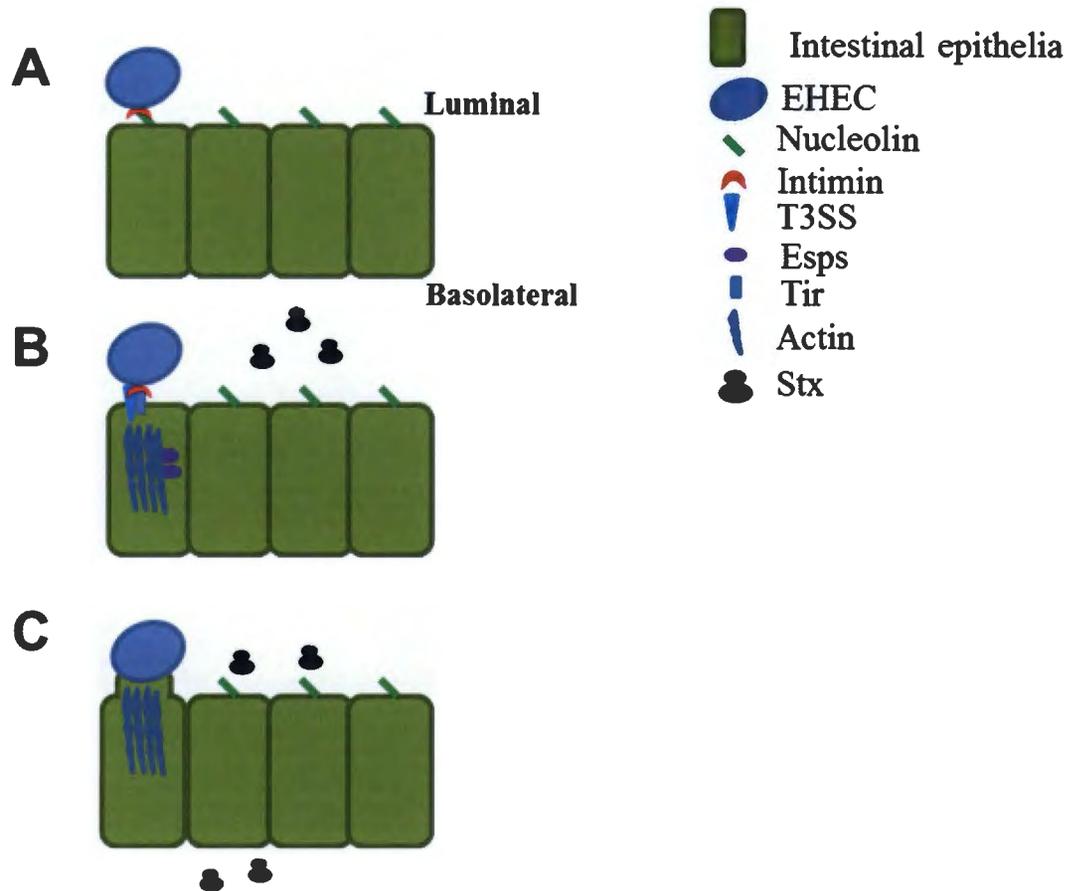
Figure 1. Model of the steps in EHEC O157:H7 pathogenesis.

    (A) E. coli O157:H7 are ingested, survive the low pH of the stomach, and then transit through the gastrointestinal tract to reach the primary site of colonization, the colonic epithelium. Intimin, the outer surface adhesion molecule of *E. coli* O157:H7, initially adheres to nucleolin, a low affinity receptor (263), on the host cell. (B) EHEC secretes its primary adhesin Tir, the translocated intimin receptor, through a T3SS into the host cell. Other *E. coli* secreted proteins (Esps) are also injected into the target cell and cause rearrangement of the actin cytoskeleton. Stx is released early in colonization. (C) The tight interaction of intimin and Tir, combined with actin rearrangement results in the characteristic attaching and effacing (A/E) lesion and the destruction of the microvilli. Stx is able to translocate across the epithelial layer, without the inhibition of protein synthesis or necrosis, to reach the basolateral vasculature (5; 110; 222).

Shiga toxins

Stx1a and Stx2a, two biologically similar though antigenically distinct AB5 toxins [50], are the primary STEC virulence factors (reviewed in (173; 195)). Stx1a and Stx2a share approximately 57% amino acid (aa) homology (204), similar crystal structures, and an identical mode of action (described below). Stx1a and Stx2a are encoded on chromosomally-inserted, inducible, lambdoid bacteriophages (303). The Stx subunits are located in operons and are transcribed with the late stage phage genes. Upon phage conversion to the lytic cycle, Stx expression is induced via the SOS response pathway. Stx1a transcription is additionally repressed in high iron concentrations by Fur (45). The mobility of the phage allows Stx loci to enter new strains through horizontal gene transfer, a feature responsible for the evolution of new STEC strains. This type of lysogenic phage conversion was evident in the summer of 2011, when an Enteroaggregative *E. coli* (EAEC) strain acquired the Stx2a phage; that *E. coli* O104:H4 Stx2+ strain was responsible for the largest outbreak of HUS ever recorded (78). The mobility of the Stx-converting phage also means that it can be lost, especially when induced in the lytic cycle (29). Therefore, absence of *stx* from a clinical sample does not necessarily mean STEC was not responsible for the illness.

Shiga toxin variants

Stx variants were originally recognized as immunologically related to Stx1a or Stx2a but with different biological activities. An increase in the number of Stx-expressing isolates with minor nucleotide alterations in the toxin genes led to an *ad hoc* classification system that blurred the distinction between biologically and/or immunologically distinct

9

toxin variants and functionally similar toxins with sequence modifications. A multicenter phylogenetic analysis resulted in a universal PCR typing system for the identification of each variant within the two Stx serogroups (248). The prototype Stx in each group, named Stx1a and Stx2a, respectively, is responsible for the most severe disease in each group.

The Stx1 group contains Stx1a and two additional variants, Stx1c and Stx1d, both of which are immunologically distinct from the prototype (210; 320). Stx1a is identical to Stx of *S. dysenteriae* type 1, with a maximum of one aa difference. Stx1a is responsible for STEC-associated human disease. Stx1c and Stx1d have decreased cytotoxicity compared to Stx1a and are rarely associated with human disease (82).

The Stx2 group is considerably more diverse. Variants identified to date include: Stx2a, Stx2b, Stx2c, Stx2d, Stx2e, Stx2f, and Stx2g. The first Stx2 variant recognized was Stx2e (169). Stx2e causes edema disease in pigs, an illness that affects the central nervous system and is often fatal [74, 75]. That toxin prefers a different functional receptor globotetraosylceramide, then does Stx2a (62) and is less active on Vero cells than is Stx2a (169). The next Stx2 variant recognized was Stx2c (251). Although Stx2c can result in human disease, it has decreased *in vitro* and *in vivo* activity compared to Stx2a (86; 251). The third Stx2 variant recognized was Stx2d. That Stx2d toxin is activatable was first recognized by Melton-Celsa *et al.* (174). These investigators incubated the toxin with mouse intestinal mucus and found that the cytotoxic activity of the toxin for Vero cells had increased. This same group also noted that that two aa, at positions 291 and 297 are changed in the A subunit of Stx2d compared to Stx2a and that

activation occurs when elastase (the substance in intestinal mucus responsible for activation (144) removes the final two aa, positions 296 and 297, from the C terminal tail of the A subunit of Stx2d (144). Activation also results in increased toxicity, compared to Stx2a, in a streptomycin-treated (Str) mouse model (176), and Stx2d is associated with the most severe forms of STEC disease, HC and HUS (27). Two aa differences in the B subunit of Stx2c and Stx2d result in decreased *in vitro* activity, compared to Stx2a (154). Variant Stx2b is similar to Stx2d; however, Stx2b cannot be activated and is rarely associated with human disease (223; 273). Stx2f and Stx2g have not been linked to human disease and, in fact, have only been isolated from animal STEC (151; 250).

Shiga toxin structure

Although Stx1a (Stx (80)) and Stx2a (81) are AB5 toxins with a similar crystal structure (Figure 2), the holotoxins only share 57% aa homology. The mature A subunits for Stx1a and Stx2a are 293 and 297 aa, respectively. The A subunit contains a proteolytic site that is cleaved by furin, or a similar protease, into the A_1 subunit (252 aa for both toxins) (Figure 2, shaded dark blue), and A_2 peptide (41 aa for Stx1a and 45 aa for Stx2a) (Figure 2, shaded light blue). The A_1 subunit remains linked to the rest of the toxin molecule through a disulfide bond between cysteines at position 242 and 261 or 241 and 260, for Stx1a and Stx2a, respectively (Figure 2, shaded yellow). The active site of the A_1 subunit, which is responsible for the catalytic activity of the toxin molecule (42), is the glutamic acid at position 167 (107) (Figure 2, shaded red). Although both Stxs share the same active site, part of the A_2 peptide occludes the active site in the Stx1a holotoxin structure, while that site is accessible in the Stx2a holotoxin (81). The A_2

11

peptide comprises the C terminus of the A subunit and non-covalently binds to the mature B pentamer. The A_2 is threaded through the center of the pentamer and provides stability to the overall holotoxin structure (14). The additional four aa of the A_2 peptide for Stx2a cause it to extend below the B pentamer, and that tail partially blocks one of the receptor binding sites (discussed below) (81).

The B subunits, 69 aa per monomer for Stx1a and 70 aa per monomer for Stx2a (Figure 2, shaded green), form homopentamers that are responsible for binding to the host cell receptor, globotriaosylceramide (Gb3) (301). Crystallization of the Stx1a mature B pentamer revealed three independent receptor- binding sites per monomer (155). Two of the binding grooves incorporate residues from adjacent monomers; therefore, the mature pentameric structure is required to bind the receptor. The crystal structure of the Stx2a B subunit revealed two binding sites per monomer (81). The extension of the A_2 tail blocks the binding site in one of the B subunit monomers, and this blockage alters the steric conformation of the binding site in the rest of the pentamer (81). The authors propose that binding site three requires all five monomers to bind Gb3 (81). Additionally, there is a conformational change in the binding cleft at site two due to a difference in the interaction of the carboxy-terminus of each B monomer with the A subunit of Stx2a compared to Stx1a (81). Despite the conformational differences in site 2 between the B pentamers of Stx1a and Stx2a, several studies have identified binding site 2 as the site with the greatest receptor binding affinity for both Stx1a and Stx2a, (138; 155; 199; 258).

12
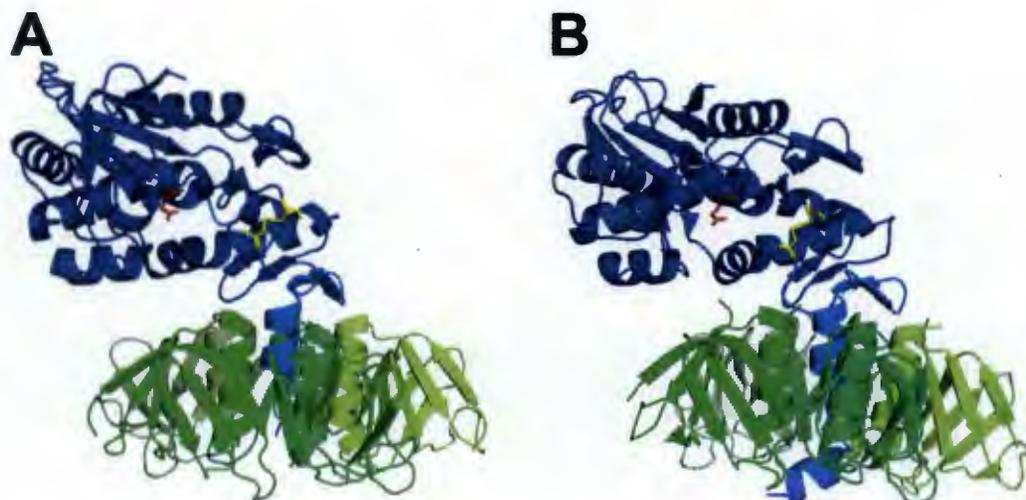
Figure 2. Crystal structure comparison of the Stxs.
Stx, equivalent to Stx1a, resolved to 2.5 Å (A) and Stx2a, resolved to 1.77 Å (B) crystals are depicted. For both toxins, the A1 subunit is colored dark blue, and the A2 peptide is colored light blue. The active site glutamic acid at position 167 is shaded red. The active site is obstructed by the holotoxin structure of Stx1a (A); however, that site is assessable for Stx2a (B). The two cysteine residues that engage in a disulfide bond to maintain attachment of the A1 subunit to the rest of the molecule after cleavage are colored yellow. The A2 peptide terminates within the B subunit for Stx1a (A), while the four aa extension of the A2 peptide, below the B subunit pentamer, is visible for Stx2a (B). Additionally, the B pentamer of Stx2a (B) takes on a slightly different conformation than the Stx1a B subunit pentamer (A). The differences between the two Stx structures may contribute to the differential toxicity between Stx1a and Stx2a. The structures were created with PyMOL Molecular Graphics System, Version 1.5.0.5 Schrodinger, LLC with sequence downloaded from www.pdb.org; Stx (Stx1a): 1R4Q; Stx2a: 1R4P

13

Stx-receptor binding

Gb3 is the functional receptor for all Stx variants except Stx2e; as mentioned above, that Stx binds preferentially to globotetraosylceramide (Gb4) (62; 158; 243). Gb3 is a glycosphingolipid (GSL), i.e., an amphipathic molecule composed of a hydrophobic ceramide that serves as a membrane anchor and a hydrophilic trisaccharide with a fatty acid (FA) tail of variable length (C14-C24) (8; 133; 219). The structure of the trisaccharide is Gal-α1-4-Gal-β1-4-Glc (159). Gb3 is necessary for Stx intoxication (excluding Stx2e) (119). Removal of the Gb3 synthase gene from otherwise sensitive wild type C57BL/6 mice rendered the knockout animals insensitive to Stx (211), while transfection of the Gb3 synthase gene sensitizes otherwise unresponsive cell lines (300). Of note, Fabry mice, animals that have a genetic disorder such that Gb3 expression is increased systemically, are less sensitive to Stx intoxication. One hypothesis as to why these mice are insensitive to the lethal effects of Stx is that toxin is sequestrated or bound to Gb3 on irrelevant cell types before it can reach its receptor (Gb3) at the functional site of intoxication that leads to death, the kidney (56).

Gb3 is mobile within the cellular membrane and often arranges into lipid rafts, detergent resistant membrane domains (DRM) with high cholesterol content (reviewed in (19)). Lipid rafts add structure to the membrane and increase Gb3-Stx binding. Since Stx binds Gb3 in a dose-dependent manner, the increased Gb3 density within a lipid raft is thought to be important for Stx pathogenesis (19; 37) and may affect the Stx intracellular transport (316). Although cholesterol is believed to be important for the maintenance of

the DRM (25; 49), two reports proposed that cholesterol may mask the majority of GSL receptors within the lipid raft (161; 167).

Receptor- positive cells express a heterogeneous makeup of Gb3 populations (49; 170; 207; 219; 252). FA chain length and degree of saturation affect Stx binding affinity (7; 8). Stx2a prefers shorter chain lengths (C16-18), while Stx1a binds preferentially to long FA chains (C20-C24) (104; 133; 158). Mutations in the Stx B subunit result in differential FA chain length affinities. For example, a mutation in the B subunit of Stx2e that results in the genotype of a mature B subunit equivalent to Stx1a, changes the receptor preference from Gb4 to Gb3 (39; 295).

Cellular sensitivity to Stx is determined by the site of tissue origination (reviewed in (19)). Gb3 mRNA is expressed in the brain, heart, kidney, spleen, colon, small intestine, and lungs of humans and mice (85; 143); however, expression on specific cells within these organs varies considerably (252; 324). Although Gb3 is expressed in human and mouse kidneys, the receptor is expressed in the glomerulus and tubules of humans while it is only expressed in the tubules of mice (85). Additionally, Gb3 expression levels vary across cell types and locations (Table 1). Human renal glomerular endothelial cells are 1,000X more sensitive than human brain endothelial cells (20; 24). Microvascular endothelial cells express up to 50X more Gb3 and are much more sensitive to Stx than are macrovascular cells, such as human umbilical vein endothelial cells (HUVECs) (207). Lastly, the microenvironment of Gb3- positive cells can influence the expression of the receptor and, therefore, sensitivity to Stx. The addition of butyrate, a metabolite that results from bacterial fiber fermentation (101), results in a systemic increase in Gb3

expression, and, consequently, an increase in Stx binding to and intoxication of target cells (324). However, the effect of the metabolite is lost soon after its removal (324), a finding that demonstrates the sensitivity of the response and the importance of physiological conditions within study parameters.

Table 1. Cell line heterogeneity of Gb3 expression

Cell Line	Abbreviation	Phenotype	Conclusion	Ref
Human renal glomerular endothelial cells Human brain endothelial cells	HGMEC HBMEC	Stx1a cytotoxicity: HGMEC 1,000X > HBMEC	Endothelia sensitivity: renal > neural	(20; 24)
Human renal microvascular endothelial cells Human umbilical vein macrovascular endothelial cells	HRMEC HUVEC	Gb3 expression: HRMEC 50X > HUVEC Stx1a cytotoxicity: HRMEC > HUVEC	Endothelia sensitivity: microvascular > macrovascular	(207)
Human brain microvascular endothelial cells Macrovascular endothelial cells	HBMEC EA.hy 962	Gb3 expression: EA.hy 962 > HBMECs EA.hy 962 FA: C24 >C16 HBMECs FA: C24=C16 EA.hy 962: Gb3 synthase only HBMECs: Gb3 and Gb4 synthase	Gb3 expression: microvascular > macrovascular + different Gb3 species	(252)
Primary human renal proximal tubule epithelial cells (cultured *in vitro* 24 h)	HRTEC	Gb3 expression: Proximal tubular cells > Vero cells Pro-inflammatory cytokines increase Stx1a cytotoxicity	Renal proximal tubules express high density of Gb3	(108)

17

Intracellular trafficking and mode of action of Stxs

Stx can translocate across intestinal epithelial cells (5; 110) that exhibit low levels of Gb3 on their surface (324) to reach the microvascular endothelial cells. Stx enters systemic circulation in a mechanism as yet to be elucidated to reach the kidneys. The Stx target site in humans is the glomerular microvascular endothelium (28); however, Stx additionally intoxicates glomerular epithelial (109), mesangial cells (299), and tubular epithelial cells (61; 108). Stx also affects pulmonary (298) and cerebral (24) endothelial cells. In mice, the primary target of Stx is distal tubular epithelial cells (130).

Upon binding to its receptor, Gb3, Stx undergoes endocytosis into host cell (see Figure 3 for model of entry and intoxication of a cell by Stx). Endocytosis primarily proceeds through the clathrin-dependent pathway; nevertheless, clathrin-independent endocytosis does occur (22). Stx undergoes retrograde transport from early endosomes through the trans-Golgi complex to the ER (244). Gb3-mediated endocytosis is required, as Stx transit initiated through a non-receptor pathway does not reach the Golgi (71; 227). The Stx A subunit may undergo cleavage into the A_1/A_2 components in the intestinal mucus (174); otherwise furin cleaves the subunit as Stx exits the Golgi (90). The A_1 subunit remains attached to the rest of toxin molecule in the ER through a disulfide bond (244). The disulfide bond is reduced as the A_1 subunit is unfolded and released into the cytosol where it acts as an N-glycosidase (42; 69; 246) to remove an adenine from the alpha-sarcin loop of the 28s rRNA of the 60 ribosome. That action prevents the association between the ribosome and elongation factor 1 with a consequent inhibition of

18
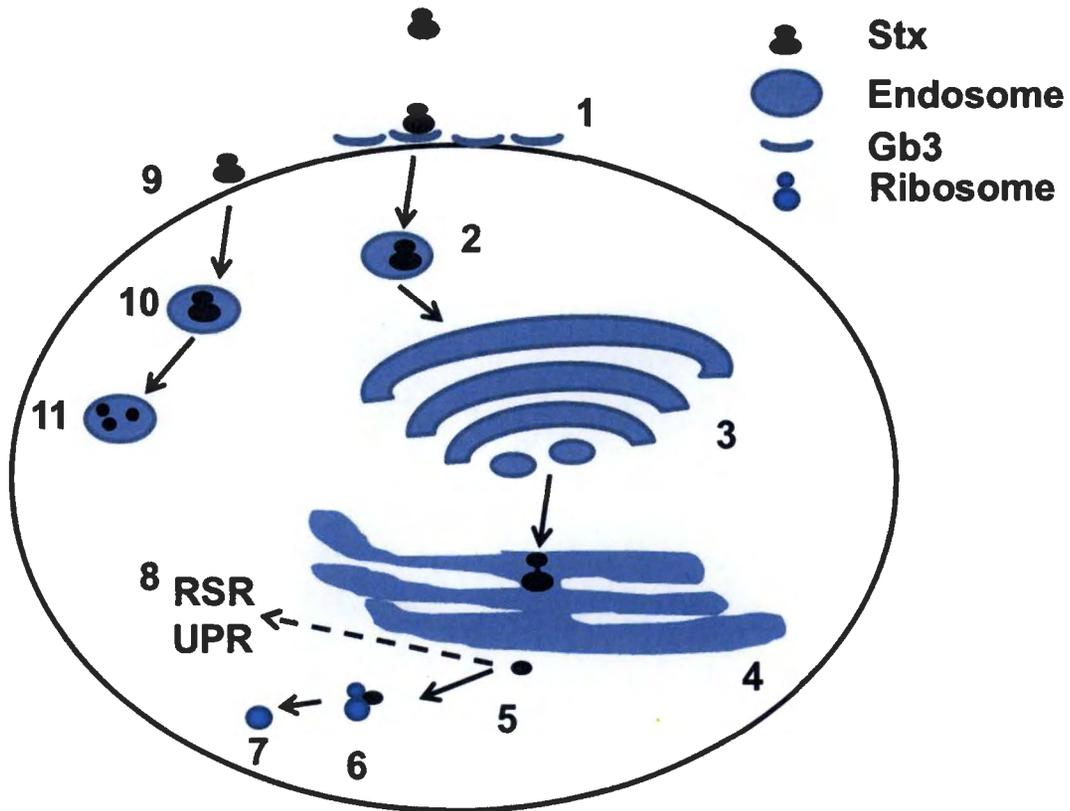
Figure 3. Stx transit through a receptor- positive cell.

(1) Systemic Stx binds to Gb3, located in a lipid raft, on a host cell membrane. (2) The toxin molecule enters the host cell through endocytosis into an early endosome and under goes retrograde transport. (3) Stx transits through the Golgi apparatus to the ER. If the A_1 subunit is not cleaved from intestinal mucus, it is cleaved by furin as it exits the Golgi. (4) The A_1 remains attached to the toxin molecule by a disulfide bond at is transits through the ER. (5) The bond is reduced and the A_1 subunit partially unfolds as it enters the cytosol. (6) The A_1 subunit binds to a ribosome and (7) depurinates the adenine on the 28S rRNA of the 60S ribosome, a process that inhibits protein synthesis and results in apoptosis. (8) Entry of the A_1 subunit into the cytosol may also trigger the ribosomal stress response (RSR) or the unfolded protein response (UPR) and result in apoptosis of the host cell. (9-11) Stx that enters a host cell without binding Gb3 does not enter the retrograde pathway and is degraded.

protein synthesis, an event that leads to cell death (208). Note that the modes of action of Stx1a and Stx2a are the same (69).

Although one Stx molecule may be sufficient to inhibit protein synthesis and result in cell apoptosis (279), additional cellular pathways may be initiated after Stx retrograde transport and release of the A_1 subunit into the cytoplasm, particularly at low Stx concentrations (reviewed in (285; 286)). Removal of the adenine from the alpha-sarcin loop results in damage to the ribosomal structure. The damage initiates signaling through the ribotoxic stress response (RSR) pathway. This signaling results in increased cytokine expression, specifically the release of NFkB, activator protein-1 (AP-1), and early growth response gene-1 (Erg-1). Circulating STEC LPS may also increase the activation of the innate immune response. Ultimately, the RSR results in DNA fragmentation, an event that triggers apoptosis (reviewed in (286)). Additionally, entry of the unfolded A_1 subunit into the cytoplasm may initiate the unfolded protein response (UPR). Signaling cascades activate the innate immune response and attenuate cellular protein translation while also initiating transcription of proteins responsible for the ER associated protein degradation pathway (ERAD). Extended signaling through ERAD due to truncated proteins from ribosomal depuration can also activate apoptosis (reviewed in (288)). However, the specific role of the UPR or ERAD pathway during an STEC infection is unknown. Limited *in vitro* analyses suggest that activation of the pathways in response to Stx differs across cell types (286).

20

Endothelial injury and the Hemolytic Uremic Syndrome

Approximately 90% of *E. coli* O157:H7- infected individuals will develop HC, and, of those, 10-20% will progress to HUS (Figure 4) (9; 40; 48; 106; 114; 171; 232; 280). HUS, the most severe consequence of STEC infection is characterized by a triad of symptoms: thrombocytopenia, hemolytic anemia, and renal failure (280). Stx is responsible for HUS as STEC are not invasive and rarely result in bacteremia. Additionally, Stx has been identified at the site of damage in human renal biopsies from infected individuals obtained from surgery or autopsy (48; 114; 129; 157; 232; 284; 297). However, the factors that determine whether an individual will progress to HUS or recover after HC are unknown. Children under five have the highest incidence of HUS, and STEC-mediated HUS is the leading cause of pediatric acute renal failure. STEC strains that express Stx2a only are associated with increased risk of HUS as compared to strains that encode Stx1a only or Stx1a and Stx2a (32; 140; 197; 212; 255).

Stx intoxication of renal glomerular endothelial cells results in activation from a normal, thromboresistant state to a thrombogenic state of vascular dysfunction (221; 321). Activated endothelial cells release pro-inflammatory cytokines and induce pro-adhesive, pro-thrombic, and pro-inflammatory genes (321). The intoxicated endothelial cells swell and detach from the basement membrane; this endothelial cell damage and detachment causes edema and exposes subendothelial collagen. The exposed collagen activates platelets that then accumulate at the site and cause thrombosis. Hemolytic anemia follows as RBC are fragmented by shear force as they transit through the occluded vessels. Renal failure results when healthy glomeruli can no longer compensate

21
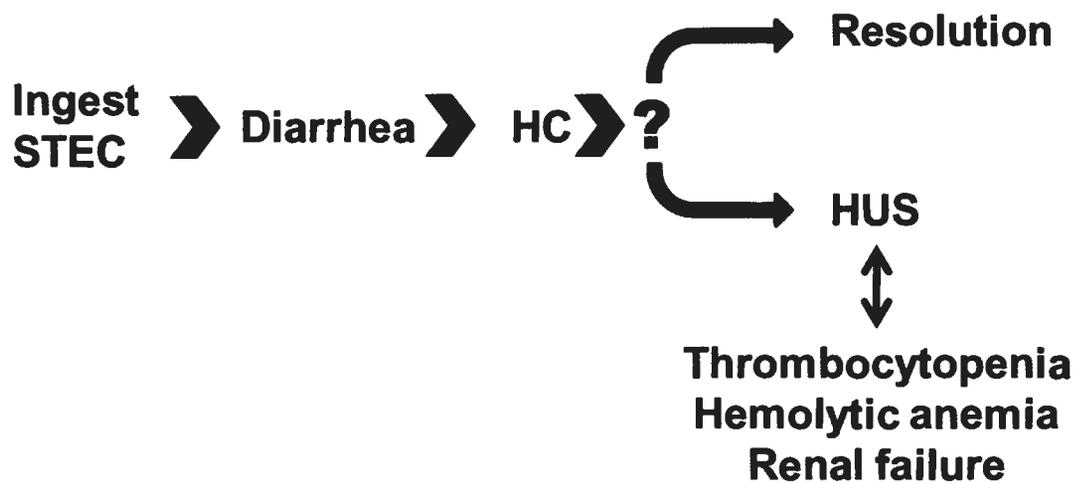
Figure 4. Progression of disease after STEC O157:H7 ingestion.
Infection begins with ingestion of the organism. Approximately three to five days later diarrhea will begin, followed by hemorrhagic colitis three days later. The infection will spontaneous resolve in the majority of individuals, however, for unknown reasons, 10-20% will develop HUS. The disease is defined by a triad of symptoms: thrombocytopenia, hemolytic anemia, and renal failure.

for the intoxicated, nonfunctional glomeruli. Tubular damage may also play a role in renal failure (48; 297) as indicated in murine models (see Chapter 2). Some studies suggest that complement activation may induce HUS (123; 186; 269), however the role of complement is controversial in STEC-provoked HUS [also called D+ for diarrhea HUS] (149). Complement dysregulation is responsible, however, for atypical HUS due to a rare genetic disorder that causes excessive activation of the complement pathway (224).

A retrospective review of HUS cases from 1950-2001 found that death or end-stage renal disease occurred approximately 12% of the time, while 25% of patients experienced long term consequences upon recovery (89). Chronic symptoms included: hypertension, proteinuria, chronic kidney disease, and decreased glomerular filtration rate (GFR). Cerebral endothelial involvement is a serious HUS sequela associated with an increased risk of fatality (205; 293). Neurological symptoms include seizures, dysphasia, cortical blindness, stroke, cerebral hemorrhage, or coma (293). Approximately 25% of patients with HUS will develop neurological symptoms (92).

Currently, there are no approved therapeutics to prevent or treat HUS (detailed below). Antibiotic treatment is contraindicated for STEC infection due to the potential increase in Stx expression and associated increased risk of HUS (318). A low antibiotic dose has the potential for increased Stx production due to induction of the lambdoid phage into the lytic cycle and increased expression of the late stage phage genes and *stx* (134). Conversely, a high antibiotic dose could result in a singular event of bacterial lysis and the release of a large bolus of intracellular Stx (93). Retrospective and prospective studies have found that antibiotics do not provide a benefit and may cause harm (242).

23

However, one report from a large STEC outbreak in Japanese school children indicated a potential benefit from treatment with fosfomycin, if delivered early in the clinical course (112). One caveat is that fosfomycin was compared to other antibiotics and not untreated controls. Anti-motility agents are not recommended due to an increased risk of neurological involvement (57). Similarly, plasma therapy is not recommended due to its association with chronic sequelae (237). Supportive therapy, such as fluid replacement with intravenous (iv) isotonic saline solution supplemented with electrolytes, is the only current treatment (6; 280). Fluid expansion counteracts vascular leakage and helps to maintain kidney function.

Therapeutics

Since antibiotics are contraindicated when an STEC infection is suspected, the development of novel therapeutics is needed to prevent HUS in at-risk individuals. Multiple therapeutic approaches have been tried at the proof-of-principle stage (reviewed in (178)); however, this section will focus on therapeutics that have advanced to human clinical trials. The first clinical trial was with the receptor analog SYNSORB Pk, a chemically synthesized oligosaccharide with a high receptor density that was designed for increased Stx binding affinity compared to Gb3. This receptor mimic was created to bind to Stx in the lumen of the intestinal tract and prevent the toxin from binding Gb3 locally or systemically (10). SYNSORB Pk was able to protect human renal adenocarcinoma cells against both Stx1a and Stx2a (277), although it only efficiently protected Vero cells from Stx1a (10). SYNSORB Pk was well tolerated in phase 1 clinical trials (11); nevertheless, it failed to prevent progression to severe sequela in

STEC-infected individuals in a double blind study (294). The lack of *in vivo* efficacy was probably because the therapeutic was delivered relatively late in the course of disease, and Stx had likely already been delivered systemically (294).

The most advanced therapeutic options in the prevention of HUS are humanized monoclonal antibodies (MAbs). Several groups have developed MAbs that have progressed through Phase I/II trials. O'Brien and colleagues developed 11E10, directed against the A subunit of Stx2a (274), and 13C4, directed against the B subunit of Stx1a (220). The antibodies neutralized the Stxs, prevented cytotoxicity of Vero cells (266; 267) and protected against lethality from Stx2a in mice (245). The MAbs were chimerized (made partially human) and renamed cαStx1 and cαStx2. Both MAbs demonstrated *in vivo* protection as cαStx1 protected against Stx1a intoxication (STEC that express Stx1a do not cause a lethal oral infection in mice), and cαStx2 prevented lethality from Stx2d- producer, B2F1, in a Str-treated mouse model (66). In both phase I (31; 63) and phase II clinical trials, the chimerized MAbs were well tolerated. Takeda's group also developed anti-Stx1a and anti-Stx2 chimerized MAbs (193; 194). The chimerized anti-Stx2 MAb, TMA-15, can neutralize Stx2a in cell culture and protect mice from intoxication (135; 319). The MAb was renamed urtoxazumab for Phase I clinical trials, where it was well tolerated; however, no efficacy data are available (146). Lastly, fully humanized anti-Stx1a and anti-Stx2 MAbs were generated in a transgenic mouse model and shown to neutralize Stx *in vitro* (189; 190). The anti-Stx2 antibody was named 5C12 and was protective in a Str-treated mouse and piglet model of infection (189; 190).

Finally, efficacy of Eculizumab, an Ab developed for the treatment of atypical

HUS, was tested as a therapy against STEC-mediated HUS. The Ab is directed against

the C5 complement protein and prevents further activation of the complement cascade.

Treatment with this antibody is thus proposed to limit the pro-inflammatory immune

response. Eculizumab was tested in a small STEC outbreak of 5 pediatric patients (148).

The authors reported a positive clinical effect, even though two patients still progressed

to HUS. Eculizumab was also used during the 2011 O104:H4 outbreak in Germany.

There was no evidence of efficacy (180); however, it is difficult to assess the results due

to different clinical courses in those HUS patients and because it was often prescribed to

the sickest patients.

Stx1a versus Stx2a

The differential *in vitro* and *in vivo* phenotypes of Stx1a and Stx2a is the basis of

experimental investigation. The paradox is that Stx1a is more cytotoxic to Vero cells (the

gold standard for cytotoxicity), while Stx2a is more toxic in animal models and human

disease (discussed above). The risk for development of HUS precludes the use of human

volunteers to study the effects of Stx, so a model system is required. To date, no one

system or animal model fully recapitulates all aspects of disease; therefore, various *in*

vitro and *in vivo* approaches are used to study Stx, both independently and in the context

of an STEC infection (described below and outlined in Table 2).

Table 2. Characterization of Stx1a and Stx2a subunits and holotoxins

Subunit analyses	Assay	Result	Conclusion	Ref
	Rabbit reticulate lysate (RRL)	A subunit protein inhibition: Stx1a = Stx2a	A subunit not responsible for different toxicities; B subunit implicated	(105; 287)
	Mass spectral sedimentation equilibrium Circular dichrosim	B subunit stability: Stx1a B 50X > Stx2a	Stx1a B subunitis more stable than Stx2a B subunit	(59)
	Mass spectrometry	Stx1a B subunit: maintains homopentamer Stx2a B subunit: decreased thermodynamic stability; dissociates into lesser oligomers	Subunit studies may not represent holotoxin phenotypes	(137)

Holotoxin analyses	Assay	Result	Conclusion	Ref
	Crystal structure comparison	Holotoxin active site accessibility: Stx2a, yes; Stx1a, no Stx1a vs Stx2a: different structural conformations Stx2a, A_2 peptide extends beyond B subunit Receptor binding sites: Stx1a, 3; Stx2a, 2	Multiple structural differences between Stx1a and Stx2a may be responsible for differential toxicity	(81)
	Mass spectrometry	Holotoxin stability at physiological conditions: Stx1a = Stx2a	Decreased stability not responsible for Stx1a decreased *in vivo* toxicity	(139)

Gb3 binding ELISA	Gb3 binding affinity: Stx1a > Stx2a	*In vitro* receptor affinity: Stx1a > Stx2a	(324)
Translocation (polarized monolayer)	Stx1a: Greater %; saturable; directional; temp/energy dependent Stx2a: does not compete with Stx1a; decreased inhibition from temp	Stx1a and Stx2a translocate via different pathways	(5; 111)
ELISA Surface plasmon resonance	Binding kinetics: Stx1a slower on/off than Stx2a Receptor density affects Stx1a > Stx2a binding Binding site 2: highest affinity for both Stxs	Stx1a and Stx2a exhibit different glycan binding preferences	(76; 88)

Relative toxicity	Cell lines (abbreviation)	Result	Conclusion	Ref
	African green monkey kidney epithelial (Vero)	Cytotoxicity: Stx1a 10X > Stx2a		(287)
	Human proximal tubule epithelial cell (HK-2)	Cytotoxicity: Stx1a > Stx2a Differential induction of ER stress response Stx1a B subunit to ER and lysosome	High membrane Gb3	(150)

Human renal glomerular microvascular endothelial cells (HRMEC) & Human umbilical vein macrovascular endothelial (HUVEC)	Cytotoxicity: HRMEC: Stx2a 1,000X > Stx1a HUVEC: Stx1a > Stx2a Stx binding sites HRMEC: Stx1a> Stx2a HUVEC: Stx1a> Stx2a	Stx2a: increased cytotoxicity for microvascular cells Stx1a: increased cytotoxicity for macrovascular cells	(165)
Human brain microvascular endothelial cells (HBMECs) & Macrovascular endothelial cells (EA.hy 962)	Cytotoxicity: HBMECs: Stx2a 1,000X > Stx1a EA.hy 962: Stx1a 10X > Stx2a Stx2a mostly apoptosis Stx1a both necrosis and apoptosis	Stx1a similar for both cell lines; Stx2a varies Stx2a: increased cytotoxicity for microvascular cells Stx1a: increased cytotoxicity for macrovascular cells	(20)
Human intestinal microvascular endothelial cells (HIMEC) & Human saphenous vein macrovascular endothelial cells (HSVEC)	Binding, cytotoxicity: HIMEC>HSVEC Gb3 expression: HIMEC > Vero HIMEC: Binding capacity: Stx1a=Stx2a Binding affinity: Stx1a 50X > Stx2a Cytotoxicity: Stx2a > Stx1a	Stx2a: increased cytotoxicity despite decreased binding; resembles *in vivo* toxicity on microvascular cells	(118)

Mouse studies	Model	Result	Conclusion	Ref
	DH5α transformed with *stx₁* and *stx₂*	Stx1a: colonizes; not lethal Stx2a: colonizes; morbidity and mortality dose dependent on plasmid expression Histology lesions similar to EHEC infection	*In vivo* toxicity: Stx2a >Stx1a Lethality is dose dependent Stx is responsible for renal lesions from intoxication and infection	(302)
	Ip intoxication	Stx1a LD$_{50}$: 400 ng Stx2a LD$_{50}$: 1 ng ATN in kidneys after intoxication of both Stxs; Stx2a lesions were more severe Anti-Stxs MAbs protect from intoxication	Purified Stx responsible for lethality *In vivo* toxicity: Stx2a > Stx1a	(287)
	IV ^{125}I- Stx1a and ^{125}I- Stx2a Gb3 TLC	Stx1a has a shorter serum half-life Lung: 10X more Stx1a vs Stx2a Kidney: 3X more Stx2a vs Stx1a ATN from Stx1a and Stx2a intoxication Murine renal Gb3 slower than lung	Stx1a is sequestered at non-functional sites; responsible for decrease *in vivo* toxicity vs Stx2a	(241)
	Oral intoxication	Stx2a LD$_{50}$: 2.9 μg Stx1a: no morbidity or mortality up to 157μg	*In vivo* toxicity: Stx2a > Stx1a	(240)

Evaluation of Stxs **in vitro**

Studies with isolated Stx subunits from Stx1a and Stx2a have been conducted by several groups of investigators in efforts to define the individual contribution of the A and B polypeptides to differential toxicities of the two holotoxin types. For example, the enzymatic activities of the Stx A subunits were measured in a cell-free rabbit reticulate lysate assay. The A subunits from Stx1a and Stx2a were found to inhibit protein synthesis equivalently (105; 287). This finding suggested that the B subunit might be responsible for the Stx1a:Stx2a differential phenotype. Therefore, a number of investigators assessed differences between the Stx1a and Stx2a B subunits (59; 137; 139). The conclusion of one such inquiry was that the Stx1a B subunit binds with greater affinity to its receptor and is more thermodynamically stable than is the Stx2a B subunit (59). However, subunit studies are dependent on the formation and maintenance of the characteristic homopentamer. The Stx1a B subunit is able to form a stable pentamer *in vitro*, while the Stx2a B subunit often dissociates into smaller oligomers (137). Since the Stx2a B subunit does not readily pentamerize, the *in vitro* profile may not be representative of the holotoxin properties. Both Stx1a and Stx2a holotoxins are equivalently stable under physiological conditions (139), observations that support the necessity of comparing holotoxins rather than B subunits alone.

Multiple *in vitro* assays have been used to examine the differences in binding (49; 76; 88; 133; 324), translocation (5; 110; 222), and cytotoxicity (20; 118; 150; 165; 287) of Stx1a and Stx2a holotoxins. As stated previously, Stx1a and Stx2a preferentially bind Gb3 FA chains of different lengths; Stx1a prefers C22-24 while

31

Stx2a prefers C16-18 (133). However, the source of Gb3 is also important to assess Stx binding. An ELISA with porcine Gb3 indicates that Stx1a binds with a greater affinity than does Stx2a (324), while Stx1a and Stx2a appear to have an equivalent affinity for rat renal Gb3 as measured by ELISA (49). Additionally, the method of analysis affects Stx-Gb3 affinity results, as data from thin-layer chromatography (TLC) assays suggest that Stx1a binds renal Gb3 with greater affinity than does Stx2a (49). Stx1a and Stx2a also bind synthetic Gb3 analog mixtures differentially. Stx1a exhibits slower on/off binding kinetics than does Stx2a; additionally, Stx1a requires a more dense receptor bed while Stx2a requires increased Gb3 diversity (76; 88).

The initial entry of Stx into the vascular system results from translocation across intestinal epithelial cells. Stx1a and Stx2a both translocate across polarized epithelial cells *in vitro* without disrupting the monolayer or inhibiting protein synthesis (5; 110; 222), however, significantly more Stx1a translocates the barrier than does Stx2a (110). Additionally, Stx1a translocates in an energy-dependent, saturable manner (5) while Stx2a is not able to inhibit the translocation of Stx1a and is not affected by temperature (110). These results suggest that Stx1a and Stx2a translocate across the intestinal epithelium through a different pathway.

Finally, the cytotoxicity profiles of Stx1a and Stx2a vary significantly depending on the cell line. The differences are likely due to the vascular nature of the cell line and heterologous Gb3 expressed on the cell surface. Differential interactions with lipid rafts may also influence cytotoxicity of Stx1a compared to Stx2a on various cell lines. One study found that although both Stxs bound lipid rafts, upon membrane

fractionation, Stx1a was primarily associated with the lipid raft section while Stx2a was not (278). Stx1a is more toxic than Stx2a on Vero cells, the cell line historically used to differentiate *in vitro* cytotoxicity differences among Stx variants (287). Stx1a is also more cytotoxic on HK-2 cells, human proximal tubule epithelial cells (150). However, Stx2a is significantly more cytotoxic than Stx1a towards human microvascular endothelial cells, the primary cell type affected in human disease (20; 118; 165).

In an attempt to reconcile the contradictory *in vitro* activities of Stx1a and Stx2a and study the effect of individual Stx subunits in the context of the holotoxin, several groups have developed chimeric Stxs (105; 117; 168; 259; 310). In these studies, the A subunit from one Stx was combined with the B subunit from the reverse Stx, either by plasmid complementation or operon fusion. A number of reports suggest that the B subunit is responsible for Stx activity. However, some groups could not purify active chimerics (259; 310), or the chimerics failed to match the expected cytotoxicity values of the native Stx with the corresponding B subunit (105; 117). The loss of activity is presumably due to decreased stability of the chimeric holotoxin. The A_2 subunit is critical to the stability of the native holotoxin (14); therefore, we created chimeric toxins in which the A_1 subunit was from one native Stx, while the A_2 and B subunit were from the opposite native Stx (Chapter 3). This design enabled us to create chimeric Stxs with cytotoxic activity equivalent to the native Stxs for the first time.

Evaluation of Stxs in vivo

Multiple animal models, from mice to non-human primates, have been developed to study STEC and/or Stx specifically, although no one animal recapitulates

33

all aspects of disease (reviewed in (172; 185)). Initial animal studies often used rabbit models, since rabbits develop diarrhea and some symptoms of human disease (84). A greyhound model was developed to study glomerular lesions, as the dogs are naturally susceptible to idiopathic cutaneous and renal glomerular vasculopathy (CRGV), an HUS-like renal glomerular disease (75). A baboon model of HUS was developed and the animals develop symptoms that approximate those of human disease (261; 272), however, a non-human primate model is financially and logistically prohibitive for the majority of animal studies. Mice, and less frequently rabbits, are the most widely used models due to ease of care and low cost associated with housing. Limitations of murine animal models are that mice do not develop diarrhea or HUS, and that Gb3 is only expressed in the tubules, not in the glomerulus (85; 226) where the primary damage in human kidney is postulated to occur based on autopsy results (157; 232).

One major focus of animal research is to determine the pathology attributable to colonization and virulence factors associated with STEC infection compared to pathology resultant from Stx alone. The first report of similar pathophysiology from Stx intoxication as compared to STEC infection was by Pai *et al.* (214). These investigators orally intoxicated infant New Zealand white rabbits with Stx1a and reported diarrhea, colonic lesions and lethality similar to rabbits infected with an O157:H7 strain. To further define the direct role of Stx expressed in the gastrointestinal tract, mice were infected with non-virulent *E. coli* DH5α strains transformed with plasmids that contained stx_1 or stx_2 (302). Str-treated mice infected with the Str^r Stx1a-producing strain were colonized but did not display any signs of morbidity or mortality.

However, mice infected with the Str^r Stx2a-producing clone succumbed to infection due to acute tubular necrosis (ATN) in the kidneys, pathological findings similar to those observed in animals infected with a mouse-virulent O157:H7 STEC strain (302). Additionally, MAb against Stx2a but not Stx1a protected mice from lethal infection with the *E. coli* O157 strain that made Stx1a and Stx2a (302). This latter study supports the conclusion that Stx secreted in the intestinal tract, independent of additional virulence factors, is responsible for the lethality of EHEC infection in a murine model. The results of the investigation by Wadolkowski *et al.* (302) also support the epidemiological observation that Stx2a is associated with kidney damage and mortality rather than Stx1a when both are made by an O157:H7 strain.

Isogenic deletion mutant strains were also used to determine the contribution of Stx in an STEC infection model. Since the deletion of Stx was the only difference between the two strains, any reduction in pathology could be directly attributed to the loss of the *stx* gene. Infant New Zealand white rabbits were initially used to study an Stx2a-producing O157:H7 clinical isolate and its isogenic deletion mutants to determine the importance of independent virulence factors (234). Stx2a did not influence colonization; however, the toxin was primarily responsible for diarrhea. Moreover, rabbits infected with the wild type O157:H7 had renal lesions, but no such lesions were found in the kidneys of the rabbits infected with the mutant (Stx negative) strain. These authors also orally intoxicated rabbits with purified Stx2a and observed renal lesions similar to wild type infection. Later, a similar study was completed in mice (236). Unlike the rabbit model, Stx promoted intestinal colonization in the murine

35

model, as the stx_2 isogenic mutant did not colonize as well as the wild type strain; additionally, the colonization defect could be complemented by a dual infection with an Stx2a- positive strain (236). Finally, the addition of exogenous Stx2a during an infection with Stx2a- positive STEC strain increased colonization levels compared to the control (183). Cumulatively, these results demonstrated that Stx is responsible for lethality resultant from EHEC infections and confirm that Stx2a is more toxic than Stx1a *in vivo*. Nevertheless, the question of why there is a difference observed *in vivo* between Stx1a and Stx2a or STEC strains that make these toxins remained unanswered.

In an attempt to further discern the factors responsible for Stx1a and Stx2a differential lethality, Tesh *et al.* peritoneally injected purified Stx1a and Stx2a, separately into mice. By this injection method, these investigators bypassed any potential differences in efficacy of Stx1a and Stx2a entering the systemic circulation from the gut (287). The results of this study confirmed the increased lethality of Stx2a compared to Stx1a, as the LD_{50} was 400X lower for Stx2a even though Stx1a was more cytotoxic on Vero cells. ATN was observed in the kidneys of mice intoxicated with both toxins; however, the damage was more severe after Stx2a intoxication. Additionally, monoclonal antibody (MAb) was protective against the Stx it was raised against, but there was no heterologous protection (287). Protection with a toxin-specific MAb further supported the conclusion that Stx is independently responsible for lethality in a murine model. Since the enzymatic activities of the A subunits of Stx1a and Stx2a are equivalent, Tesh *et al.* concluded that the binding properties of the B subunits of the two types of Stxs were likely responsible for differences in lethality

(287). In a separate study, Rutjes *et al.* intoxicated mice iv with iodinated Stx1a and Stx2a to track toxin dissemination (241). They observed differential tissue targeting of Stx1a and Stx2a with 10X more Stx1a bound in the lungs and 3X more Stx2a bound in the kidneys. These authors surmised that Stx1a bound its receptor, Gb3, with an increased affinity, a phenomenon that effectively sequesters that toxin at nonfunctional sites, while Stx2a accumulated in the kidneys (target organ). Additional intoxication studies by other groups confirmed CNS involvement after Stx intoxication (205; 292). Indeed, mice intoxicated ip with a lethal dose of Stx2a exhibited hind limb paralysis, and Stx2a was found in the neurons of those mice (205). Furthermore, histological evaluation of brain sections from intoxicated mice revealed that the neurons were physically altered (205). In another investigation, mice developed damaged astrocytes and neuronal edema after a sub-lethal dose of Stx2a given iv (292).

Although intoxication animal models clearly pinpoint Stx as the virulence factor responsible for lethality in STEC infections, the models do not recapitulate all symptoms of human disease, especially in relation to HUS. Analyses of sera from patients with confirmed EHEC O157:H7 infections reveal the presence of anti O157 LPS Ab (30; 50). Therefore, some groups have attempted to create HUS animal models with the co-administration of Stx and LPS. The combination of Stx2a and LPS has been reported to have a synergistic effect on intoxication in mice and rabbits in that the pathology observed is greater than that seen in tissues of animals that received Stx or LPS alone (17; 113; 131; 216). Animals injected with both LPS and Stx exhibit neutrophilia, thrombocytopenia, red cell hemolysis, an increase in both creatinine and

blood urea nitrogen (BUN), along with glomerular fibrin deposition and microthrombi. However, these models are somewhat controversial. Increased weight loss was reported in rabbits when Stx2a and LPS were given in combination, but there was no statistically significant difference in that amount of weight loss compared to animals that received Stx2a alone (17). Also, the only additional HUS symptoms observed in mice after intoxication with Stx2a and LPS in combination that are not found after Stx2a only intoxication are thrombocytopenia and fibrin deposition (113; 131; 216). Additionally, the time of LPS delivery affected the outcome of the model; mice were actually protected from the lethal effects of Stx2a if LPS was delivered prior to Stx2a intoxication (17; 113; 131; 216). Since Stx is directly responsible for mortality in an infection and intoxication model, the protective effect of LPS may signify that the model is not representative of a natural infection. Other studies reported that there was no synergy observed with addition of LPS in Stx2a intoxication model (276) or that LPS was not required to induce HUS-like disease when repeated low doses of Stx were injected as seen initially in baboons (283) and later in mice (245). Therefore, LPS may (or may not) increase symptoms of disease after STEC infection of humans, but it is not required for lethality in an STEC infection- or Stx intoxication- animal model.

An Stx oral intoxication model was developed after reports of preformed Stx in food sources (103; 309) and the discovery that Stx can remain toxic in milk subjected to current pasteurization processes (229). There are only a few reports in the literature about oral intoxication of animals with Stx. These publications include the two Stx oral intoxication studies conducted in infant rabbits (described above) (214; 234), and a

study by Rasooly *et al.* in which they were the first to report oral intoxication of mice with Stx2a (230). These investigators found that a low dose of 0.25 was not lethal, while 50 µg was lethal. They also reported lesions in the kidneys similar to those acquired from EHEC O157:H7 infection of mice. Recently, we expanded the Stx intragastric (ig) intoxication model in mice (Chapter 2). We found that the Stx2a LD_{50} was 2.9 µg, while up to 157 µg of Stx1a did not result in morbidity or mortality. Additionally, pathological lesions and renal serum biochemical values were similar after ip versus ig intoxication. Furthermore, we were able to protect and rescue mice with MAb 11E10 that was raised against the Stx2a A subunit. We believe that the demonstration that oral intoxication by Stx2 can lead to morbidity and even mortality in mice may be an important observation for public health as ingested preformed Stx may contribute to disease during an STEC outbreak.

Hypotheses

Stx is the primary virulence factor responsible for human disease after infection with STEC. Prior reports have established that Stx is sufficient to induce pathology after ip and iv intoxication. We propose that toxin can survive transit through the GI tract, reach its systemic target of the kidneys, and result in a lethal event in mice. Additionally, we theorize that the B-subunit is responsible for the difference in cytotoxic activity of Stx1a and Stx2a *in vitro* and *in vivo*. Although reports by our laboratory and others (105; 117; 259; 287; 310) have provided suggestive evidence that B subunit variations between Stx1a and Stx2a are key to the differential toxicities of

Stx1a and Stx2a *in vitro* and *in vivo,* technical issues have heretofore prevented acquisition of definitive data in support of this hypothesis.

Specific Aims

Specific Aim 1: Develop and characterize an oral intoxication model of Stx1a and Stx2a. For that purpose I propose to:

Sub Aim 1a: Establish the oral LD_{50} of Stx1a and Stx2a

Sub Aim 1b: Investigate the histopathology in tissues of mice after oral intoxication

Sub Aim 1c: Determine whether a MAb raised against Stx1a or Stx2a can protect and/or rescue mice from intoxication

Specific Aim 2: Define the contribution of Stx subunits towards cytotoxicity and mouse lethality through comparative analyses of native (Stx1a and Stx2a) and chimeric Stxs. For that purpose I propose to:

Sub Aim 2a: Determine the *in vitro* activity profile of Stx chimerics in relation to the native toxins

Sub Aim 2b: Establish the ip and ig $LD_{50}s$ of the chimeric Stxs as a platform to determine the importance of subunits towards *in vivo* toxicity

CHAPTER 2

Oral intoxication of mice with Shiga toxin type 2a (Stx2a) and protection by anti-Stx2a monoclonal antibody 11E10

Russo LM, Melton-Celsa AR, Smith MA, Smith MJ, O'Brien AD.

Department of Microbiology and Immunology, Uniformed Services University of the Health Sciences, Bethesda, MD, USA.

L.M. Russo is solely responsible for the work presented in this chapter, with the following exceptions: A.R. Melton-Celsa, M.J. Smith, and A.D. O'Brien assisted with experimental design and analysis and M.A. Smith was the veterinary pathologist who performed the histological review.

Note: The figure, table, and reference numbers have been adjusted to follow the format of this dissertation.

ABSTRACT

Shiga toxin (Stx) producing *E. coli* (STEC) cause foodborne outbreaks of hemorrhagic colitis, and less commonly, a serious, kidney-damaging sequela called the hemolytic uremic syndrome (HUS). Stx, the primary virulence factor expressed by STEC, is an AB_5 toxin with two antigenically distinct forms, Stx1a and Stx2a. Although both toxins have similar biological activities, Stx2a is more frequently produced by STEC that cause HUS than is Stx1a. Here we asked whether Stx1a and Stx2a act differently when delivered orally by gavage. We found that Stx2a had a lethal dose 50% (LD_{50}) of 2.9 μg, but no morbidity occurred after oral intoxication with up to 157 μg of Stx1a. We also compared several biochemical and histological parameters in mice intoxicated orally versus intraperitoneally with Stx2a. We discovered that both intoxication routes caused similar increases in serum creatinine and blood urea nitrogen, indicative of kidney damage, as well as electrolyte imbalances and weight loss in the animals. Furthermore, kidney sections from Stx2a-intoxicated mice revealed multifocal, acute tubular necrosis (ATN). Of particular note, we detected Stx2a in kidney sections from orally intoxicated mice in the same region as the epithelial cell type in which ATN was detected. Lastly, we showed reduced renal damage, as determined by renal biomarkers and histopathology, and full protection of orally intoxicated mice with monoclonal antibody (MAb) 11E10 directed against the toxin A subunit; conversely, an irrelevant MAb had no therapeutic effect. Orally intoxicated mice could be rescued by MAb 11E10 6 hours but not 24 hours after Stx2a delivery.

INTRODUCTION

Shiga toxin (Stx)-producing *Escherichia coli* (STEC) are foodborne pathogens with an estimated infectious dose of less than 50 organisms (291). While multiple STEC serotypes are associated with disease, illness associated with infection by *E. coli* O157:H7 accounts for over 63,000 of the 113,000 total STEC cases each year in the U.S. (247). Bovine and other ruminants are the natural carriers of STEC, and contamination of meat generally occurs during beef processing, with up to 40% of the outbreaks from beef (102; 215). However, contaminated fresh produce is also responsible for both outbreaks and sporadic cases of STEC in the U.S. (215; 228).

Upon STEC infection, the most common disease manifestation is hemorrhagic colitis. In 5-15% of patients, a serious sequela of STEC infection, the hemolytic uremic syndrome (HUS), may occur (127; 171). The HUS is characterized by a triad of symptoms: microangiopathic hemolytic anemia, thrombocytopenia and acute kidney failure (124). Currently, there is no vaccine to prevent or therapeutic to cure STEC infection, as antibiotics are contraindicated due to the potential up regulation of bacteriophage production of Stx (317).

An STEC strain may encode for Stx1a (equivalent to Stx from *Shigella dysenteriae* type 1) and/or Stx2a, two antigenically distinct but biologically similar toxins (200; 312). Stx1a and Stx2a share about 57% amino acid homology, an analogous crystal structure, and an identical mode of action (179). Stx1a and Stx2a are AB5 toxins. The A subunit is responsible for the catalytic activity of the toxin molecule, and the B subunit, a homopentamer, is required for the toxin to bind to Stx host cell receptor, globotriaosylceramide (Gb3) (156; 158). Once bound to its receptor, Stx undergoes

43

retrograde transport through the cell; the enzymatically active portion of the toxin is then released into the cytoplasm where it depurinates a single adenine residue from the 28S rRNA of the 60S ribosome (69; 246). This ribosomal injury results in the inhibition of protein synthesis and ultimately cell death (206). Although Stx1a and Stx2a have the same receptor and mode of action, epidemiologic studies indicate that strains that encode Stx2a are more likely to be associated with food-borne outbreaks and severe disease, such as the HUS, than are those that make Stx1a only or Stx1a and Stx2a (32; 213; 255).

Although no one animal model recapitulates all aspects of STEC pathogenesis, the capacity of the Stxs to cause disease has been demonstrated by either infection or intoxication models in mice, rats, pigs, baboons, and greyhounds (see reviews (177; 187)). For example, oral infection with certain strains of STEC in mouse models or injection of mice with either Stx1a or Stx2a results in renal injury and death (Reviewed in (185)). Monoclonal antibody (MAb) against the toxin is able to protect those animals from disease and death (66; 267), findings that further establish a role for Stx in pathogenesis. Only a few studies that examine oral intoxication by Stx in animals have been reported. In two such investigations, purified Stx (specific toxin type(s) unknown, (214)) and Stx2a (234), were found to be lethal after intragastric (i.g.) gavage of infant New Zealand white rabbits. More recently, Rasooly *et al.* demonstrated that i.g. administration of 50 µg, but not 0.5 µg, of Stx2a is lethal in Swiss Webster mice (230). Here, we further defined the oral toxicity of the Stxs in mice. We found that although Stx1a was not lethal via the oral route, Stx2a has an i.g. LD_{50} of 2.9 µg. We further showed that the renal pathology caused by Stx2a by both the i.g. and i.p. route of

intoxication was similar. Finally, we protected mice from oral Stx2a intoxication by passive antibody transfer of MAb 11E10 against the Stx2a toxin A subunit.

(A portion of this work was presented at the 8th International Symposium on Shiga Toxin [Verocytotoxin] Producing *Escherichia coli* Infections, Amsterdam, The Netherlands, 6 to 9 May 2012 [(239)].)

MATERIALS AND METHODS

Bacterial strains and growth conditions.

E. coli K12 DH5α strains transformed with pLPSH3 (288) or pJES120 (153) encode Stx (equivalent to Stx1a, and called Stx1a from here on for simplicity) or Stx2a, respectively. Both strains were grown in Luria Bertani (LB) broth or LB agar supplemented with 100 µg/mL ampicillin for maintenance of the recombinant plasmid.

Purification of Stx1a and Stx2a.

Both toxins were purified by affinity chromatography with 5 mL AminoLink Coupling Resin (Thermo Scientific) columns.

Column preparation:

MAb to the B subunit of either Stx1a or Stx2a was covalently bound to the column resin in pH 7.2 coupling buffer according to manufacturer's instructions. MAb 13C4 (274) was purified from hybridoma supernatant by fast protein liquid chromatography over a HiTrap Protein G HP 5 mL column (GE Life Sciences, Pittsburgh, PA), desalted (HiTrap Desalting column, GE Life Sciences) into phosphate-buffered saline (PBS), and used for purification of Stx1a (approximately 7 mg MAb/column) while MAb BC5 BB12 (64) in ascites fluid, a gift from Dr. Nancy Strockbine, was diluted into PBS and used for Stx2a purification (approximately 13 mg MAb/column).

Cell lysate preparation:

An overnight culture of the *E. coli* K12 strain that contained the plasmid that encoded the *stx* of interest was sedimented by centrifugation (5,000 x g) and the pellet resuspended at 4 mL per g in sonication buffer (50mM NaPO4, 200mM NaCl). The

resuspended cell pellet was disrupted by sonication. The cell lysate was sedimented by centrifugation (20,000 x g), and the supernatant was filtered prior to toxin purification.

Toxin purification:

Cell lysates were applied to the column in accordance with the manufacturer's instructions for sample application except as noted below. All column elutions were recovered via gravity instead of centrifugation. The cell lysate flow-through was reapplied to the column for additional toxin binding. The column contents were washed consecutively with three column volumes each: sonication buffer, high salt buffer (0.5 M NaCl, 50 mM NaPO4) to further remove non-specific contaminants, and sonication buffer to prevent protein denaturation resultant from the high salt concentration. Toxin was eluted (0.1 M glycine, pH 2.8) in 1mL fractions into 200 μL neutralization buffer (1M Tris HCL pH 9.5). The fractions that contained toxin were dialyzed against PBS in Slide-A-Lyzer dialysis cassettes (Thermo Scientific). Toxin activity was confirmed on Vero cells as previously described (91). The endotoxin level was less than 0.025 EU per μg Stx2a (data not shown) as determined by the Limulus amebocyte lysate chromogenic endpoint assay (Hycult). When necessary, Millipore Amicon Ultra 30K, 15 mL concentrators were used in accordance with manufacturer's instructions to concentrate the toxin preparation. The protein concentration in the toxin preparations was determined with a bicinchoninic acid (BCA) assay (Thermo Scientific).

Specific toxin concentration determination.

To normalize for differences in purity among the toxin preparations, we used densitometry analyses of stained gels to determine the percent of toxin in each preparation relative to the total protein in each sample as follows. Purified toxins were

separated on NuPAGE Novex 4-12% Bis-Tris gel(s) (Invitrogen). The gel(s) were then stained with Oriole fluorescent gel stain (BioRad) and scanned with ImageQuant LAS 4000 (GE Healthcare). The scanned image was analyzed with ImageQuant TL software (GE Healthcare) to determine what contribution to the total protein was made by the bands that comprised the A and B subunits of the toxins. The concentration of purified toxin was then calculated by multiplying the percent of toxin in the preparation by the total protein concentration measured in the BCA assay. The densitometry analyses of the individual A and B subunit bands suggested that the proportion of A to B subunits in each preparation was at or close to the expected ratio of 1:5 and that the purity of the preparations ranged from 82 to 95 percent (data not shown).

Mice.

All animal studies were approved by the Institutional Animal Care and Use Committee of the Uniformed Services University of the Health Sciences and were conducted in strict accordance with the recommendations of the Guide for the Care and Use of Laboratory Animals (296). Female BALB/c mice, 5-6 weeks old, were obtained from Charles River Laboratories (Wilmington, MA) and used for all experiments. Food and water were removed for 18 and 2 h, respectively, prior to all i.g. intoxication studies. Mice were gavaged with 0.2 mL of toxin/PBS dilutions or PBS as control for oral intoxication or injected with 0.1 mL Stx/PBS dilution for all i.p. intoxication studies. Mice were weighed daily and monitored for morbidity and mortality for two weeks post-intoxication. When the starting weights of mice were similar among groups, we graphed the mean weights of animals in each group on that day. However, when the initial mean weights of the mice in groups differed by more than 5% we plotted the

percent weight change per day. Two way Analysis of Variance (ANOVA) was used to determine a significant difference in weight change among intoxication groups. The Stx2a i.g. intoxication LD_{50} and 95% confidence interval (CI) values were determined by probit regression analysis with log transformation of the values.

Serum biochemistry and histopathology.

Mice received Stx2a diluted in PBS or PBS alone as a control through i.p. or i.g. administration. Three or four days post intoxication, mice were anesthetized with isoflurane (VetEquip Incorporated, Pleasanton, CA), and blood was collected via cardiac puncture. After the blood clotted, the serum was separated by centrifugation at 6,000 x g for 10 min, and sent to BioReliance (Rockville, MD). Serum samples were analyzed by an automated clinical chemistry analyzer (Cobas 600 series) and reported through a laboratory information management system (LIMS). For the initial studies, a full serum panel was done. However, only the kidney-specific markers showed differences from the expected normal range (http://www.criver.com/files/pdfs/rms/balbc/rm_rm_r_balb-c_mouse_clinical_pathology_data.aspx), so all subsequent serum analyses were limited to the renal panel: blood urea nitrogen (BUN), creatinine, sodium (Na), potassium (K), chloride (Cl), and albumin. One way ANOVA was used to determine statistical significance between the experimental and control groups.

After blood collection, the mice were euthanized and necropsied. For some studies, kidney, small intestine, cecum, large intestine, and/or liver were collected, fixed in formalin, and sent to Histoserv (Germantown, MD) to be embedded in paraffin and sectioned. Sections from all organs were stained with hematoxylin and eosin

(H&E). The semi-quantitative severity modifier of a morphologic diagnosis, such as mild, moderate, or severe, was used to describe lesions. Additionally, serial sections from some of kidney samples analyzed with H&E were stained with periodic acid-Schiff (PAS). PAS stains polysaccharides, including basement membranes and brush boarders of certain epithelial cells. Therefore, proximal tubules, which have a thick brush border, can be distinguished with the PAS stain from distal tubules that lack a prominent brush border. Slides were read by a veterinary pathologist who was blinded to the study group identifications.

Immunofluorescence.

Slides with unstained kidney or intestinal sections were deparaffinized by incubation in Histoclear (National Diagnostics; Atlanta, Ga) twice for three min each time. The tissue was then rehydrated in a graded ethanol (ETOH) series as follows: three incubations for three min in 100% ETOH, followed by three min in 95% ETOH, three min in 90% ETOH, and finally three min in 70% ETOH. The slides were rinsed in deionized water and heated in 1X citrate pH 6 antigen retrieval buffer (Ag Plus Buffer, Novagen) at 95°C for 10 minutes. The slides were then rinsed in deionized water and blocked overnight at 4°C in 1% goat serum diluted in antibody (Ab) diluent reagent solution (Invitrogen). Slides were incubated with primary Ab (polyclonal rabbit αStx2a (144) diluted 1:500 in Ab diluent solution) for one h at room temperature. Slides were washed 3X with PBS before the secondary Ab, goat anti-rabbit-Alexa-fluor 488 (Invitrogen) diluted 1:500 in Ab diluent, was applied for one h at room temperature. Finally, slides were washed 3X with PBS and the coverslip was mounted with Vectashield (Vector Laboratories, Inc, Burlingame, CA), which contained the counter

stain, 4', 6-diamidino-2-phenylindole (DAPI). Slides were observed on an Olympus BX60 microscope with a BX-FLA fluorescent attachment.

Passive Ab transfer.

MAb 11E10 (BEI Resources/Hycult), directed against the Stx2a A subunit (220; 267), was used for all passive Ab transfer studies. TFTB1 (BEI Resources), an irrelevant Ab which recognizes the ricin B subunit (87), was included as an IgG2a isotype control. Additionally, each experiment included a group that received Stx2a only as a positive control for toxin activity. A dose of 7.5 µg Stx2a was used for all Ab protection and rescue experiments because that amount of toxin is invariably lethal in the oral intoxication model. Both MAbs and Stx2a were diluted in PBS for all experiments.

Ab Protection:

For the preliminary study, mice received 2 µg of 11E10 or TFTβ1 i.v. by tail vein 24 h prior to i.g. intoxication with 7.5 µg Stx2a. In all subsequent experiments, mice received 2, 4, or 40 µg of Ab i.v. one h before intoxication.

Statistical Analyses of Antibody Protection Data:

The percent weight change values were first transformed into log ratios (log $((Y/100)+1)$ where Y is percent change) to make the data more normally distributed with more homogenous variance. Next, two-way repeated measures ANOVA with Tukey's post-hoc tests were used to determine statistical significance of weight loss among Ab dose groups. Since repeated measures ANOVA is only an appropriate tool for evaluation of complete data sets, analyses started on day 2. Although there was no

significant group effect (p = 0.06), there was a significant interaction effect (p = 0.0002), a finding that indicates that the difference among groups varies over time. Tukey's post hoc tests were used to determine statistical significance on individual days.

Ab Rescue.

MAbs 11E10 or TFTβ1 (4 μg) were delivered i.v. at 6, 24, 48, or 72 h after Stx2a i.g. intoxication. An Ab protection group, which received 4 μg one h prior to intoxication, was included as a positive Ab control.

RESULTS

Stx2a but not Stx1a is lethal for mice after oral intoxication.

We determined the LD_{50} of Stx2a in mice by the oral intoxication route. Groups

of mice were gavaged with Stx2a at concentrations from 0.25 μg through 15 μg toxin.

Significant weight loss and death were observed at Stx2a concentrations of 2 μg or

greater (Figure 5A & B). The LD_{50} for Stx2a after oral intoxication was calculated to be

2.9 μg (CI 1.4-5.0 μg), 1,000X greater than the Stx2a i.p. LD_{50} of approximately 2 ng

[(287) and confirmed with our toxin lot, not shown]. The mean time-to-death (MTD)

was 4.9 days. In contrast, no morbidity or mortality was observed after i.g. intoxication

of up to 157 μg Stx1a (data not shown).

Kidney damage and electrolyte imbalances occur in mice intoxicated i.p. or i.g. with Stx2a.

After we determined the oral Stx2a LD_{50}, we compared the serum biochemistry

values after i.p. or i.g. intoxication. Mice were challenged with 6X the i.p. or i.g. Stx2a

LD_{50} (13.2 ng or 17 μg, respectively) or PBS as a control. Serum biochemistry markers

from all groups were evaluated three days post intoxication. The serum biochemistry

markers from the i.p. and i.g. PBS control groups were within the normal range and

statistically indistinguishable (only i.g. shown, Table 3, row 1). Independent of the

route of intoxication, and with the exception of albumin, the serum biochemical values

related to kidney function from Stx2a-intoxicated mice were significantly different than

those from the PBS control group values (Table 3). Specifically, the BUN and

creatinine levels rose significantly after intoxication, and there was an imbalance of the

electrolytes Na, Cl, and K.
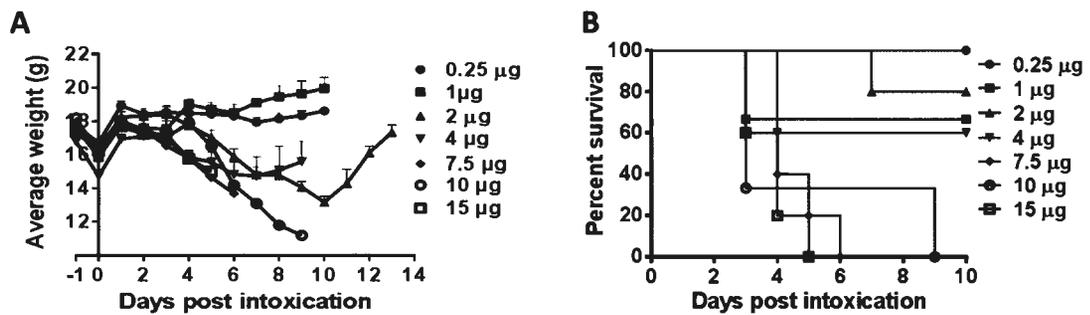
Figure 5. Morbidity and mortality after i.g. intoxication by Stx2a in mice.
(A) Mean weight of mice over the course of the experiment for each Stx2a concentration tested in the oral intoxication model. Sample size (n) =5 for all doses except 1 and 10 μg, where n=3. Error bars indicate standard error of the mean. There was a significant dose-over-time interaction, such that mice that received 2 μg or more Stx2a experienced significant weight loss compared to animals that received 0.25 or 1 μg toxin (p<0.05). The weight gain in the no toxin group (PBS only) was statistically similar to the 0.25 μg Stx2a group, p<0.05, so, for simplicity, only the 0.25 weight data were plotted. (B) Mouse survival percentage over time at each Stx2a concentration. The PBS-only control group had 100% survival, not shown.

54

Table 3. Mean renal panel serum biochemistry values

Agent, route	n	Dose	Time of blood collection[a]	BUN (mg/dl)	Cre (mg/dl)	Na (mmol/L)	K (mmol/L)	Cl (mmol/L)	Albumin (g/dl)
				Level (range)[f]					
PBS i.g[b]	8	0.2 ml	D3 pi	33.9 (25-40)	0.24 (0.2-0.28)	135.5 (132-137)	19.9 (13.7-24.5)	105.3 (102-108)	3.3 (3.2-3.5)
Stx2a i.p.[c]	4-9	13.2 ng	D3 pi	193.9 (81-246)	0.95 (0.67-1.2)	119.5 (99-128)	30.2 (23.2-45)	84.8 (67.3-91.1)	4.1 (3.9-4.2)
Stxa2 i.g.[c]	8-9	17 μg	D3 pi	116.6 (82-245)	0.61 (0.44-1.1)	105.9 (76-121)	37.3 (25.6-67.3)	77.2 (68.9-88.8)	3.7 (1.9-4.3)
Stx2a i.g.	2	2 μg	Wt loss plateau	114.5	0.50	119.0	37.3	87.1	3.7
Stx2a i.g.	4	2 μg	+1D recovery	35.8 (34-38)	0.20 (0.14-0.24)	135.8 (134-139)	25.3 (23.3-27.2)	106.6 (106-109)	3.3 (3.2-3.4)
Stx2a i.g.	2	7.5 μg	D4 pi	275	1.62	NV	NV	NV	NV
+TFTB1[d]	5	7.5 μg	D4 pi	213.2[e] (150-269)	1.23[e] (.99-1.41)	NV	NV	NV	NV
+11E10[d]	4	7.5 μg	D4 pi	30.5[e] (25-40)	0.24[e] (0.2-0.28)	NV	NV	NV	NV

[a] Blood collection times were dictated by parameters for each study.

[b] Serum biochemistry values from i.p. and i.g. PBS control mice were not statistically different (p < 0.05)

[c] The serum chemistry values were significantly different (p < 0.01) from PBS control except the K in the Stx2a i.p. group and the albumin values in both groups.

[d] Four μg of Ab

[e] P <0.0001, TFTB1 versus 11E10

[f] NV, no value returned

Renal tubular damage is seen in kidney sections of mice orally intoxicated with Stx2a.

We next examined intestinal, liver, and renal tissues for damage after Stx2a i.g. intoxication. Four days post i.g. intoxication with 7.5 μg Stx2a (~2.5X LD_{50}) mice were euthanized and the intestinal tracts and kidneys removed. For comparison, we also collected the kidneys from mice intoxicated i.p. with 13.2 ng or i.g. with 17 μg Stx2a (6X LD_{50}) on day three (the intestinal tract does not exhibit damage after i.p. intoxication, (287)). The earlier time point (day 3 as opposed to day 4) of kidney collection was necessitated by the earlier MTD and the increased Stx2a i.g. dose for i.p.-intoxicated mice. No lesions were noted in the small intestine, cecum, or large intestine of mice orally intoxicated with Stx2a (Figure S1 A-C). We next reviewed kidney sections stained with H & E from mice given PBS or Stx2a i.g. No lesions were observed in renal sections from PBS control mice (Figure 6A). In contrast, we found diffuse tubular dilation and basophilia in the renal cortex of mice intoxicated i.g. with 7.5 μg Stx2a (Figure 6B) or 6X LD_{50}s of Stx2a regardless of route of toxin administration (not shown). We then used the PAS stain to examine kidney sections. As expected, no renal lesions were detected in the kidneys of either i.p. (not shown) or i.g. PBS control mice (Figure 6C). However, we observed minimal to moderate, multifocal acute tubular necrosis (ATN) of distal tubules characterized by tubules lined with degenerating, necrotic, or sloughed epithelial cells, independent of dose or route of intoxication (2.5X LD_{50} dose shown Figure 6D).
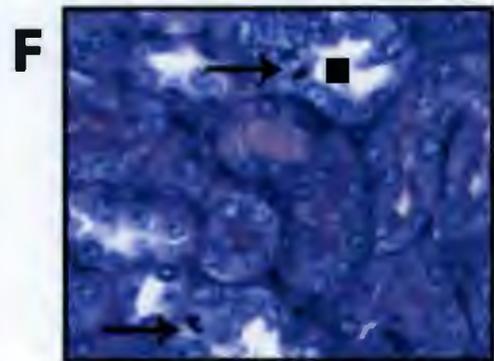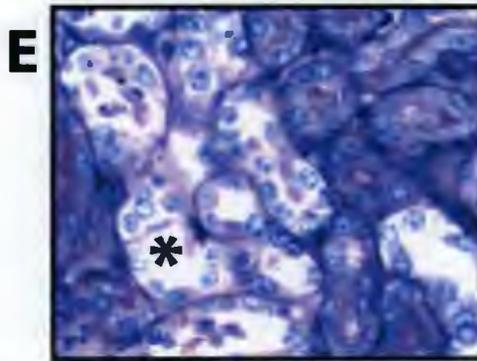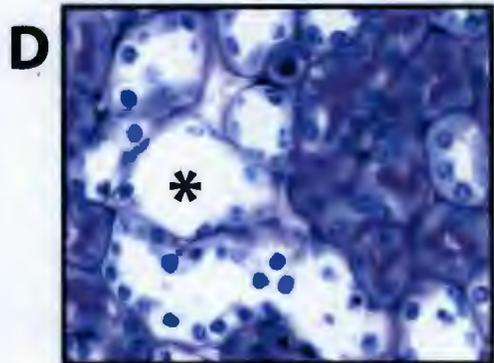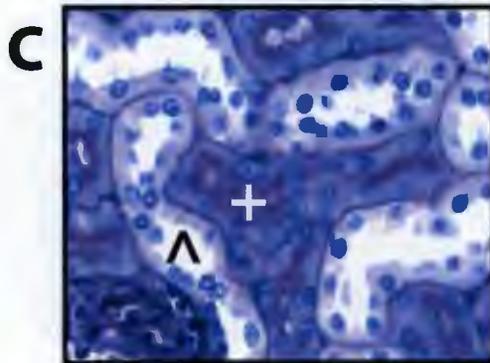
Stx2a is present in the kidneys of intoxicated mice.

We next asked if we could detect Stx2a in the kidneys of mice after parenteral (i.p.) or oral intoxication. Only a minimal green fluorescent background was observed in kidney sections from mice given PBS i.p. (Figure 7A) or orally (not shown). However, we were able to confirm the findings of Rutjes *et al.* that Stx2a can be found in kidney sections after parenteral (in our case i.p. in their studies i.v.) intoxication (241) (Figure 7B). Moreover, we also detected Stx2a in kidney sections from i.g. intoxicated mice (17 µg) (Figure 7C). The Stx2a-positive cells appeared to be tubule epithelial cells for both i.p.- and i.g.-intoxicated mice as the Stx2a staining-pattern in the tubules coincided with the histopathological location of renal damage in the intoxicated mice (Figure 6D).

Morbidity in Stx2a-intoxicated mice correlates with kidney function.

Because we observed significant weight loss followed by rapid weight gain in the majority of mice intoxicated i.g. with 2 µg of Stx2a, we speculated that mice given 2 µg of Stx2a i.g. might exhibit kidney damage even though they typically recovered from that toxin dose (Figure 5A & B). In a subsequent study, we found that mice intoxicated with 2 µg of Stx2a, a sub-LD_{50} dose, and sacrificed when weight loss began to plateau (day 8 or 9 in this experiment) exhibited similar serum biochemistry profiles and kidney histopathology to mice intoxicated with 6X LD_{50} (Table 3 Row 4, Figure 6E). Stx2a was also detected by immunofluorescence in the kidneys of those same mice (not shown). In mice given 2 µg of Stx2a and allowed to recover one day after the weight loss plateau, serum biochemistry values returned to control levels and kidney histology improved (the ATN was less severe and tubules contained regenerating

59

epithelial cells) (Table 3 Row 5, Figure 6F). Three days after the rebound in weight, no

kidney lesions were noted (data not shown).
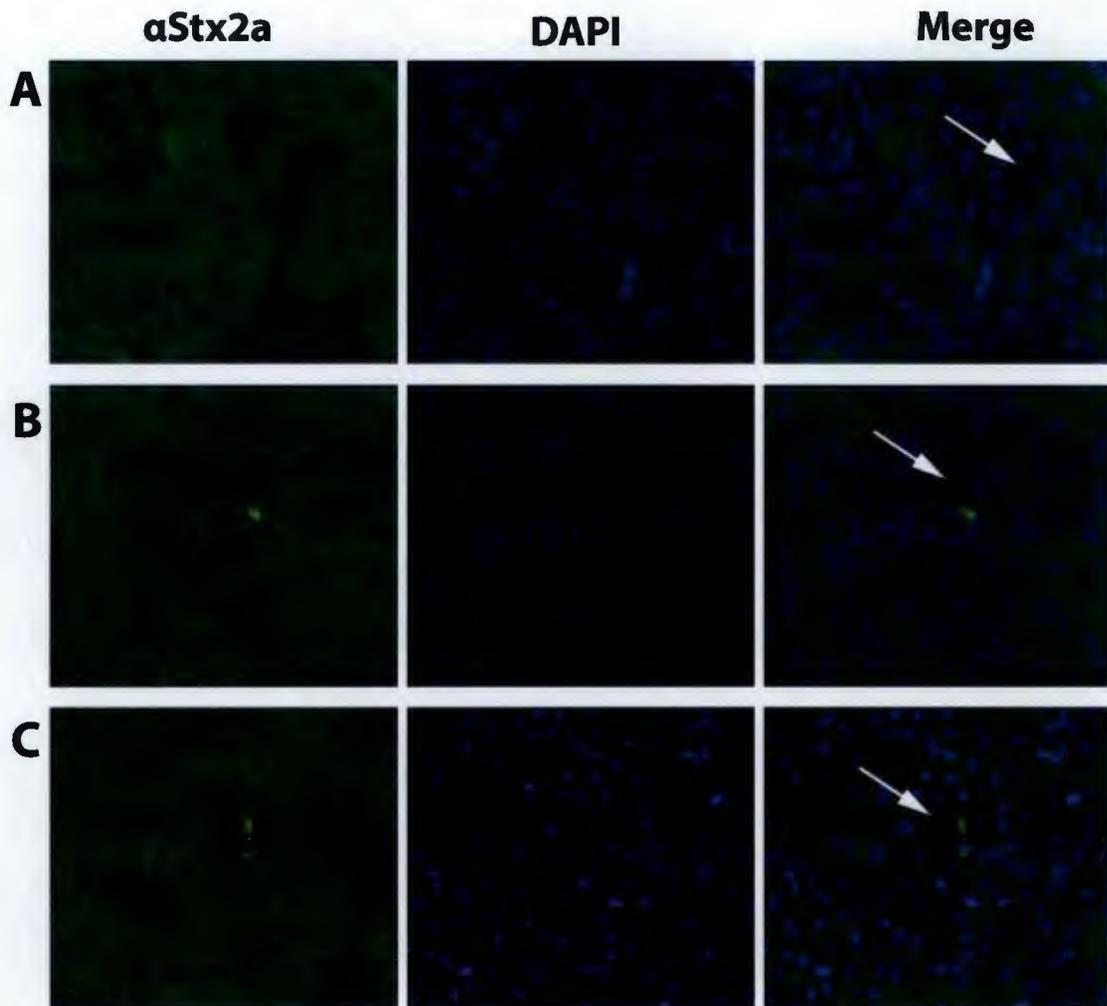
Figure 7. Staining to detect Stx2a in kidney sections from PBS-treated or intoxicated mice.
Immunofluorescence of kidney sections treated with rabbit polyclonal αStx2a combined with goat αrabbit conjugated to Alexa488. DAPI stained the cell nuclei. I.g. PBS control sections (A) were negative for Stx2a. Stx2a-positive cells adjacent to tubule lumens (bright green fluorescence) were detected in kidney sections from mice i.p. intoxicated with 13.2 ng (B) and i.g. intoxicated with 17 μg of Stx2a (C). (↑) lumen of tubule. Magnification: 400X.

Anti-Stx2a MAb fully protects mice when given before intoxication.

We next tested whether i.g.-intoxicated mice could be protected from morbidity and/or mortality with a MAb to Stx2a. In a pilot study, mice received 2 μg of 11E10 (anti-Stx2a) or TFTB1 (isotype-matched control) i.v. 24 h prior to i.g. intoxication with 7.5 μg Stx2a. A positive control group received only Stx2a i.g. (In this study and all subsequent experiments, MAbs and Stx2a were diluted in PBS.) In this preliminary study, complete mortality was observed in the Stx2a only and Stx2a plus TFTB1 groups while MAb 11E10 prevented mortality though not morbidity (Figure 8A, Row 1; Figure 8B). Protected mice experienced weight loss that peaked on day seven post-intoxication of 1.9 g or 11% compared to their starting weight before they recovered and exhibited positive weight gain by day 14 (data not shown). For our next study, in the hopes of limiting morbidity in the toxin-treated mice, we altered the time of administration of the 11E10 from -24 h to -1 h so that higher levels of MAb would be present during the intoxication window. We found that although the mice were protected from lethality as expected, they still experienced weight loss before recovery (Figure 8A, Row2; Figure 8B). Therefore, in an attempt to reduce morbidity in the subsequent protection experiment, the amount of MAb administered was doubled. Mice that received 4 μg 11E10 were completely protected (Figure 8A, Row 3), and in addition, their weight loss was reduced, although not to a statistically significant level (p= 0.055) (Figure 8B). In a final attempt to further reduce or prevent Stx2a-mediated morbidity, 10-fold more 11E10 was administered in the next study. Although the 11E10 again protected (Figure 8A, Row 4), the level of weight loss in the intoxicated,

A

Protection by 11E10 in mice given 7.5 µg Stx2a ig

Ab dose, µg	Time of Ab Rx, h	Dead/Total (MTD) Treatment		
		11E10	TFTB1	No Ab
2	-24	1/7 (6)	8/8 (4.6)	5/5 (4.8)
2	-1	0/5	ND	8/8 (4.4)
4	-1	0/13	10/10 (5)	10/10 (5)
40	-1	0/9	8/8 (4.7)	8/8 (5)

B
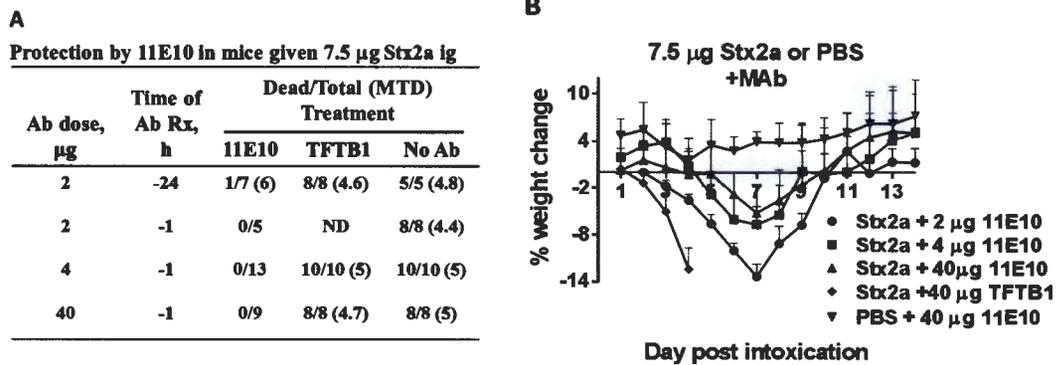
Figure 8. MAb 11E10 prevented mortality and limited morbidity due to Stx2a i.g. intoxication.

(A) Mortality results from four independent Ab studies. Two, four, or 40 µg 11E10 protected mice from Stx2a i.g. intoxication while TFTB1, the irrelevant MAb, had no therapeutic effect. ND, not done. (B) Percent weight change from day 0 to day 14 of antibody treated, Stx2a-intoxicated or PBS control groups. Each group received Ab one h prior to intoxication. The PBS control group experienced positive weight gain over the course of the experiment, with no effect from of 40 µg 11E10. Error bars indicate standard deviation. There was a significant interaction effect ($p = 0.0002$) which indicates that the percent weight change varies over time between Ab treatment groups. The difference in percent weight change was significant between the groups given 2 or 4 µg 11E10 on days 3, 7, and 9 and between the 2 µg and 40 µg groups on days 5-8. There was no difference between the 4 and 40 µg groups.

treated animals was similar to that from the previous protection experiment in which mice received 4 μg MAb, i.e., there was no statistical difference in weight loss in mice treated with 4 or 40 μg MAb (p < 0.064) (Figure 8B).

We next compared mouse weight change after administration of 4μg MAb in the i.p. and i.g. intoxication models to evaluate if MAb protection from morbidity might be greater in the i.p. than the i.g. model. As was done previously, an Stx2a-only group served as a positive control for mortality, and MAb TFTB1 was included as an isotype-matched control for 11E10. One h after injection of treatment groups with 4 μg MAb, mice received 2.5X the i.p. or i.g. LD_{50}, 5.7 ng or 7.5 μg respectively. All mice in the Stx2a-only positive control groups succumbed to intoxication, but the MTD was longer in i.g.-intoxicated animals (5 days) compared to that of mice given toxin i.p. (3.4 days). As expected, TFTB1 did not alter morbidity or survival in either the i.p. or i.g. intoxicated groups (data not shown). In contrast, all mice given11E10 survived and had positive weight gain by day14 post-intoxication. However, weight loss began earlier in the 11E10-treated animals intoxicated i.p., and those mice lost significantly more weight prior to recovery than MAb-treated mice given toxin i.g. (p<0.05) (Figure 9).

Level of renal serum markers and degree of histopathology in kidneys of Stx2a-intoxicated and Mab-protected mice are related.

We analyzed sera from i.g.-intoxicated mice treated with nothing or MAbs TFTB1 or 11E10 (MAbs given one h prior to intoxication) to determine if there were alterations in the values for the renal damage markers BUN and creatinine. Compared to animals given 11E10 then i.g. Stx2a, mice intoxicated with Stx2a only or
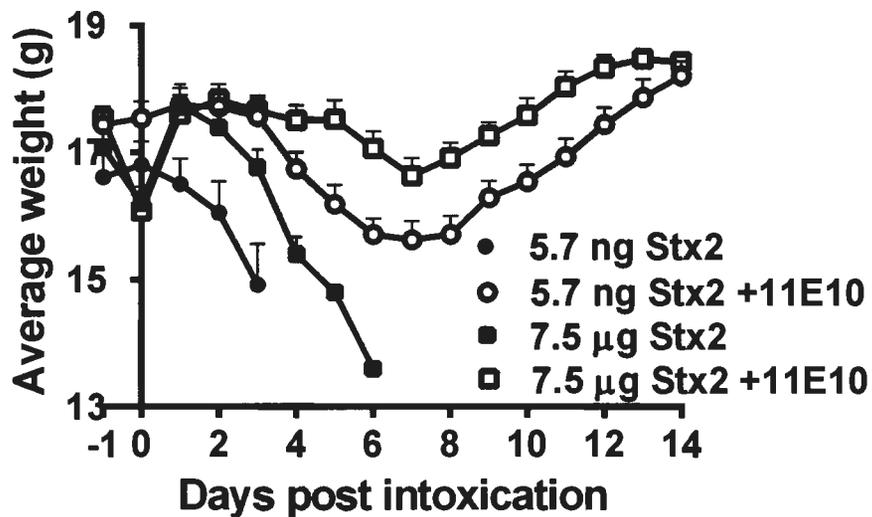
Figure 9. Average weight over time in Stx2a-intoxicated mice given 11E10 or no treatment one hour before toxin administration.
Mice were intoxicated with 2.5X the Stx2a i.p. (circles) or i.g. (squares) LD_{50} and received 11E10 (open symbols) or no treatmens (closed symbols). Although MAb 11E10 was protective in both intoxication models, i.p.-intoxicated mice exhibited significantly more morbidity than i.g.-intoxicated mice (p <0.05). Additionally there was a significant difference in weight between the Stx2a i.p. and i.g. 11E10 protected groups on days 5, 6, 8, and 11.

administered TFTB1 and then intoxicated with Stx2a exhibited a significant increase in

BUN and creatinine levels ($p < 0.0001$) (Table 3, Rows 6-8). However, the renal

biochemistries from mice protected with 11E10 were indistinguishable to those of the

PBS controls from previous experiments ($p > 0.05$) (Table 3, Row 1).

Finally, the effect of MAb treatment on kidney histopathology was evaluated.

Moderate ATN was detected as expected in kidneys from the Stx2a-only control group

(similar to the pathology previously described in Figure 6D) and from mice treated with

TFTB1 (Figure 10A). The pathologist did not note any difference in kidney lesions

between Stx2a only and TFTB1-treated, Stx2a-intoxicated mice. ATN was also

observed in mice given 11E10 and then i.g. Stx2a, although the lesions were minimal

rather than moderate, and there was increased evidence of regeneration of distal tubules

(Figure 10B).

MAb can rescue Stx2a-intoxicated mice.

We tested the capacity of 11E10 to rescue mice after oral intoxication with

Stx2a. MAbs 11E10 or TFTB1 were administered i.v. at 6, 24, 48, or 72 h post i.g.

intoxication with approximately 2.5X LD_{50} (7.5 µg) Stx2a. None of the mice treated

with TFTB1 or in the Stx2a-only group survived toxin challenge. Additionally, all

TFTB1-treated and Stx2a-only groups had a similar MTD, a finding that indicates that

the addition of fluids alone had no therapeutic effect (since the TFTB1 was given in

PBS) (data not shown). Mice that received 11E10 one h prior (a control) or six h after

intoxication were completely protected from Stx2a. In contrast, only one mouse was

rescued when 11E10 was given at 24 h post intoxication, and no mice were rescued if

the MAb was administered at 48 or 72 h after toxin (Table 4). Both the -1 h and +6 h treatment groups also exhibited similar patterns of weight loss throughout the experiment and both groups displayed positive weight gain by day 14 (data not shown).
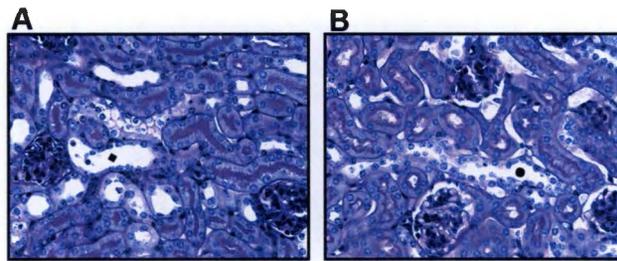
Figure 10. PAS-stained kidney sections from MAb protection/Stx2a i.g. intoxication study.
(A) Moderate ATN (♦) of distal tubules was observed in kidneys of mice in Stx2a +TFTB1 groups. (B) Minimal ATN (●) and increased regeneration of distal tubules were seen in Stx2a + 11E10-treated mice.

Table 4. Rescue by 11E10 of Stx2a i.g.-intoxicated mice

11E10 treatment relative to i.g. Stx2a, h	Dead/total	MTD (days)
-1	0/8	
+6	0/10	
+24	9/10	4.4
+48	10/10	4.4
+72	8/8	4.3
Stx2a only	8/8	4.4

DISCUSSION

That Stx [specific toxin type(s) unknown] alone can recapitulate some of the symptoms of STEC disease was first reported by Pai *et al.* (214). These investigators found that infant New Zealand white rabbits orally intoxicated with Stx develop diarrhea and succumb to intoxication in an analogous manner to rabbits challenged with *E. coli* O157:H7 (214). Similarly, Ritchie *et al.* showed that rabbits orally intoxicated with Stx2a develop inflammation comparable to rabbits infected with an Stx2a-producing STEC strain (234). Additionally, Rasooly *et al.* recently reported that oral intoxication of mice with high doses of Stx2a was lethal (229). We extended such observations with the determination that the LD_{50} for Stx2a in BALB/c mice by the oral route is 2.9 µg and that both i.p. and i.g. Stx2a intoxication routes lead to similar systemic pathologies in those animals. Additionally, our data illustrated that similar renal damage occurred even in mice intoxicated with a sub-LD_{50} Stx2a dose and that survival in those animals correlated with a return to normal serum chemistry values and tubule regeneration. Finally, we demonstrated protection and rescue of mice from Stx2a oral intoxication through passive transfer of MAb 11E10.

In contrast to the oral lethality of Stx2a, we found that Stx1a was not lethal by the intragastric route. We speculate that if, similar to Stx2a, the i.g. LD_{50} for Stx1a is 1,000X greater than the i.p. LD_{50} (as it was for Stx2a), more than 500 µg Stx1a per mouse would be necessary to observe lethality. However, it is not practical to purify such large quantities of toxin to test the hypothesis that Stx1a is potentially lethal by the oral route. Our finding that Stx1a is not lethal by the oral route as far as we can test may not be surprising since STEC strains that only produce Stx1a are not lethal in mouse models of oral infection (302).

70

We did not observe lesions in any section of the intestinal tract from Stx2a i.g.-intoxicated mice, a finding that suggests the toxin reached systemic circulation without injury to the intestinal epithelial cell lining. We also examined the liver for damage because we thought that organ had the potential to absorb a large concentration of Stx2a as the toxin traveled through the hepatic portal system. However, we did not observe lesions in the livers of orally intoxicated mice nor did we detect alterations in the hepatic serum biochemistry values (data not shown). Therefore, we concluded that the liver is not a target site for Stx2a in mice, a contention supported by the observation that Gb3 concentrations are low in that organ (85).

We found that once sufficient Stx2a entered systemic circulation, independent of the route of intoxication (i.p. or i.g.), similar elevations in renal serum biochemistry values occurred. The elevated BUN and creatinine values suggest acute renal failure which is characterized by reduced glomerular filtration rate (GFR). Although the pathophysiologic mechanism of GFR is not fully understood, it likely involves reduction in blood flow to or within the kidney. The apparently reduced GFR is not related to problems with the glomerulus in these mice. In addition, the significant reduction in sodium and chloride levels due to Stx2a exposure indicate renal tubular malfunction (163; 280). We do not believe the changes in serum biochemistry values after Stx2a-intoxication are a result of hemoconcentration due to dehydration because the experimental serum albumin levels were equivalent to albumin levels from control mice.

Our immunofluorescence data suggest that once Stx2a reached the kidney, it targeted tubular epithelial cells because the toxin staining was in the cells adjacent to

71

the renal tubule lumen. The toxin molecule likely killed those cells, events that would lead to ATN. ATN causes loss of renal function, which, in turn, can result in mortality. ATN is the same pathology that occurs in STEC mouse infection models. Overall these results demonstrate that oral intoxication with Stx2a alone recapitulates disease noted after infection of mice with STEC in various models (185).

The specificity of the PAS stain revealed approximately equivalent proportions of distal and proximal tubules in both control and experimental mice (data not shown). The PAS stain further indicated that the Stx2a-mediated lesions were in distal rather than proximal tubules [as we had previously believed (287)], because of the absence of a brush border in the affected tubules. The hypothesis that distal rather than proximal tubules are more affected by Stx2a is supported by a study that showed that distal tubules have higher concentration of Gb3 receptors on the cell surface than do proximal tubules (130).

We were surprised to find that the renal pathology and serum biochemistry values due to a sub-LD_{50} oral Stx2a dose were similar to those found after i.g. delivery of 6X LD_{50} of toxin if the mice were necropsied when weight loss reached its nadir. In contrast, once the sub-LD_{50}-intoxicated animals began to gain weight, they had serum biochemistry values similar to control mice and exhibited less severe kidney histopathology. We believe that although the types of histopathology observed in the sub-LD_{50} and 6X LD_{50} Stx2a groups were similar when assessed at the point of lowest weight for the sub-LD_{50} group, the magnitude of damage was greater in the higher-dose group. We further speculate that those mice that received a sub-LD_{50} dose survived if they were able to regenerate tubular epithelial cells (observed in Fig. 6F) and restore a

minimum threshold of kidney function. This study also demonstrated the importance of timing when collecting samples after intoxication; we note that damage can occur yet go undetected because of subsequent repair if samples are taken too long after toxin insult.

We protected all mice from 2.5X LD_{50}s of Stx2a with a single passive transfer of 4 µg 11E10. Although there was a reduction in weight loss at the 4 µg compared to the 2 µg11E10 dose, a 10-fold increase to 40 µg of the MAb did not result in a further decrease in morbidity. Thus, there appears to be a threshold for levels of antibody that can decrease morbidity in intoxicated animals. We also found that mice treated with 11E10 then given Stx2a had normal kidney function 4 d post-intoxication as indicated by serum BUN and creatinine levels. Although minimal renal ATN was observed in the MAb-treated Stx2a-intoxicated mice, there were increased instances of tubule regeneration compared to animals that received Stx2a only. Our study suggests that 11E10 pre-treatment reduced kidney damage in Stx2a-intoxicated mice. Finally, since we observed no protective effect by irrelevant MAb TFTB1, an IgG2a isotype control, we conclude that fluid alone was not protective.

We also observed that in mice treated with 11E10, greater morbidity occurred after i.p. than i.g. Stx2a intoxication. I.p.-intoxicated animals exhibited a shorter time-to-death of approximately one and a half days compared to mice given toxin i.g. The reduced MTD in i.p.-intoxicated mice suggests that Stx2a reached the target site of the kidneys earlier when delivered to the peritoneum as compared to from the gastrointestinal tract. Although ATN was probably present at increased levels in i.p.- as

compared to i.g.-intoxicated mice, kidney function was not lost and the mice were able to recover.

We demonstrated rescue of mice with 4 μg of 11E10 at six but not 24 h post oral intoxication with Stx2a. A recent study in which mice were orally intoxicated with Botulinum neurotoxin serotype A (BotA) then treated by passive Ab transfer demonstrated that differences of just one to two h in antibody administration time points resulted in the loss of the capacity to rescue intoxicated animals (51). We speculate, therefore, that similar to BotA, once Stx2a is sequestered in target tissues (the kidneys), passive Ab transfer is not able to rescue intoxicated animals. However, the rescue timeframe could probably be increased if a larger MAb dose was provided, or if additional doses were delivered. In support of the latter hypothesis, another group was able to rescue baboons 24 h after intravenous intoxication with Stx2a by providing the therapeutic TVP, an acetylated tetravalent peptide, daily until day four (271). We believe that passive Ab transfer is a viable therapeutic option for STEC infections. Furthermore, for someone infected with STEC, the rescue timeframe would likely be extended as compared to the oral intoxication model as Stx would be delivered at a continual low dose rather than in a single large bolus. Previous research in our lab demonstrated that low levels of active Stx2a could be found in the feces of mice with an intact commensal flora up to 72 h post-infection with an Stx2a-producing O157:H7 strain (184).

Finally, we found that an oral Stx2a dose of 2 μg (~0.1 mg/kg) was sufficient to cause weight loss and renal injury but not death in mice. If mice and humans are equivalently susceptible to Stx, then we calculate that 1.8 mg Stx2a would be sufficient

to cause some disease in an 18 kg child. However, we believe humans are more susceptible to Stx than are mice because, unlike mice, people have Gb3 in the glomeruli in addition to the tubules (36; 232; 287). Therefore, we believe that the oral toxicity of Stx2a is potentially relevant as a public health issue. There is a possibility that preformed Stx could occur in contaminated food which might contribute to morbidity (103; 229; 309) and possibly enhance colonization by the organism as Stx2 has been shown to increase adherence of O157:H7 to tissue culture cells and in animal models (183; 236).

Figure S1. Intestinal tract histology (H&E).
No pathology was observed in any section of the small intestine (A), cecum (B), or large intestine (C) from PBS- or Stx2a-i.g. intoxicated mice. 400X magnification. Inlays show nearby tissue at 100X magnification. Cecum inlay (B) contains a Peyer's patch that is not present in the high magnification field.

CHAPTER 3

Comparisons of Native Shiga Toxins (Stxs) Type 1 and 2 with Chimeric Toxins Indicate that the Source of the Binding Subunit Dictates Degree of Toxicity

RUSSO LM, MELTON-CELSA AR, SMITH MJ, and O'BRIEN AD

Department of Microbiology and Immunology, Uniformed Services University of the Health Sciences, Bethesda, MD, USA.

L.M. Russo is solely responsible for the work presented in this chapter with the following exceptions: A.R. Melton-Celsa, M.J. Smith, and A.D. O'Brien assisted with experimental design and analysis and M.J. Smith created the chimeric Stx operons.

Note: The figure, table, and reference numbers have been adjusted to follow the format of this dissertation.

ABSTRACT

Shiga toxin (Stx)-producing *E. coli* (STEC) cause food-borne outbreaks of hemorrhagic colitis. The main virulence factor expressed by STEC, Stx, is an AB_5 toxin that has two antigenically distinct forms, Stx1a and Stx2a. Although Stx1a and Stx2a bind to the same receptor, globotriaosylceramide (Gb3), Stx2a is more potent than Stx1a in mice, whereas Stx1a is more cytotoxic than Stx2a in cell culture. In this study, we used chimeric toxins to ask what the relative contribution of individual Stx subunits is to the differential toxicity of Stx1a and Stx2a *in vitro* and *in vivo*. Chimeric stx_1/stx_2 operons were generated by PCR such that the coding regions for the A_2 and B subunits of one toxin were combined with the coding region for the A_1 subunit of the heterologous toxin. The toxicities of purified Stx1a, Stx2a, and the chimeric Stxs were determined on Vero and HCT-8 cell lines, while polarized HCT-8 cell monolayers grown on permeable supports were used to follow toxin translocation. In all *in vitro* assays, the activity of the chimeric toxin correlated with that of the parental toxin from which the B subunit originated. The origin of the native B subunit also dictated the 50% lethal dose of toxin after intraperitoneal intoxication of mice; however, the chimeric Stxs exhibited reduced oral toxicity and pH stability compared to Stx1a and Stx2a. Taken together, these data support the hypothesis that the differential toxicity of the chimeric toxins for cells and mice is determined by the origin of the B subunit.

78

INTRODUCTION

Shiga toxin (Stx)-producing *E. coli* (STEC) are Gram-negative, enteric pathogens with an estimated infectious dose of less than 50 organisms (291). Among the multiple serotypes associated with disease, O157:H7 is responsible for more than 63,000 of the 175,000 total estimated STEC cases each year (247). Ruminants, especially cattle, are the natural carriers of STEC, and these bacteria most commonly enter the food chain during beef processing (2; 12; 95; 228). Outbreaks and sporadic cases of STEC infection have also been attributed to contaminated fresh produce, person-to-person spread, and environmental sources (3; 228). Upon *E. coli* O157:H7 STEC infection of humans, the most common disease manifestation is hemorrhagic colitis. A more severe sequela, the hemolytic uremic syndrome (HUS), characterized by microangiopathic hemolytic anemia, thrombocytopenia and acute kidney failure, occurs in 5-15% of *E. coli* O157:H7-infected individuals (35; 127; 128; 171).

Stx is the primary virulence factor associated with disease caused by STEC. This group of organisms may encode for Stx1a and/or Stx2a, two biologically similar, though antigenically distinct toxins with analogous crystal structures and identical modes of action [reviewed in (175)]. The Stxs are AB_5 toxins; the A subunit, which has a protease sensitive site near the C-terminus, is cleaved into two parts. The A_1 subunit is responsible for the catalytic activity of the toxin molecule, and the A_2 peptide, which threads through the center of the B pentamer, links the binding moiety to the catalytic subunit (80; 81). The homopentameric B subunit binds to the host cell receptor, globotriaosylceramide (Gb3) (160), a glycolipid that that is primarily expressed on endothelial cells. After Stx binds Gb3, the toxin undergoes retrograde transport through the Golgi network to the endoplasmic reticulum (244). The A_1 subunit is released into

the cytoplasm from the endoplasmic reticulum and depurinates a single adenine residue from the 28S RNA of the 60S ribosome, an injury that halts protein synthesis and leads to cell death (209; 246).

Although Stx1a and Stx2a are biologically similar, Stx2a is associated with an increased number of outbreaks and more severe disease (32; 116; 140; 197; 212; 213). These latter observations correlate with reports that Stx2a has a parenteral 50% lethal dose (LD_{50}) for mice that is 100-fold lower than that of Stx1a (104; 287). Conversely, Stx1a has a 50% cytotoxic dose (CD_{50}) for Vero cells that is 10X lower than that of Stx2a (287). Multiple methods and approaches have been used to study the paradox of the differential *in vitro* (on Vero cells) and *in vivo* (in mice) toxicities of Stx1a and Stx2a. There is no difference in the enzymatic activity between Stx1a and Stx2a in a cell-free rabbit reticulocyte lysate assay of protein synthesis inhibition (105; 287); therefore, the A subunit is not responsible for the differential toxicity of Stx1a and Stx2a, at least at the level of the ribosome. Multiple studies propose that the biological differences between Stx1a and Stx2a are specific to the B-subunit. For example, Stx1a binds Gb3 *in vitro* with a greater affinity than does Stx2a (104; 158; 287; 324), a finding that may explain the greater toxicity of Stx1a on Vero cells. In contrast, *in vivo*, a higher binding affinity for the receptor may reduce overall toxicity if secondary targets (non-lethal) are bound. Indeed, after intravenous (iv) injection into mice, radiolabelled Stx1a demonstrates increased binding to murine pulmonary and splenic tissues but decreased kidney binding (kidney damage is responsible for the lethality of the Stxs to mice), and a shorter serum half-life, compared to Stx2a (241).

Chimeric Stxs have been used to study the contribution of the individual A and B subunits to toxin function. Ito *et al.* purified individual toxin subunits and then recombined them to form recombinant Stx2a, and chimeras Stx1aA/Stx2aB2 and Stx2aA/Stx1aB (117). Although that group observed equivalent cytotoxicity for the recombinant Stx2a as compared to native Stx2a and found no difference in the cytotoxicities of Stx1aA/Stx2aB2 and Stx2aA/Stx1aB, they did not report Stx1a activity. Because of the lack of data for Stx1a and the relative equivalent toxicity of Stx1aA/Stx2aB2 and Stx2aA/Stx1aB, no conclusion about the relative contribution of the A or B subunits to toxicity of the prototype toxins could be made (117). Another study took a similar recombinant approach to produce and then assess chimeric Stx function, and showed that the cytotoxicity of the chimerics correlated with the source of the B subunit; however, the activity of all toxins tested was below what would be expected, a result that may indicate the recombined toxins did not fold properly (105). Weinstein *et al.* tried two genetic approaches (operon fusions and co-transformation of two compatible plasmids that each encoded an individual toxin subunit into a K-12 strain) to produce hybrid Stx1a/Stx2a molecules but neither method produced a functional Stx1aA/Stx2aB2 chimeric (310). Furthermore, the Stx2aA/Stx1aB chimeric had a cytotoxic profile that was closer to that of Stx2a than Stx1a, but the caveat to that result is that the level of toxin in the preparations was not quantitated (310). Another group that used an operon fusion to produce an Stx2aA/Stx1aB chimera reported that that hybrid toxin had cytotoxicity, Gb3 binding, and LD_{50} values that were intermediate between the Stx1a and Stx2a values (259). Taken together these studies do not provide

a definitive answer to the question of which toxin subunit is responsible for the differential toxicity of Stx1a and Stx2a for Vero cells and mice.

We believe that previous analyses of hybrid Stxs may have been limited by decreased stability of the chimeric toxins. Because the A_2 peptide is critical for native holotoxin stability (14), our approach was to create chimeric Stxs in which the A_2 peptide comes from the same origin as the B subunit. We then assessed those toxins for purity, cytotoxicity, and lethality in mice by the intraperitoneal (ip) and oral routes. We found that the toxicity of the chimeric toxins for Vero and HCT-8 cells, and by ip delivery into mice, correlated with the origin of the B subunit. However, the chimeric Stxs exhibited reduced activity after oral intoxication.

Ethics Statement.

All animal studies were approved by the Institutional Animal Care and Use

Committee of the Uniformed Services University of the Health Sciences. These studies

were conducted in strict accordance with the recommendations of the Guide for the

Care and Use of Laboratory Animals (296). Animals were housed in an

environmentally controlled room approved by the American Association for

Accreditation of Laboratory Animal Care (AAALAC).

Bacterial strains and growth conditions.

E. coli K12 DH5α strains were transformed to encode the native Stxs (Stx1a,

pLPSH3 (288); Stx2a, pJES120 (153)) or the chimeric Stxs, as described below. All

bacterial strains were grown in Luria Bertani (LB) broth or LB agar supplemented with

100 µg/mL ampicillin for maintenance of all recombinant plasmids.

Construction of chimeric toxin operons.

Chimeric stx_1A_1: stx_2A_2 stx_2B and stx_2A_1: stx_1A_2 stx_1B operons were created by

splicing by overlap extension (SOE) PCR as previously described (268). Specifically,

the Stx1a clone, pMJS1, was used to amplify the PCR products stx_1A_1 and stx_1A_2 stx_1B

using primers MJS1 (268) and $2A_2/1A_1$

(5'CTCTCTTCATTCACGGCGCGAACAGATCGCGATGCATGATGATGACAATT

CAG-3') and primers $1A_2$ (5'GTTGCCAGAATGGCATCTGATGAG-3') and MJS2,

respectively (268). The Stx2a clone, pMJS2, was used to amplify the PCR products

stx_2A_1 and stx_2A_2 stx_2B with primers MJS5 (268) and $1A_2/2A_1$

(5'CTCATCAGATGCCATTCTGGCAACACGCGCCCCCTGATGATGGCAATTCA

G-3') primers MJS6 (268) and 2A$_2$ (5'TCTGTTCGCGCCGTGAATGAAGAGAG-3'), respectively. The *stx$_1$A$_1$* and *stx$_2$A$_2$stx$_2$B* amplification products were spliced together by PCR to create the 122 operon (with the junction from Stx1a to Stx2a after first R of RSVR in Stx1a). The *stx$_2$A$_1$* and *stx$_1$A$_2$ stx$_1$B* amplification products were spliced together by PCR to create the 211 operon (with the junction from Stx2a to Stx1a after first R of RVAR in Stx2a). The PCR products were ligated into pBluescript II KS(-) (Stratagene, La Jolla, CA), transformed into *E. coli* DH5α, and named pMJS122 and pMJS211, respectively.

Purification of Stx1a, Stx2a, and chimeric toxins.

All four toxins (Stx1a, Stx2a, 211 and 122) were purified by affinity chromatography with five mL AminoLink Coupling Resin (Thermo Scientific) columns, as described previously (240). Briefly, monoclonal antibody to either the Stx1a or Stx2a B subunit was covalently bound to the column resin in pH 7.2 coupling buffer according to manufacturer's instructions. Monoclonal 13C4 (274), purified from hybridoma supernatant, was used for purification of Stx1a and chimeric 211 (approximately 7 mg 13C4/column) while monoclonal BC5 BB12 (64), from *ascites* fluid, a gift from Dr. Nancy Strockbine, was used for Stx2a and chimeric 122 purification (approximately 13 mg/column). An independent column was used for the purification of each toxin.

Toxin purification:

The *E. coli* K12 strain that contained the plasmid that encoded for the *stx* of interest was grown overnight, sedimented by centrifugation (5,000 x g), resuspended 40X in sonication buffer (50mM NaPO$_4$, 200mM NaCl), and disrupted by sonication. The cell

84

lysate was sedimented by centrifugation (20,000 x g) and placed over the appropriate affinity column. After purification, Stx was dialyzed against PBS in Slide-A-Lyzer dialysis cassettes (Thermo Scientific) and concentrated (Millipore Amicon Ultra 30K) according to manufacturer's instruction, if necessary. The protein concentrations of the Stx preparations were determined with a bicinchoninic acid (BCA) assay (Thermo Scientific).

Specific toxin concentration determination.

Differences in the purity of toxin preparations were normalized as described previously (240). Briefly, purified toxins were separated on a sodium dodecyl sulfate-polyacrylamide gel (SDS-Page), and the gel was stained with Oriole fluorescent stain (BioRad). The stained gel was scanned with ImageQuant LAS 4000 (GE Healthcare) and analyzed with ImageQuant TL software (GE Healthcare). Densitometry analysis of the Oriole-stained gel was used to determine the percent of the total protein bands that comprised the A and B subunit bands. Then the percentage of the preparation that could be attributed to toxin was multiplied by the total protein in each sample (as determined by BCA assay). Densitometry analysis of the A and B subunit bands also confirmed the expected 1:5 subunit ratio, respectively, in each preparation.

Cell culture.

Vero cells (CCL-81, American Type Culture Collection [ATCC], Manassas, VA) were maintained in Eagle's minimal essential medium (EMEM) (Lonza, Inc., Walkersville, MD) while HCT-8 cells (CCL-244, ATCC), a human epithelial colorectal adenocarcinoma cell line, were maintained in RPMI-1640 medium (ATCC). All media were supplemented with 10% FBS, 10 U/mL penicillin, and 10 μg/mL streptomycin.

Cytotoxicity assay.

The Vero cytotoxicity assay has been described previously (91; 251). Briefly, Vero cells were seeded in 96-well plates at a concentration of 10,000 cells per well and incubated at 37°C, 5% CO_2 for 24 hours. Serial dilutions of toxin samples in fresh media (EMEM plus supplements as described above) were overlaid onto the cells, and the plates were incubated for an additional 48 h. The cells were then fixed with formalin and stained with crystal violet. The absorbance of the wells at 630 nm was measured spectrophotometrically. Cytotoxicity assays were done on HCT-8 cells in the same manner as for Vero cells, except that the cells were incubated for 48 hours prior to the application of toxin. For each toxin sample, CD_{50} was determined by the reciprocal of the toxin dilution that caused death of 50% of the cells in the monolayer compared to control cells. Specific toxin activity was calculated as the CD_{50}/mL divided by the toxin concentration in mg/mL.

Toxin-Gb3 binding enzyme-linked immunosorbent assay (ELISA).

An ELISA to quantitate Gb3-toxin binding was conducted as previously described (324). Briefly, wells of an Immobilon 2HB 96-well plate (Thermo Electron Corp) were coated with decreasing concentrations of purified Gb3 glycosphingolipids (Matreya) suspended in 100% ethanol and dried overnight. The wells were then overlaid with 20 ng of toxin. Polyclonal rabbit anti-Stx1a and -anti-Stx2a antibodies (each at 1:5000) were used in combination as the primary antibody for the detection of all four toxins, while goat anti-rabbit-HRP antibody (1:2,000) was used as the secondary. Statistical significances of the differences in how well toxins bound to Gb3

were determined via Two-Way ANOVA with Tukey's adjustment for multiple comparisons.

Transwell assay.

We followed the protocol published by Hurley *et al.* to establish polarized HCT-8 cells (110). Transwell permeable supports (Corning) with polycarbonate membrane transwell inserts were seeded with $2\text{-}5 \times 10^5$ HCT-8 cells. Media was changed every two days until the cells were polarized (8-10 days) as determined by Millicell-ERS resistance reader (Millipore Corporation, Bedford, Mass.) and a transepithelial electrical resistance (TEER) above 2,000 Ω/cm^2. Once the cells were polarized, 20 ng of toxin was added to the upper chamber. All cells remained polarized through 24 hours post-intoxication as the TEER did not drop below 2,000 Ω/cm^2. The amount of toxin translocated from the apical to the basolateral side of the cells was determined as follows. A 40 µL sample of media from the lower chamber was removed and the toxicity in that sample measured on Vero cells. The Vero cell toxicity of the basolateral sample was compared to a standard toxicity curve of known toxin concentrations, and then the value was corrected for the total volume in the lower chamber. The statistical significance of the amount of translocated Stx was determined via the Students t-Test.

Mice.

All experiments were conducted with 5-6 week old, female BALB/c mice from Charles River Laboratories (Wilmington, MA). Mice were housed in filter-top cages with access to food and water ad libitum, unless otherwise stated.

Lethal dose 50% (LD$_{50}$) studies.

Mice were injected by the ip route with 0.1 mL of toxin/PBS at varying dilutions for ip LD$_{50}$ studies. The ip LD$_{50}$ values were confirmed for the native toxins with a total of 25 or 41 mice for Stx1a and Stx2a, respectively (4-5 mice per dose). A total of 45 mice were used for the chimeric 122 studies, with 3-5 mice per dose. A total of 48 mice were used for the chimeric 211 ip LD$_{50}$ studies, with 5-6 mice per dose. Mice were gavaged with 0.2 or 0.3 mL of toxin/PBS dilutions for the ig LD$_{50}$ studies. Food and water were removed for 18 and 2 hours, respectively, prior to oral intoxication. A total of 20 mice were used for the chimeric 122 studies, while five mice were used for the chimeric 211 study. We used the minimum number of animals required to attain statistical significance. No analgesics were administered since non-steroidal anti-inflammatory drugs (NSAIDs) could confound or mask the effect of Stx, and alter the LD$_{50}$ values. All mice were weighed daily and monitored at least twice per day for morbidity and mortality for two weeks. The animals were checked every 6 h during the time period when mortality was expected. Mortality was an endpoint for the LD$_{50}$ studies, however mice that exhibited signs of extreme morbidity were humanely euthanized by an overdose of inhalational isoflurane followed by cervical dislocation or CO$_2$ overdose, in accordance with the AVMA Guidelines on Euthanasia. Extreme morbidity was defined as two or more of the following symptoms: $\geq 25\%$ weight loss, ruffled fur, lethargy, labored breathing, hunched posture, inability to remain upright, or impaired ambulation that prevents the animal from reaching food and water. LD$_{50}$ and 95% confidence interval (CI) values were determined by Probit regression analysis with log transformation of the values. The relative median potency, defined as the ratio of two LD$_{50}$s, along with the CI for the ratio, was calculated to determine statistical

significance among the Stxs. If the calculated CI did not include 1.0, then the two LD_{50}s were significantly different with $P < 0.05$.

Active toxin in feces of ig-intoxicated mice.

Fecal samples were collected 3, 9, 12, 24, and 48 hours after ig intoxication (same mice from the ig LD_{50} studies). At each time point, mice were transferred to an individual cage with no bedding for 30-40 minutes. Fecal pellets were collected, weighed, and EMEM 1:10 w/v was added. The fecal samples were frozen at -20°C until all time points were completed so that they could be analyzed simultaneously. The samples were thawed, mixed by vortex and then filter-sterilized (0.45 micron). The sterile fecal supernatant was applied to Vero cells as described for the cytotoxicity assay above, and the total level of toxicity present in each sample was determined. The basal level of fecal cytotoxicity was determined from stools of unintoxicated control mice, and that value was subtracted from all experimental sample values. The geometric mean for each group was then calculated. The amount of toxin present was then calculated by dividing the geometric mean CD_{50} by the specific activity of that toxin (CD_{50}/ug). The Students t-Test was performed on log_{10} transformed cytotoxicity CD_{50} values.

pH stability of Stxs.

The effect of pH and temperature on toxin stability was measured as previously published (287). The pH buffers used were: pH 7, 100 mM Tris; pH 5, 100 mM sodium acetate; and pH 3, 100 mM glycine. Briefly, toxin was diluted to 10^7 CD_{50} in 0.2 mL of PBS. Twenty microliters of each toxin was then added to 180 µL of the pH buffers or PBS as a control. Samples were incubated at either 37°C or 60°C for one hour, then

immediately placed on ice and neutralized 1:10 v/v with 1 M Tris, pH 7.5. Toxin activity was then determined by the Vero cell cytotoxicity assay described above. To determine the fold change in Stx activity, the log transformed CD_{50} values from experimental samples were divided by the log transformed CD_{50} value of the PBS control. The mean value from four biological replicates is reported. Statistical significance of fold-change differences was determined with a 1-way ANOVA with Tukey's correction for multiple comparisons.

Construction, purification, and analysis of chimeric and native toxins.

We created two chimeric stx_1/stx_2 operons, purified the toxins produced by those operons, and evaluated them in comparison with Stx1a and Stx2a in several assays as described below. The chimeric toxins consisted of the A_1 subunit from either Stx1a or Stx2a and the A_2 peptide and B subunit from the heterologous toxin (see schematic in Figure 11A). The chimeric toxins were named according to the origin of the A_1, A_2, and B subunits, i.e. 122 or 211. We determined the cytotoxicity profile of the toxin panel (Stx1a, Stx2a, 122, and 211) on Vero and HCT-8 cells (Figure 11B). The Vero cell specific activities of the native toxins were similar to those previously reported (287); Stx1a was 3.8×10^9 CD_{50}/mg, while Stx2 was approximately 10-fold lower at 4.2×10^8 CD_{50}/mg (Figure 11B). The activity of the chimeric toxins was equivalent to the native toxin with the homologous B-subunit, such that 211 and 122 had specific activities of 1.0×10^9 and 1.9×10^8 CD_{50}/mg, respectively. Similar toxicity results were obtained on HCT-8 cells, although the overall activity of the toxins was 10-fold lower than observed for Vero cells as expected (Figure 11B). (HCT-8 cells exhibit reduced sensitivity to Stx due to decreased expression of the toxin receptor, Gb3, on the cell surface (324)).

Next, we determined the binding profile of the chimeric toxins for Gb3. Previous reports showed that Stx1a binds Gb3 in a dose-dependent manner and with a higher affinity than Stx2a (49; 324). When the chimeric toxins were examined for the capacity to bind Gb3 by ELISA, we found that the Gb3-binding capacity of the chimeric toxins was again dependent on the origin of the B-subunit. Stx1a and 211 bound Gb3 with a significantly greater affinity than Stx2a or 122 ($p < 0.01$) (Figure 12).

91

Stx Type	Construct A₁ Subunit A₂ B-Subunit	Specific Activity (CD₅₀/mg) Vero Cells	HCT-8 Cells
Stx1a		3.8×10^9	2.1×10^8
211		1.0×10^9	1.1×10^8
Stx2a		4.2×10^8	3.2×10^7
122		1.9×10^8	1.3×10^7
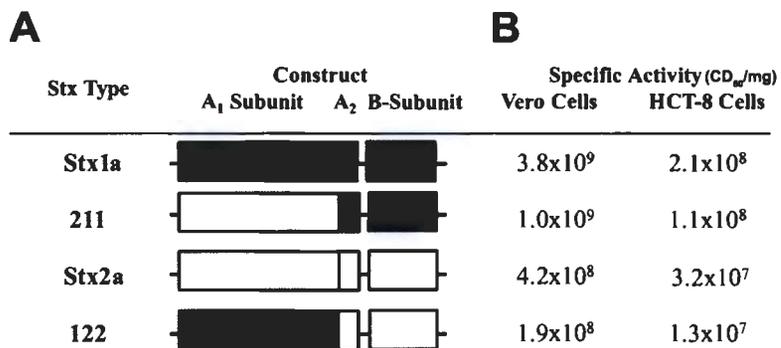
Figure 11. Native and chimeric Stx operon structure and activities.
(A) Illustration that depicts the origin of the individual subunits, A_1, A_2, or B, in the native and chimeric operons. Stx1a is in black, while Stx2a is in white. The chimerics are named such that the number represents the native toxin from which that subunit originated. (B) Specific activities of the toxin panel after intoxication of Vero and HCT-8 cells. Geometric mean of representative of seven biological replicates.
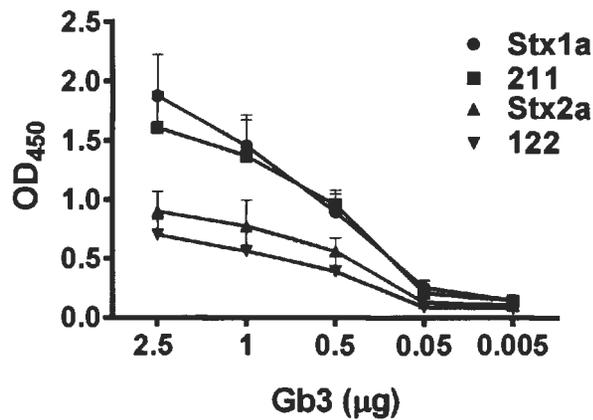
Figure 12. Binding of toxin panel to Gb3 as measured by ELISA.
All four toxins bound Gb3; however, Stx1a and 211 bound Gb3 with a
significantly higher affinity than Stx2a or 122 ($p< 0.01$). Additionally,
when toxins with identical B subunits were compared, Stx1a vs 211 and
Stx2a vs 122, there was no difference in binding ($p > 0.05$). Error bars
represent standard error of the mean (SEM); n=four biological replicates.
Toxin-Gb3 binding was compared by Two-Way ANOVA with Tukey's
adjustment for multiple comparisons.

Our next step was to investigate the translocation properties of the toxins through polarized HCT-8 cell monolayers by the procedure published by Hurley *et al.* (110). As expected, the HCT-8 cells remained polarized for 24 hours after 20 ng of any of the Stxs were applied to the apical transwell chamber (data not shown). However, a significantly greater amount of Stx1a or 211 translocated through the HCT-8 polarized monolayers to the basolateral chamber than did Stx2a or 122 at 0.5, 2.5, and 24 hours post intoxication ($p \leq 0.05$) (Figure 13). For example, after 24 hours, 0.57 and 0.71 ng of Stx1a and 211, respectively, had translocated while only 0.14 and 0.07 ng of Stx2a and 122, respectively, were recovered from the basolateral chamber.

Ip lethality of the toxin panel.

We next determined the ip LD_{50}s of the toxin panel. The ip LD_{50} values for Stx1a and Stx2a were 430 ng and 2.2 ng respectively (Table 5), values that are consistent with previous reports (287). The 122 chimeric had an equivalent LD_{50} to that of Stx2a at 2.3 ng ($p > 0.05$), while 211 had an LD_{50} closer to that of Stx1a at 2300 ng, results that again show that the relative toxicity of the chimeric is dependent on the source of the B subunit. The LD_{50}s corresponding to the Stx2 B subunit were statistically lower compared to LD_{50}s associated with the Stx1 B subunit ($p < 0.05$). The mean time-to-death (MTD) for ip intoxicated mice was analogous for all four toxins, at approximately 4.3 days.

94
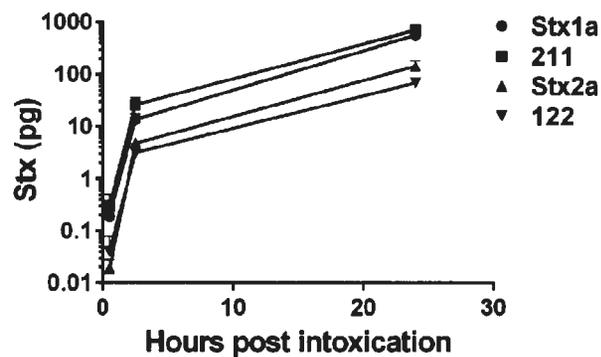
Figure 13. Stx translocation through a polarized HCT-8 cell monolayer after 20 ng was applied to the apical chamber.
The Stx1a B subunit was associated with statistically greater toxin translocation compared to the Stx2a B subunit. A greater amount of Stx1a and 211 was recovered from the basolateral chamber as compared to Stx2a and 122 at 2.5 and 24 h ($p < 0.05$). Error bars represent SEM. n=4 biological replicates

95

Table 5. Ip LD$_{50}$ of native and chimeric toxins

Toxin	LD$_{50}$, ng[*]	95 % CI[*]
Stx1a	430	250-620
211	2300	1300-4600
Stx2a	2.2	2.0-2.6
122	2.3	1.7-3.1

*LD$_{50}$ and confidence intervals were determined by Probit analysis after taking the log of the values.

Oral intoxication of chimeric Stxs.

We continued our *in vivo* analysis of the chimeric Stxs with a determination of the oral toxicity of those preparations. We recently reported that the i.g. LD_{50} of Stx2a is 2.9 μg/mouse (240). Although extreme weight loss and death were observed at Stx2a concentrations of 2 μg or greater, we observed only minimal weight loss and no mortality with 122 at doses of 15 μg or below (data not shown). We next gavaged 35 or 130 μg of 122 into new groups of mice (approximately 10- or 40-X the Stx2a ig LD_{50}, respectively). At the 35 and 130 μg doses of 122, we observed weight loss in both groups and one death in the 130 μg cohort (Figure 14A & B). From these results we concluded that the 122 ig LD_{50} is greater than 130 μg and more than 10X the Stx2a ig LD_{50}. We found no morbidity or mortality after intragastric administration of 157 μg Stx1a (240) or 211 at doses up to 70 μg (data not shown).

Higher percent of active Stx2a recovered than active Stx1a from feces.

To determine whether the toxins were shed differentially into the feces, or if large amounts of the toxins were shed into the stool after oral intoxication, we collected stool from mice fed Stx1a, Stx2a, 211, or 122 at 3, 9, 12, 24, and 48 hours post intoxication and measured the cytotoxicity from those samples on Vero cells. Fecal samples were also collected from control mice to determine the baseline toxicity of stool for Vero cells. After subtracting the background fecal toxicity, we determined the CD_{50}/mL attributable to the active toxins in stool. Once we measured the CD_{50} for each toxin present in the stool, we used the specific activity of the toxins to calculate the actual amount of toxin (μg) excreted at each time point. The highest levels of toxin in stools were found at the three hour time point for all four toxins. Active Stx2a was
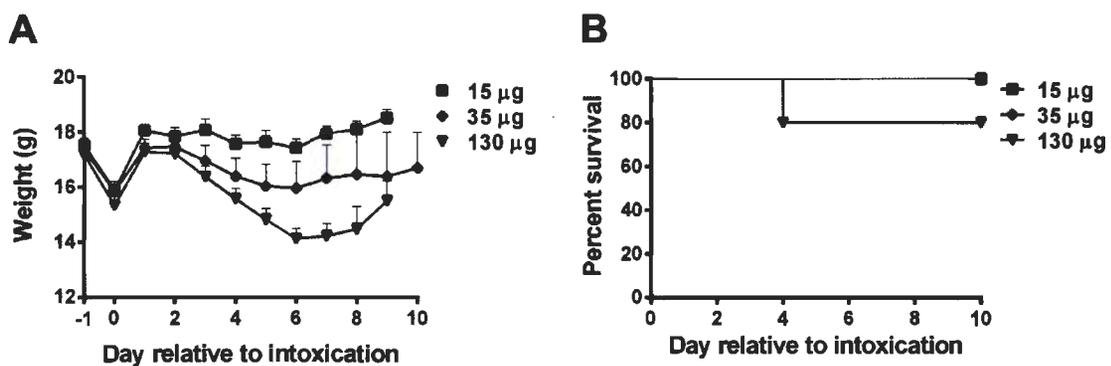
Figure 14. Morbidity and mortality after ig intoxication with chimeric 122.
Ig intoxication of up to 15 μg 122, 5X the Stx2a LD_{50} of 2.9 μg [38], did not result in morbidity or mortality. Weight loss was observed after intoxication with 35 and 130 μg 122 (A) and one animal in the 130 μg group succumbed to intoxication on day 4 (B). Error bars represent SEM; 15 μg: n=10; 35 and 130 μg: n=5

98

recovered from mice gavaged with 2, 7.5, or 15 μg of Stx2a for up to 48 hours post intoxication, whereas the toxin was only detectable in the feces of mice given 0.25 μg ig for 12 hours (Figure 15A). Chimeric 122 was only detected up to 24 hours post intoxication, and there was a significant reduction in toxin excreted from three to nine hours (p< 0.05) (Figure 15B). Stx1a was also detectable in the feces up to 48 hours post-intoxication (Figure 15C), while chimeric 211 was only found in the first 12 hours (Figure 15D). When the calculated toxin output was compared to the initial intoxication dose, we found that a relatively low percentage of each Stx was recovered from stool. For example, when 15 μg of Stx2a were given ig, we detected 1.8 μg in the feces at three hours post-intoxication. Levels of active Stx2a in fecal samples were recovered at a higher percentage of the initial dose over time compared to the rest of the toxin panel (Figure 15A-D), except for the 157 μg Stx1a dose at the 3 h timepoint. Overall, we recovered a higher percentage of active native Stxs compared to the chimeric Stxs when equivalent amounts of toxin were gavaged (Figure 15A-D). In particular, significantly less 122 than Stx2a was detected at three hours in the 0.25 and 15 μg groups and for all groups at the remaining time points (p< 0.05) (Figure 15A &B). In addition, significantly more Stx1a than 211 was recovered from the groups that received 70 μg at all time points (p <0.05) (Figure 15D). We next tried to determine the total concentration of toxin in the feces (active and possibly inactive) with an Stx ELISA. However, the levels of Stx in the feces were below the high limit of detection in the ELISA (not shown) (270).
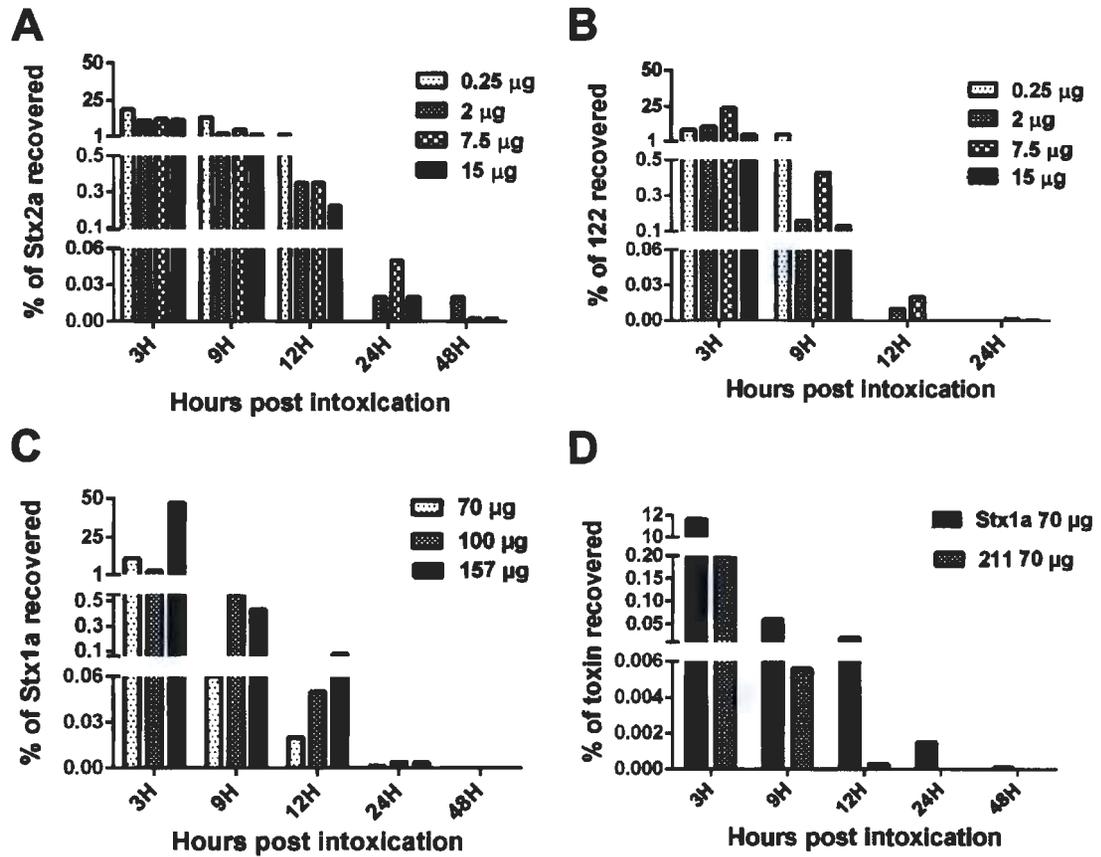
Figure 15. The percent of active toxin recovered from feces compared to toxin input.

The amount of active toxin detected was divided by the amount administered and multiplied by 100 to determine the percent of active Stx2a (A), 122 (B), Stx1a (C), or 211 (D) recovered from the stool. A significantly greater amount of active Stx2a was recovered than active 122 at 9, 12, 24 hours post intoxication at all concentrations fed (t-Test $p<0.05$). A significantly greater amount of active Stx1a was recovered than active 211 at three, nine, and 12 hours post intoxication (Students -Test $p\leq0.05$).

Chimeric toxin stability was reduced in acidic conditions.

Because we observed that the lethality of the chimeric toxins was reduced *in vivo* as compared to the native toxins, especially after ig intoxication, and since previous reports indicated that holotoxin stability is critical for toxin activity (14), we tested the stability of the toxin panel after exposure to acidic conditions. We found that while none of the toxins exhibited altered toxicity when incubated at pH 7 or pH 5 as compared to PBS control (data not shown), the entire toxin panel showed reduced toxicity when incubated in pH 3 buffer at 37°C or 60°C, with a greater reduction in activity at 60°C. The chimeric toxins exhibited an increased susceptibility to inactivation at pH 3 when compared to the native toxins (Table 6). At both 37°C and 60°C, the reduction in activity of chimeric Stxs was significantly greater than the reduction observed in the native Stx with a corresponding B subunit ($p < 0.05$).

Table 6. Fold change of Vero cytotoxicity after incubation in a buffer of pH 3 compared to pH 7.4 (PBS) for 1 h at 37 C or 60 C.

Stx type	37°C	60°C
Stx1a	1.0[a]	0.79[a]
211	0.88[a]	0.46[a]
Stx2a	0.94[b]	0.62[b]
122	0.74[b]	0.48[b]

[a,b] The reduction in activity of the chimeric was significant at both temperatures (P<0.05).

DISCUSSION

The major finding from this study was that the toxicity difference between Stx1a and Stx2a on cells and ip in mice is mediated by the B subunit. For this investigation, we evaluated purified chimeric toxins in which both the A_2 peptide and B subunit originated from the same native toxin. Although another group had created chimeric Stxs with hybrid A_1/A_2 subunits, they used plasmid complementation to combine the chimeric A_1/A_2 with the B subunit, and the cytotoxic activities of those chimerics were significantly lower than those of the native Stx with the corresponding B subunit (121). The structural design of our chimeric toxins is likely the reason that they exhibited *in vitro* cytotoxicity equivalent to the native toxin with the corresponding B subunit. We also believe it was critical that we quantitated the toxin level in purified preparations based on toxin antigen rather than total protein concentration. Other groups of investigators who examined Stx1a/Stx2a chimeras either reconstituted the toxins from purified subunits and observed lower cytotoxicity values than expected (104) or did not get the expected difference in toxicity between Stx1a and Stx2a (117), or they used an operon fusion method but did not produce an active Stx1aA/Stx2aB hybrid (259; 310), or they focused solely on the capacity of Stx2a and the Stx1aA/Stx2aB chimeric to bind human serum amyloid component P (HuSAP) (168).

Although our finding that the B subunit is responsible for the differential toxicity of Stx1a and Stx2a on Vero and HCT8 cells and ip in mice was not surprising based on previous studies (105; 117; 259; 310), our investigation was the first in which a complete set of toxins and chimeras (Stx1a, Stx2a, and each hybrid, 211 and 122) were compared in both *in vitro* and *in vivo* assays. Furthermore, this is the first report in

103

which the Vero cell specific activity of the chimeric toxins was equivalent to the activities associated with the native toxin. However, we found that although Stx2a and 122 have an identical mouse LD_{50} by the ip route, the 211 chimeric demonstrated about a 5-fold higher ip LD_{50} than did Stx1a. In contrast, Shimizu *et al.* found that the LD_{50} of an Stx2aA/Stx1aB hybrid is approximately 2-fold lower than that of Stx1a (259), perhaps because that hybrid bound to Gb3 with a lower affinity in their hands than did Stx1a, and a lower binding affinity to Gb3 is associated with a lower LD_{50} in mice (241). The decreased *in vivo* lethality as compared to *in vitro* toxicity of 211 in our hands may be due to a reduced stability of the holotoxin as compared to Stx1a as measured by sensitivity to pH, and perhaps exacerbated *in vivo* by the requirement of the toxin to travel from the peritoneal cavity to the kidney. By comparison, *in vitro* the toxin is overlaid directly onto the target cell and is not subject to multiple potentially harsh environments.

We previously established that the oral mouse intoxication LD_{50} for Stx2a is 2.9 μg, 1,000X greater than the ip LD_{50} (240). However, in this study we found that 122 was not lethal to mice at 35 μg. Nevertheless, mice gavaged with 130 μg of 122 displayed morbidity profiles similar to mice gavaged with 2 μg of Stx2a and one mouse died. These observations indicate that 130 μg of 122 is close to the ig LD_{50}. We anticipate that the ig LD_{50} of 211 would be at least 1,000X greater than the ip LD_{50} (as we found for Stx2a),and, therefore, more than 2.3 mg/mouse.

We hypothesize that oral intoxication is likely the most strenuous test of the activity of the toxins because the molecule must pass through the gastrointestinal tract (GI) before entering the bloodstream. As a corollary to that theory, we initially

speculated that 1,000X more toxin is required for ig compared to ip intoxication because a portion of toxin is inactivated by the acidic conditions in the intestines. We found however, that less than 25% of the Stx2a and 50% of Stx1a gavaged, respectively, could be found in the stool, a result that indicates that most of the active Stx is not combined into stool. Overall, we recovered a greater percentage of active Stx2a than Stx1a from stool, even though a higher amount of Stx1a was gavaged and Stx2a was more lethal than Stx1a. These latter differences between the native toxins may be due to unique binding and/or translocation patterns during transit through the GI tract, and we did observe greater Stx1a binding to Gb3 and translocation in the HCT-8 cells *in vitro*. We do not believe a significant reduction in activity of the native Stxs occurred in the GI tract, as we did not find Stx antigen in the stool at levels above that detected by Vero cell assay, and because we and others showed that the toxins are stable at pH 3 and 37°C (139). Additionally, the Stxs were not readily inactivated by proteases in the mucus *in vitro* (data not shown). We believe, therefore, that after oral intoxication, a combination of factors results in less toxin reaching the target cells in the kidney, which therefore results in an increased ig LD_{50} compared to the ip $LD_{50.}$

Our results indicate that the B subunit of each toxin is critical for the differential toxicity between Stx1a and Stx2a and, further, that the B subunit is particularly critical for proper delivery of the toxins from the GI tract. However, a major question still remains: why is Stx2a more potent *in vivo* that Stx1? Our findings suggest that the differential mouse lethality of Stx1a and Stx2a may occur at the level of dissemination from the GI tract within the animal or directly at the level of toxicity to the kidney. That

Stx2a has a 1000-fold lower CD_{50} for renal endothelial cells than Stx1a suggests the difference occurs at the site of the kidney (165).

Chapter 4

Discussion

Dissertation overview.

My primary goal for this doctoral project was to examine the paradox that Stx1a is more cytotoxic *in vitro* than is Stx2a on most cell types, while Stx2a is more toxic *in vivo* compared to Stx1a. To investigate that relationship, I developed two specific aims. My first aim was to compare the features of intoxication by Stx1a and Stx2a when orally administered to mice (Chapter 2). For that purpose, I determined the Stx2a ig LD$_{50}$, defined the histopathology after intoxication, and, finally, protected, and rescued mice with a monoclonal antibody (MAb) against Stx2a. However, I did not observe morbidity or mortality after oral intoxication with Stx1a. My second aim was to define the contribution of individual Stx1a and Stx2a subunits in intoxication through the use of chimeric Stxs (Chapter 3). I validated and extended previous observations that holotoxin stability is required for Stx activity and that the B subunit is responsible for the binding and toxicity profile of the holotoxin. The data presented in chapters two and three advanced our understanding of the *in vitro* and *in vivo* properties of the Stxs.

Synopsis of chapter two

Preliminary unpublished data from Dr. Michael Smith who was a member of our group suggested that oral inoculation of Stx2a into mice could be lethal for the animals. While we were completing the work detailed in chapter two, the first report to demonstrate lethality of mice after intragastric (ig) intoxication with Stx2a was published (230). We then went on to expand the finding in that publication by the development of a well-defined and reproducible oral intoxication model that permitted us to calculate the ig LD$_{50}$ of Stx2a as 2.9 μg (Figure 5) (240). We also determined that intraperitoneal (ip) and ig intoxication profiles are similar, as mice developed acute

tubular necrosis (ATN) of epithelial cells and irregular renal panel serum

biochemistries, specifically, elevated levels of creatinine and blood urea nitrogen, and

dysregulated electrolytes. However, ip intoxicated mice exhibited greater morbidity and

a shorter mean time to death (MTD) compared to ig intoxicated mice, presumably

because Stx can reach the kidneys faster when it does not have to traverse the

gastrointestinal (GI) tract. Additionally, we did not observe any intestinal lesions after

ig intoxication, a finding that supports the hypothesis that Stx translocates across

epithelial cells without cell damage (5; 110; 222).

We also observed that ig intoxication of 2 μg of Stx2a, a sub-LD_{50} dose,

resulted in extreme weight loss followed by rapid recovery. To understand the

pathology of Stx2a intoxication and recovery, we euthanized mice on various days after

the increase in weight gain. Mice sacrificed at their weight loss nadir displayed ATN

and irregular renal panel serum biochemistries (describe above). The observed

histopathology of the sub-LD_{50} dose was similar to that of a dose 6X the LD_{50};

however, we believe the extent of tubular damage was greater in mice intoxicated with

the increased dose. When the animals were given one or two days to recover after

intoxication with sub-LD_{50} doses of Stx2a, their serum biochemistries returned to

normal and the tubular pathology was reduced with indications of tubular epithelial cell

regeneration. No renal lesions were observed in these mice after three days of weight

gain. These observations indicate that tubular function is an important predictor of

morbidity and mortality in Stx2a-intoxicated mice. Recovery from Stx2a intoxication is

possible due to tubular epithelial cell regeneration as long as a minimum number of

tubules remain functional.

Finally, MAb 11E10, against the Stx2a A subunit, was protective when delivered 1 h prior to ip or ig intoxication, and rescued mice up to 6 h after intoxication. These findings confirm that Stx2a is responsible for lethality in the oral intoxication model and that MAbs are a viable therapeutic option if delivered early in the clinical course. Stx has a short serum half-life (162; 241), a property that reduces the treatment window as the toxin is quickly bound to target tissues where it appears to no longer be available for neutralization by antibody.

Our findings are consistent with epidemiological data that infection with an Stx2a- positive O157:H7 strain is associated with more severe disease compared to an Stx1a- positive strain (32; 140; 197; 212; 255). One main difference between our oral intoxication mouse model and clinical O157:H7 infection is that the mice develop renal lesions in the tubules while the primary human renal lesion is believed to be glomerular. However, two reports have identified tubular epithelial cells as the primary target for Stx intoxication of human kidneys (48; 297). Unlike tubular epithelial cells, glomerular endothelial cells are not able to regenerate after Stx intoxication due to irreversible scaring of glomerular fenestrations that renders the glomerulus non-functional (192; 232; 322). The overall low percentage of long term sequela from O157:H7 infection supports the hypothesis that tubular epithelial cells are a primary renal target during human infection, and that glomerular involvement results in chronic sequela.

Synopsis of chapter three

We demonstrated that Stx chimerics in which the A_2 peptide and B subunit originate from the one native Stx and the A_1 subunit originates from the other native Stx

are more stable than Stx chimerics in which the entire mature A subunit originates from one native Stx and the B pentamer originates from the opposite native Stx. The A_2 peptide is critical for holotoxin stability (14), and the failure of previous reports to purify an active Stx1aA/ Stx2aB chimeric (105; 310) is probably due to lack of holotoxin stability. Our chimerics were the first to exhibit cytotoxicity equivalent to that of the native Stx with which they share the B subunit. From this result, we concluded that the chimeric holotoxin structure was maintained. Our *in vitro* tests confirmed previous reports that the B subunit is responsible for the binding profile of the toxin molecule (105; 117; 259; 287; 310). Our Stx chimerics exhibited equivalent properties to the native Stx with which they shared the corresponding B subunit, as determined by Gb3 binding in an ELISA, cytotoxicity on Vero and HCT-8 cells, and translocation across a polarized HCT-8 monolayer. However, the *in vivo* activities of the chimeric Stxs were reduced compared to the native toxins. We surmise that although the A_2 peptide increased the stability of the chimerics, it was not sufficient to overcome *in vivo* conditions. The hypothesis of decreased *in vivo* stability of the chimeric Stxs is supported by the reduced percentage of active chimeric toxin recovered in the stools of mice (Figure 15) compared to native toxin and by the increased impact of elevated temperature and reduced pH on activity of the hybrid toxins compared to native molecules.

The question as to why Stx1a is not as toxic *in vivo* as is Stx2a remains. Both Stxs were equivalently stable after incubation at 37°C in pH 3, and, therefore, we predict that each toxin can transit through the GI tract without undergoing a substantial degree of degradation. However, we recovered a greater overall percentage of active

111

Stx2a from the stool, even though the mice were intoxicated with higher dose of Stx1a than Stx2a. Since our *in vitro* stability data suggest that both Stxs are equivalently stable *in vivo*, the recovery of significantly more Stx2a indicates that Stx1a and Stx2a exhibit different binding or translocation properties through the GI tract. It is also possible that Stx1 is not toxic because once systemic, it fails to reach the target site of the kidneys.

Investigations into the lack of Stx1a *in vivo* toxicity by the oral route

The results discussed in chapters two and three increased the body of information on the determinants of Stx toxicity. Nevertheless, the original paradox remains: Stx1a is more cytotoxic toward Vero cells, while Stx2a is more toxic to mice. We propose two hypotheses for the reduced *in vivo* toxicity of Stx1a after oral intoxication. Either Stx1a is not able to exit the intestinal tract and therefore never enters the vascular system to reach the kidneys; or Stx1a binds to Gb3 and is sequestered at nonfunctional sites systemically, and therefore fails to reach the kidney in significant concentrations to cause morbidity and mortality. In support of the latter tenant, Rutjes *et al.* inoculated iodinated Stx1a or iodinated Stx2a, at equal concentrations, iv into mice and reported that 10X more Stx1a went to the lungs while 3X more Stx2a went to the kidneys (241). As mentioned earlier, these investigators suggested that since Stx1a binds Gb3 with a greater affinity than does Stx2a, Stx1a is likely sequestered at nonfunctional tissue sites when systemically administered while Stx2a reaches the kidneys at a concentration high enough for lethality. We conducted two additional experiments to test our two hypotheses as to why Stx1a was not toxic when given orally, even at high doses.

Stx1a versus Stx2a dissemination

To determine the *in vivo* dissemination pattern of each toxin after ig intoxication and discern the location of the potential barrier of Stx1a toxicity, we covalently labeled Stx1a and Stx2a with a fluorescent tag (Alexa Fluor-750; Life technologies). The tag did not affect the cytotoxic activity of either Stx. We intoxicated mice ig with 150 µg of labeled Stx1a or Stx2a. The mice were euthanized after six hours, and their systemic organs were necropsied and imaged with the Carestream *In vivo* MS FX Pro. Unpublished preliminary data suggest that Stx1a and Stx2a have a similar dissemination pattern after oral intoxication (Figure 16). We were surprised to observe that an equivalent amount of both Stxs transited to all of the systemic organs tested, with the highest signal for both toxins in the kidneys. That equal amounts of Stx1a and Stx2a reach the kidneys, suggests the block in Stx1a toxicity occurs systemically at the target site.

Stx1a and Stx2a co-intoxication

The dissemination experiment disproved both of our initial hypotheses as to the basis for decreased Stx1a *in vivo* toxicity. We now speculate that Stx1a and Stx2a likely intoxicate cells to which they bind in the kidney with different efficiency, i.e. they bind equivalently but differentially kill cells to which they bind. We are currently designing assays to test that possibility, but as a corollary to that idea, we propose that Stx1a and Stx2a compete for binding at the target site of the kidneys. Our reasoning behind that prediction is that both Stxs were found by imaging at equal concentrations in the kidneys but only Stx2a is associated with severe disease after STEC infection or
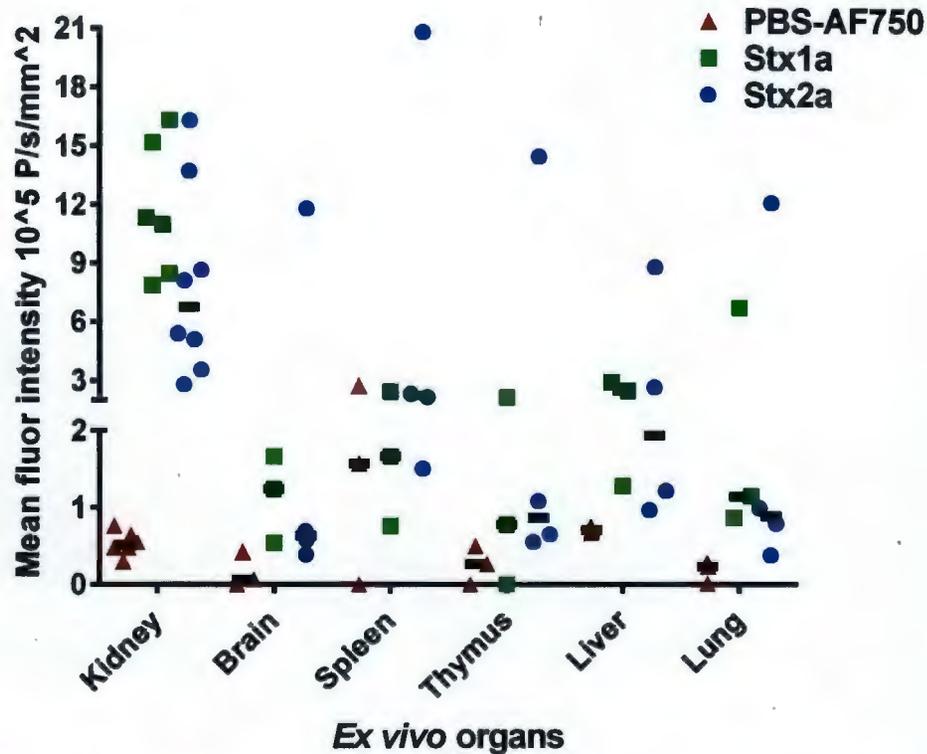
Figure 16. Fluorescence intensity of *ex vivo* systemic organs after oral intoxication with labeled Stx1a and Stx2a.

Mice were orally intoxicated with fluorescently labeled Stx1a (green), Stx2a (blue), or PBS spiked with free label as control (red). Six hours after intoxication, the animals were euthanized and systemic organs were necropsied. Both Stx1a and Stx2a disseminated to systemic organs, with the greatest signal in the kidneys, while the free label was unable to accumulate systemically. Each symbol is an individual organ, left and right kidneys are included separately. Data are from two biological replicates for Stx2a and one for Stx1a. Black bar represents the median value. Statistical significance was determined by the Kruskal-Wallis test with Dunn's correction for multiple comparisons. The mean fluorescent intensity, reported as photon/second/mm^2 (P/s/mm^2) was statistically greater in the kidneys of Stx1a and Stx2a intoxicated mice compared to PBS controls (p<0.02). There was no statistical difference between Stx1a and Stx2a in any organ (p>0.08). Alexa Fluor-750 label (Life Technologies). Imaging software: Molecular Imaging (MI) software (Bruker BioSpin Corporation; Woodbridge, CT).

oral intoxication. A potential competition between the Stxs is also suggested by previous reports on the link between the toxin profiles of O157:H7 strains and likelihood of an infected patient developing HUS. Specifically, epidemiological studies indicate that an individual is more likely to develop HUS if infected with an Stx2a-only-expressing O157:H7 strain than either an Stx1a-only producing strain or an Stx1a, Stx2a-postivie isolate (32; 140; 197; 212; 255). Additional support for the hypothesis that interference may occur between Stxs comes from the work of Kiarash *et al.* who found that Stx1a and Stx2c compete with each other for binding to preferred Gb3 analogues *in vitro* (133). Stx1a prefers Gb3 with long fatty acid (FA) chains and can out compete Stx2c binding to Gb3 with FA chains of C22. Conversely, Stx2c prefers Gb3 with shorter FA tails and can out compete Stx1a binding to Gb3 with FA chains of C18 (133). Additionally, the Stx1a B subunit has previously been shown to neutralize Stx1a holotoxin *in vitro* cytotoxicity (26; 38), and unpublished observations from Drs. James Sinclair and Zhimei Liu in our laboratory indicate that excess concentration of the Stx1a B subunit can neutralize Stx2a cytotoxicity *in vitro*.

To assess whether Stx1a impedes the toxicity of Stx2a *in vivo*, we orally intoxicated mice with 7.5 μg Stx2a, a 100% lethal dose, in combination with an equivalent concentration Stx1a (7.5 μg) or PBS as control. Preliminary data indicate that Stx1 competes with Stx2 for binding at the kidneys (Figure 17). Mice that were intoxicated with Stx2 and PBS lost weight sooner and had a significantly shorter MTD compared to the co-intoxication cohort of Stx2a and Stx1a, even though those mice received 2X the total Stx concentration. Since an equal concentration of Stx1a and
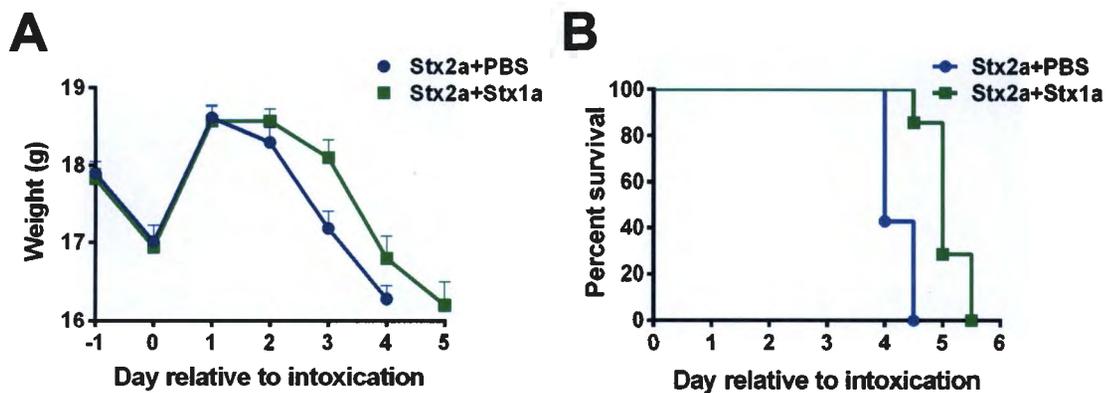
Figure 17. Stx1a competes with Stx2a in a co-intoxication model.
Morbidity (A) and mortality (B) were delayed in mice that received Stx1a in combination with Stx2a compared to mice intoxicated with Stx2a and PBS. (A) Mean weight (g) of the two experimental groups over the course of the experiment. Each group; n=7. Error bars indicate the standard error of the mean. There was a significant difference in weight on day three ($p = 0.0041$), as calculated by two-way ANOVA. (B) Mouse survival percentage for both experimental groups over the course of the experiment. The extension in MTD of mice intoxicated with Stx2a+Stx1a compared to mice intoxicated with Stx2a and PBS, five and four days respectively, was statistically significant ($p = 0.001$).

116

Stx2a disseminated to the kidneys in the first of our unpublished studies on toxin transit from the gut (Figure 16), the delay in toxicity of Stx2a in the presence of Stx1a likely occurred at the target sites in the kidney. At that location, Stx1a may bind to a more heterogeneous Gb3 population on renal tubules and compete with Stx2a for receptor binding or Stx1a may induce a change in the Gb3 membrane composition that preferentially allows Stx1a binding.

Conclusions

The two preliminary experiments discussed above provide additional insights into the Stx oral intoxication pathway. Through our dissemination study with fluorescently labeled Stxs, we showed that Stx1a did not remain localized in the GI tract and reached systemic organs. We did not anticipate that equal concentrations of Stx1a and Stx2a would disseminate to the kidneys since we have not observed morbidity or mortality after ig intoxication with an Stx1a dose 50X the Stx2a LD_{50}. Stx1a is known to cause disease (120; 253; 262; 304); however, a much larger amount of toxin is required as evidenced by a 100X increased ip LD_{50} dose compared to Stx2a (287). Additionally, we demonstrated that after oral intoxication Stx1a did not bind more systemic sites throughout the mouse than did Stx2a. Together, these results suggest that the difference in intoxication profiles between Stx1a and Stx2a occurs at the cellular level of the kidney.

The co-intoxication experimental findings support the hypothesis that Stx intoxication profiles are affected at the kidney. The localization and composition of Gb3 is critical for toxin binding (7; 8; 19; 133; 158; 207; 219). Stx1a can compete with Stx2 for receptor binding sites and Gb3 FA chain lengths are likely responsible. Stx1a

117

and Stx2a bind with greater affinity to particular FA subsets; nevertheless, their general

binding patterns overlap. Stx1a may bind to a wider variety of FA chain lengths,

initially preventing Stx2a from binding Gb3. Stx1a may intoxicate cells at the target

site of the kidney to a lesser degree or be trafficked through a different pathway than

Stx2a. However, once sufficient Stx1a is endocytosed into the cell, Stx2a is able to bind

the free Gb3 receptor and intoxication results in lethality. Another possibility is that

initial binding of Stx1a induces a change in the makeup of Gb3 on the cell membrane.

Together, these data correlate with epidemiological evidence that O157:H7

strains that produce Stx2a only are associated with more severe disease than strains that

produce Stx1a and Stx2a. The decreased disease severity observed after infection with

an O157:H7 that expresses both Stxs may be due to Stx1a competing with Stx2a for

binding receptors at the site of the kidney. It is possible the variation in the percentage

of patients that progress to HUS across O157:H7 outbreaks is affected by the ratio of

Stx1a and Stx2a produced by the strain.

Model of Stx1a and Stx2a intoxication.

The model of Stx intoxication is illustrated in Figure 18. Oral intoxication of

Stx1a and Stx2a delivers the toxins directly to the stomach. The Stxs maintain activity

as they transit through the stomach due to high pH stability of the holotoxin molecules

(Table 6). Stx1a and Stx2a enter the intestinal lumen where epithelial cells express a

minimal concentration of the receptor Gb3 (324). Stx1a and Stx2a then translocate

across intestinal epithelial cells without inhibiting protein synthesis (Figure 13) at a

level that would kill the cell, as no lesions were observed in the intestinal tracts of
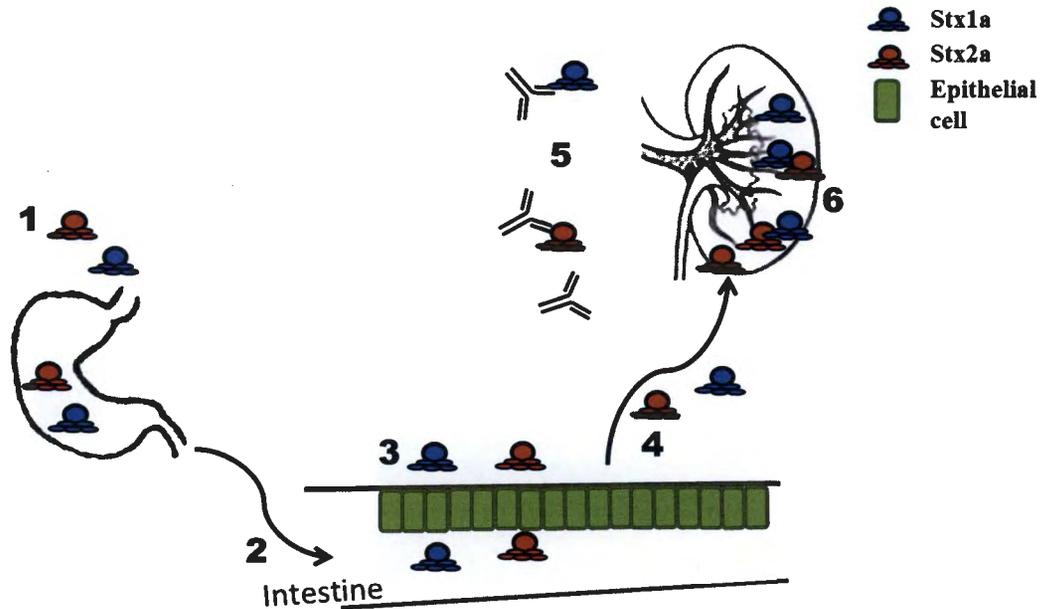
Figure 18. Model of Stx1a and Stx2a intoxication.
(1) Stx1a and Stx2a are delivered into the stomach via ig intoxication. (2) The Stxs transit through the stomach to the intestines. (3) A portion of Stx1a and Stx2a translocate across the intestinal epithelial cell layer, while some active toxin continues through the intestinal tract and is excreted in the feces. (4) The Stxs enter the vascular system and transit to systemic sites through the blood stream. (5) MAbs, when present, can neutralize Stx, and protect mice from death. (6) Stx1a and Stx2a both transit to the kidneys at equal concentrations; however, Stx2a is associated with increased disease severity. When Stx1a and Stx2a are intoxicated in combination, Stx1a competes with Stx2a and delays clinical symptoms and MTD. The Gb3 receptor expression on kidney tubular epithelial cells likely impacts the binding affinity of Stx1a and Stx2a at the target site, thereby affecting the degree of toxicity.

orally-intoxicated mice (Figure S1). However, not all Stx translocates across the epithelia, as evidenced by the detection of active Stx in the stool (Figure 15). Stx1a and Stx2a enter the vasculature and transit to systemic organs through the blood stream. MAb can protect and rescue mice from Stx2a if delivered early in the clinical course (Figures 8 & 9; Table 4). (Additionally, MAbs protect against Stx1a ip intoxication (287)). When intoxicated separately, equivalent concentrations of Stx1a and Stx2a reach the target site of the kidney (Figure 16); however, Stx2a results in morbidity and mortality, while no morbidity is observed after intoxication of up to 157 µg Stx1a. In a co-intoxication experiment with equal concentrations of each Stx, I hypothesize that Stx1a competes with Stx2a, and delays morbidity and mortality (Figure 17). Stx binding affinity is likely determined by the unique Gb3 makeup of the kidney tubular epithelial cells. Although Stx1a binds Gb3 with greater affinity *in vitro* (Figure 12), the Gb3 species in the kidney may favor the type of Stx2a binding that leads to greater levels of cellular intoxication compared to Stx1a.

Future directions.

Future aims for this project are derived from the preliminary dissemination and co-intoxication experimental results. Since the dissemination experiment demonstrated that Stx1a reaches the kidneys, we plan to compare the renal panel serum biochemistries of mice orally intoxicated with Stx1a to mice intoxicated with an equivalent concentration of Stx2a. We also plan to necropsy the systemic organs for pathological review to determine if there are any renal lesions after Stx1a oral intoxication. The renal panel biochemistry values combined with histopathology results will enable us to determine whether Stx1a is effectively intoxicating renal cells *in vivo*.

120

It is possible that renal cells do not express the Gb3 population to which Stx1a prefers to bind to or that Stx1a intoxicates at a slower rate and the tubules are able to regenerate in time to avoid outward signs of morbidity.

Second, we plan to extend our preliminary co-intoxication experiment in which we intoxicated with equivalent concentrations of Stx1a and Stx2a. Although we believe equal concentrations of both Stxs is biologically relevant, we want to determine the actual ratio of each Stx expressed by an O157:H7 strain. We plan to use an immunoblot (154) to determine the relative amount of Stx1a and Stx2a produced *in vitro* by an O157:H7 strain and repeat the co-intoxication experiment based on that result. If more Stx1a is expressed than Stx2a, we may be able to enhance the competition phenotype and delay or reduce morbidity. We also plan to conduct a dose response experiment, to determine both the minimum amount of Stx1a needed to compete with Stx2a and the maximum Stx1a amounts for *in vivo* competition with Stx2a.

Finally, we plan to combine our fluorescently labeled Stx oral intoxication model with our Stx co- intoxication model. Our initial findings suggest that during single intoxication studies, Stx1a and Stx2a transit systemically in an equivalent dissemination pattern. However, preliminary data also imply that the Stxs compete for binding, at least at the location of the kidney, when both toxins are administered at the same time. We plan to use a combination of fluorescently labeled and non-labeled Stx for our competition studies. We will orally intoxicate with a set dose of labeled Stx and compete with either an equal or excess amount of the unlabeled, heterologous Stx to determine whether the dissemination pattern of either or both Stxs is affected in dual intoxication studies.

Overall conclusions.

Oral intoxication with Stx2a results in *in vivo* toxicity that correlates with the severe disease associated with Stx2a- positive O157:H7 strains. Oral intoxication is biologically relevant as it resembles the release of toxin in the GI tract after ingestion of O157:H7 infected food source. The stability and binding of the holotoxin determine the degree of toxicity once Stx is systemic. EHEC O157:H7 pathogenesis in general and Stx intoxication specifically, is a complex, integrated process, dependent on Stx genotype, host cell location, tissue type origination, and Gb3 population. Variations of any one of these factors likely contribute to an individual's ability to resolve the infection or progress to Stx-dependent sequela. Animal intoxication models are practical systems that can be used to more fully dissect the Stx intoxication process in general and to explore the differences between Stx1a and Stx2a intoxication specifically.

Appendix A

Identification of Host Genetic Factors Involved in Colonization of Mice by *E. coli* O157:H7

Russo L.M [1], Melton-Celsa A.R.[1], Abdeltawab N.F.[2], Kotb M.[3], O'Brien A.D.[1]

[1]Department of Microbiology and Immunology, Uniformed Services University of the Health Sciences, Bethesda, MD, USA.

[2]Department of Pharmacy and Biotechnology, Cairo University, Giza, Egypt.

[3]Department of Molecular Genetics, Biochemistry, and Microbiology, University of Cincinnati, Cincinnati, OH, USA.

The data presented in this appendix are preliminary and are intended to be submitted for publication upon completion of analysis.

L.M. Russo is solely responsible for the work presented in this chapter, with the following exceptions: M. Kotb developed the model and assisted with preliminary experimental design, A.R. Melton-Celsa and A.D. O'Brien assisted with experimental design, and analysis and N.F. Abdeltawab performed the QTL statistical analysis.

Note: The figure, table, and reference numbers have been adjusted to follow the format of this dissertation.

ABSTRACT

Enterohemorrhagic *E. coli* (EHEC) are responsible for foodborne outbreaks that can result in severe human disease in a significant portion of infected individuals. During an outbreak, differential disease outcomes are observed after infection with the same EHEC O157:H7 strain. One question of particular interest is why do some infected people resolve infection after hemorrhagic colitis (HC) whereas others progress to the hemolytic uremic syndrome (HUS). Host age and infection dose have been implicated; however, these parameters do not fully account for all of the observed variation in who develops HUS. Therefore, we hypothesize that host genetic factors may play a role in progression to HUS. To test this theory, we used a mouse model of oral infection with *E. coli* O157:H7. To provide the genetic diversity required to study the variable infection outcome after *E. coli* O157:H7 challenge, we orally inoculated animals in the advanced recombinant inbred (ARI) BXD panel that was created by intercrossing C57BL/6J (B6) and DBA/2J (D2) mice and then inbreeding the individual strains to homozygosity.

The founder strains (B6 and D2) were infected with either 86-24, a wild type O157:H7 Stx2a positive strain, or TUV86-2, an Stx negative isogenic mutant. Colonization levels were determined in the intact commensal flora (ICF) infection model. We found a significant difference in colonization levels between the founder strains after infection with TUV86-2, but not with 86-24. This observation suggests that a host factor that may be masked by Stx affects O157:H7 colonization in some genetic backgrounds. We then determined the TUV86-2 colonization levels of 29 BXD strains in the ICF model. Analysis of the known genetic makeup of the BXD strains compared to the observed colonization levels may identify a quantitative trait locus (QTL).

124

Preliminary analyses of the resultant data identified a possible QTL on chromosome 13 on days three and four post infection. Additional BXD strains will be selected to refine or refute the identified QTL.

INTRODUCTION

Enterohemorrhagic *E. coli* (EHEC) are Gram-negative, enteric pathogens associated with many foodborne outbreaks. Serotype O157:H7 accounts for the greatest incidence of disease due to a single Shiga toxin- producing *E. coli* (STEC) serotype in the United States. Indeed, *E. coli* O157:H7 is estimated to be responsible for 63,000 of the estimated 113,000 STEC cases per year (247). Shiga toxin (Stx), the primary virulence factor, is an AB5 toxin that inhibits protein synthesis and leads to cell death (69). The A subunit is responsible for the catalytic activity of the molecule, and the B subunit binds to the host cell receptor, globotriaosylceramide (Gb3). An EHEC strain may encode Stx1a and/or Stx2a, two biologically similar though antigenically distinct toxins. EHEC strains also encode other virulence factors, located on the locus of enterocyte effacement (LEE) pathogenicity island (195). Intimin, the primary adhesion binds to its receptor Tir, or translocated intimin receptor, which is secreted into the host cell through a type three secretion system (T3SS). The tight adhesion of intimin and Tir create attaching and effacing (A/E) lesions that destroy the intestinal microvilli, decrease fluid absorption, and, result in diarrhea. Hemorrhagic colitis (HC) that often occurs immediately after or concurrently with *E. coli* O157-mediated diarrhea is believed to be a consequence of the action of Stx on small vessel endothelial cells in the colon (171).

Cattle and other ruminants are the natural carriers of EHEC O157:H7, and contamination most often occurs during beef processing (12; 13; 102). Initially, ground beef was responsible for the majority of outbreaks (16; 65); however, contaminated fresh produce and non-pasteurized beverages are also responsible for disease (41; 58; 83; 136; 181). Epidemiological analysis suggests that O157:H7 strains that produce

Stx2a only are responsible for more severe disease than EHEC strains that produce Stx1a only or Stx1a and Stx2a (32; 140; 197; 212; 255). After ingestion of even low doses of *E. coli* O157:H7, the most common disease manifestation is HC; this presentation of bloody diarrhea occurs in approximately 90% of infected individuals (280). A serious sequela of *E. coli* O157:H7 infection, the hemolytic uremic syndrome (HUS), as defined by thrombocytopenia, hemolytic anemia, and kidney failure, occurs in 10-20% of individuals (280). It is not known why some individuals spontaneously clear infection while others progress to HUS. Infectious dose and age of the patient have been implicated; however, these factors alone do not account for the total observed disease variance.

Host genetic factors are believed to be an important determinant for O157:H7 related disease outcome; however, traditional laboratory animal models have been inbred to reduce heterogeneity in an intentional reduction of genetic complexity so as to minimize variability between experiments (54). Therefore, a new animal model was required to study the diverse phenotypic variations and reflect the complex genetic structure of the human population. Mouse geneticists looked to model the genetic diversity of recombinant inbred (RI) panels developed to investigate phenotypic variance in Arabidopsis (164), maize (77; 152), and Drosophila (198). To create an RI panel, two founder strains are intercrossed and the homologous recombination that occurs during meiosis results in a mosaic genetic makeup of the progeny strains. The individual RI strains are then inbred to homozygositiy and genotyped to determine the location of crossover events. The heterozygosity of the RI panel is determined by the number of recombination events that occurred between the founder strains. A systems

genetic, genome wide analysis compares the known genotypes of the RI strains to the observed phenotypes to identify a quantitative trait locus (QTL), or region of the chromosome responsible for the variation in the trait of interest (4).

The first murine RI panel was designed by Ben Taylor and colleagues who intercrossed C57BL/6J (B6) and DBA/2J (D2) mice to create the RI BXD panel (281). The initial intercross of the founder B6 and D2 strains resulted in 32 unique F1 BXD strains that were inbred for 20 generations to reach 99% homozygosity. The BXD strains were identified numerically, BXD1 through BXD32. Later, nine additional BXD RI strains were added to the panel, BXD33 through BXD42 (282). The BXD stains were genotyped and extensively analyzed (315). There were a total of 1,848 recombinations in the BXD panel, with an average of 48.1 recombinations per strain. Although the RI BXD panel was the best genetic tool available to study mammalian genetics, it was still not possible to fully resolve complex genetically linked traits, such as the response to infectious disease agents. The number of recombination events was not great enough and the distance between recombinations was too wide to identify individual QTLS.

A new complex RI panel, the advanced recombinant inbred (ARI) BXD panel was developed as a multicenter consortium between Princeton University (Princeton, New Jersey) and University of Tennessee Health Science Center (UTHSC) (Memphis, Tennessee) (218). The BXD strains were then transferred to The Jackson Laboratory (Jackson Labs) (Bar Harbor, ME) for distribution. The advancement of the ARI panel was that the F1 individuals were randomly intercrossed for 9-14 generations to increase the number of recombinations, and then the individual BXD strains were inbred for 20

128

generations to attain 99% homozygosity (218). The additional intercrosses resulted in 4X the total number of recombinations and 3X the number of unique recombinations. The ARI BXD strains were added to the original BXD panel as BXD strains 43-103 (218). The genomes of both founder strains, B6 (308) and D2 (47; 307), have been sequenced and 1.8 million differences, or single nucleotide polymorphisms (SNPs) were identified. The ARI BXD panel was genotyped in 2005 through collaboration of the Complex Trait Consortium and The Welcome Trust (256). The ARI BXD panel has a total of 4,366 recombinations with an average of 82.4 recombinations per strain (256). Additionally, the average distance between recombinations was reduced compared to the original RI panel. The BXD strains were genotyped at 13,367 SNPs evenly spaced over the genome, and 7,636 SNPs were identified as unique markers (256). A subset of 3,795 SNPs differentiate the BXD strains and are primarily used for QTL mapping (256).

The BXD panel was originally used to study the genetic makeup of physical characteristics, such as forebrain weight (166), bone density (142), and taste (231). Addiction response to alcohol (60; 306), cocaine (34; 99), and methamphetamine (96) has also been investigated. Recently, the BXD ARI panel has been used to explore genetic traits underlying response to infectious diseases such as influenza (33), streptococcal sepsis (1; 15), Chlamydia (182) and Ebola (323) infections. A comparison of the human and murine genome reveals a high degree of similarity (191). Therefore, a direct translation of findings to humans is theoretically possible when a link is established between a gene identified through infection of advanced genetic murine lines and a particular response to that microbe (reviewed in (238; 260)). We thus

theorize that host genetic factors that impact colonization by O157:H7 in a mouse model may represent human factors responsible for severe disease. In this study, we observed a statistically significant difference in colonization levels in the murine founder strains (B6 and D2) after infection with TUV86-2. The difference indicates the presence of a potential QTL involved in O157:H7 colonization. Preliminary analysis of colonization data from 29 ARI BXD strains infected with TUV86-2 suggests that chromosome 13 may be important; however additional analysis is required to refine or refute the QTL.

METHODS

Mice.

All animal studies were approved by the Institutional Animal Care and Use Committee of the Uniformed Services University of the Health Sciences and were conducted in strict accordance with the recommendations of the Guide for the Care and Use of Laboratory Animals (296). Animals were housed in filter top cages with access to food and water *ad libitum* unless otherwise noted, in an environmentally controlled room approved by the American Association for Accreditation of Laboratory Animal Care (AAALAC). BXD founder strains (B6 and D2) were purchased from The Jackson Laboratory. We originally obtained BXD strains through a collaboration with investigators at the University of Cincinnati (UC) who had acquired their BXD breeding pairs from UTHSC. Thirteen BXD strains (BXD #: 32, 44, 49, 51, 55, 73, 75, 86, 87, 96, 97, 98, 103) were analyzed from UC. Due to contracting issues, the final BXD strains were acquired from the Jackson Labs colony. Similar colonization levels between mice from UC and Jackson Labs were confirmed with additional testing of four BXD strains (BXD #: 73, 83, 87, 103) whose analysis had been completed from the UC colony (data not shown). Nine BXD strains (BXD #: 45, 48, 61, 62, 66, 69, 70, 84, 100, 101) were tested twice, once from UC and once from Jackson Labs, while five BXD strains (BXD #: 60, 71, 73a, 99, 102) were only analyzed from the Jackson labs colony. Female mice, approximately 5-6 weeks, old were used for all experiments. A minimum of two biological replicates were conducted for each BXD strain. A total of 29 BXD strains have been tested to date, with 321 mice total (BXD strains n = 6-17; B6 and D2 n= 48).

E. coli O157:H7 strains and growth conditions.

Colonization studies with the BXD founder strains (B6 and D2) were conducted with two EHEC O157:H7 strains: 86-24, an Stx2a positive clinical isolate, and TUV86-2 an Stx-negative isogenic mutant, created by site directed mutagenesis to inactivate the *stx* gene (94; 97; 236). BXD colonization studies were conducted only with TUV86-2. Both EHEC strains are resistant to nalidixic acid (Nal) and were grown in Luria broth supplemented with Nal. An overnight culture (~18 h) was pelleted by centrifugation (5,000 X g) and resuspended 1:100 in phosphate buffered saline (PBS) supplemented with 20% sucrose.

Intact commensal flora (ICF) infection model.

Colonization levels were determined in the ICF infection model as previously reported (184). Briefly, food and water were removed from the mice for 20 and 2 hours, respectively, prior to infection. Mice were fed a high inoculum, approximately 10^{10} colony forming units (CFU) in 100 µL by pipette tip. Each experiment included three mice per strain, with six to seven strains total. B6 and D2 strains were included in all experiments as an internal control for colonization levels. Mice were weighed daily and colonization levels were reported as CFU per g feces on days one through four post infection.

To determine the CFU per g feces, mice were placed in individual cages with no bedding for 30-40 minutes. After this time, mice were returned to their original cage and fecal pellets were collected, weighed, and resuspended 1:10 w/v in PBS. The fecal slurry was further diluted 1:10 in PBS and plated on sorbitol MacConkey (SMAC) ager supplemented with Nal to select for the inoculating strain. The dilution that contained

between 30-300 colonies was counted to determine CFU per g feces. The limit of detection for this model is 100 CFU per g.

Preliminary QTL mapping.

Preliminary QTL analysis was conducted on colonization data from the founder strains (B6 and D2) and the 29 BXD strains analyzed (321 mice total: BXD strains n = 6-17; B6 and D2 n= 48). Mouse age, weight, inoculum dose, and CFU/g feces for each day post infection were entered into Web QTL (provided by the Gene Network (http://www.genenetwork.org/webqtl/main.py)) and paired with the BXD strain genotype. WebQTL analyzes the experimental phenotypic data and compares it to the known genotypes of the BXD strains (52; 305). The program performs regression analysis to determine the likelihood ratio statistic (LRS) of a QTL at each of the SNPs tested along the genome (100). To determine the threshold for significance of a potential QTL, 2,000 permutation tests are conducted (55) to test the null hypothesis that there are no associations between phenotypic traits and genotypes. The phenotypic data is randomly shuffled with the known genotypic data, and if the LRS score changes due to the permutation, there is likely a QTL at that position. The variance of the data determines the minimum LRS score required for a suggestive or significant QTL. A QTL can be highly significant (p < 0.001), significant (p <0.05), or suggestive (p <0.63) (147).

RESULTS

Statistically significant colonization difference between murine parental strains infected with TUV86-2.

We used the ICF infection model to determine the colonization levels of two isogenic EHEC O157:H7 strains in the BXD founder mice. After infection with 86-24, an Stx2a positive strain, both B6 and D2 mice had an average colonization level of 10^6 to 10^7 CFU/ g feces on day one post infection (Figure 19A). The colonization levels did not vary significantly between B6 and D2 over the course of the experiment, as both murine strains maintained colonization through day four. We next determined colonization levels of B6 and D2 mice infected with TUV86-2, an Stx negative isogenic mutant. The initial colonization levels were similar to those after infection with 86-24, as the geometric mean colonization levels of the founder murine strains was 10^6 and 10^8 CFU/ g feces (Figure 19B). However, a significant difference in colonization levels developed by day three post infection, such that D2 mice maintained colonization while B6 mice began to resolve the infection (Figure 19B). The significant difference in colonization was maintained on day four.
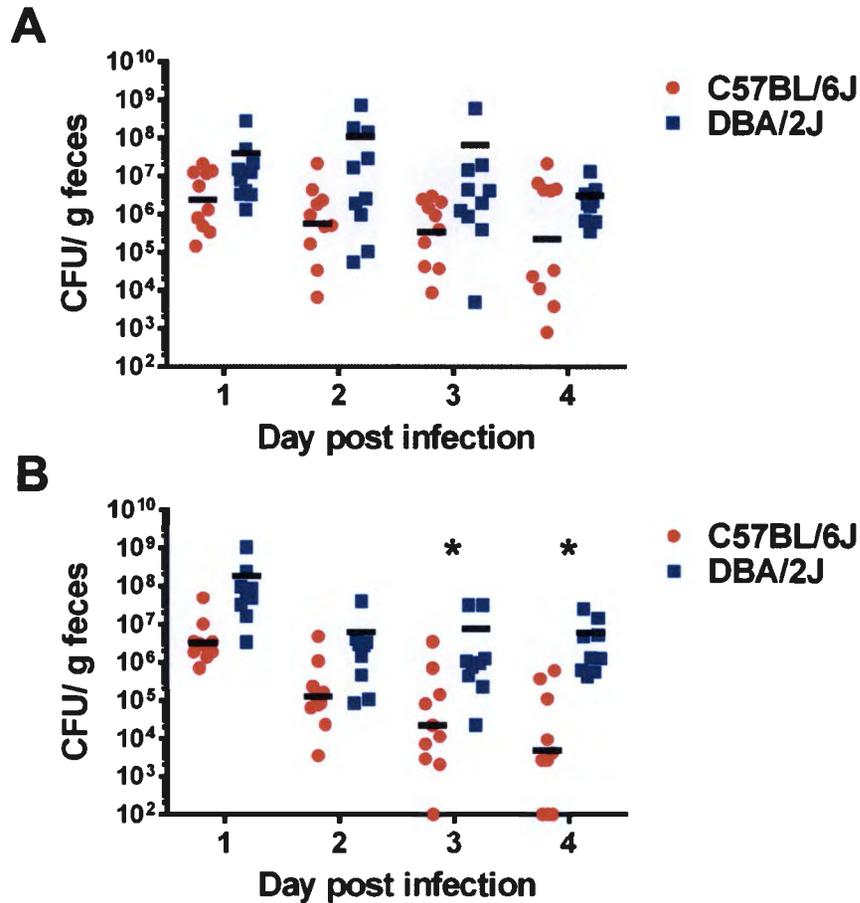
Figure 19. Colonization levels in BXD parental strains after infection with two EHEC O157:H7 strains.
C57BL/6J (B6) and DBA/2J (D2) strains were infected with isogenic O157:H7 strains 86-24 (Stx2a+) (A) or TUV86-2 (Stx-) (B). Individual colonization levels are depicted as CFU/ g feces over the course of the experiment. Black bars represent the geometric mean. The difference in colonization levels between B6 and D2 mice was significant on day 3 and 4 as D2 mice maintained colonization while B6 mice cleared the infection (p $\leq$ 0.003). n=10

Colonization differences between parental and BXD strains infected with TUV86-2.

Since there was a significant difference in the colonization levels of the founder mice after infection with TUV86-2, we decided to only infect the BXD mice with TUV86-2. All of the BXD strains tested became colonized with TUV86-2 after oral inoculation with the organism; indeed, the geometric mean of the initial colonization levels in the different strains ranged from 10^4-10^7 CFU/ g feces (Figure 20). That the colonization patterns of the BXD strains differed over the course of the experiment, suggests that the strains exhibited variable susceptibility to O157:H7 infection. Some BXD strains, such as BXD 99 and 102, were susceptible and maintained high colonization levels similar to D2 mice. Other BXD strains, such as BXD 51, 75, 96, and 97, were relatively resistant and displayed a colonization pattern similar to B6 mice. We noted, however, that some BXD strains, such as BXD 66 and 101 cleared the infection earlier in the experiment than did B6 mice. There were also BXD strains, such as BXD 60, 62, 71, 87, and 100 that gained and lost colonization levels over the course of the experiment.
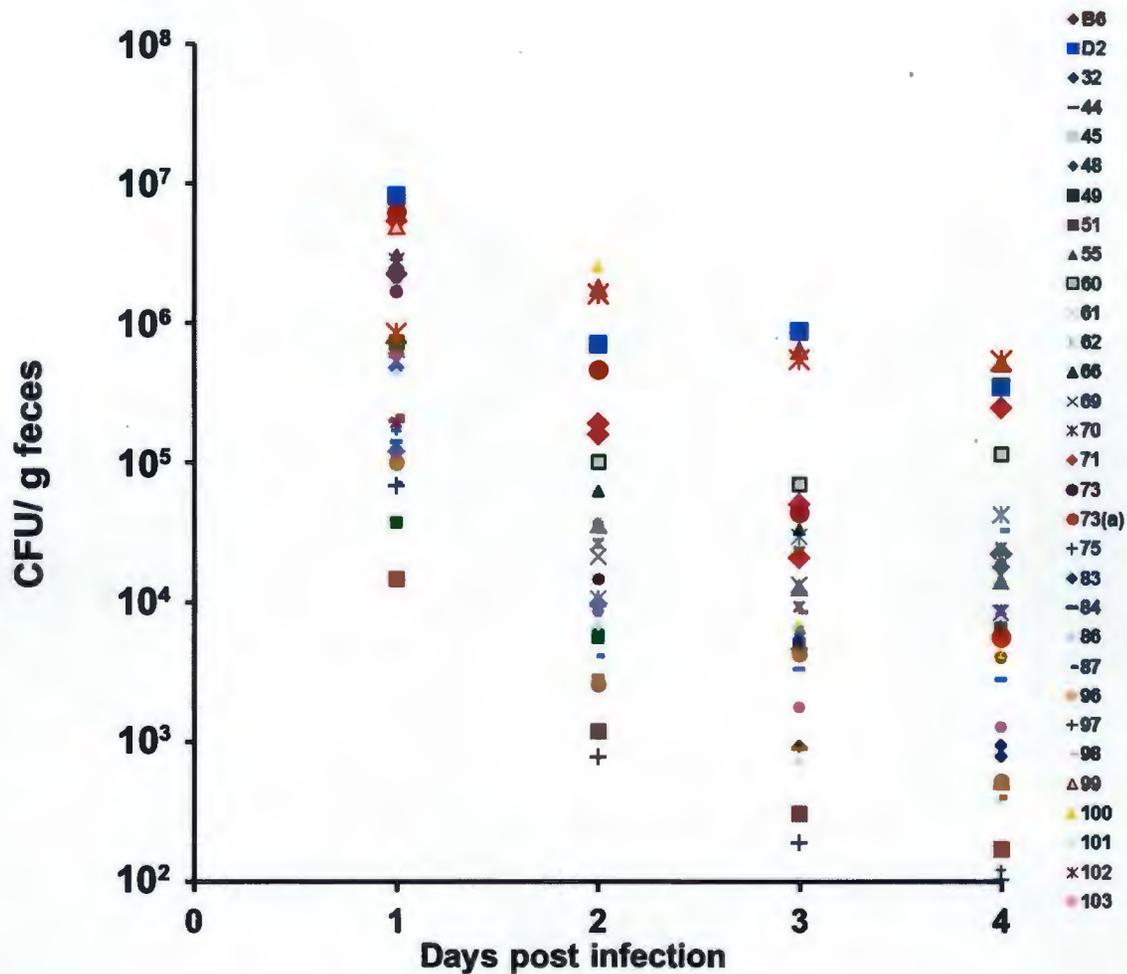
Figure 20. BXD colonization levels after infection with TUV86-2.
The BXD strain geometric mean colonization levels are depicted as CFU/ g
feces over the course of the infection. The mosaic genotypic nature of the
BXD panel is illustrated by the spread of colonization levels across the
multiple strains. Several strains segregate into colonization level clusters.
The pattern of colonization varies across the BXD strains. Some strains
maintain colonization, other steadily lose colonization, while a subset of
strains lose and gain colonization levels over the experiment. Parental n =
48; BXD n = 6-17 per strain; 321 mice total.

Preliminary analysis reveals possible QTL on chromosome 13.

Colonization data from the 321 total mice across 29 unique BXD strains and the two founder strains was sufficient to generate the statistical power required for preliminary QTL analysis. We used WebQTL to analyze the data and map potential QTLs based on CFU/ g feces. We did not obtain a QTL from the colonization data from day two post infection (Figure 21A). The colonization data from day three post infection identified two suggestive QTLs, one on chromosome seven and a second QTL that approached statistical significance, on chromosome 13 (Figure 21B). The potential QTL on chromosome 13 was also identified on day four post infection (Figure 21C).

.
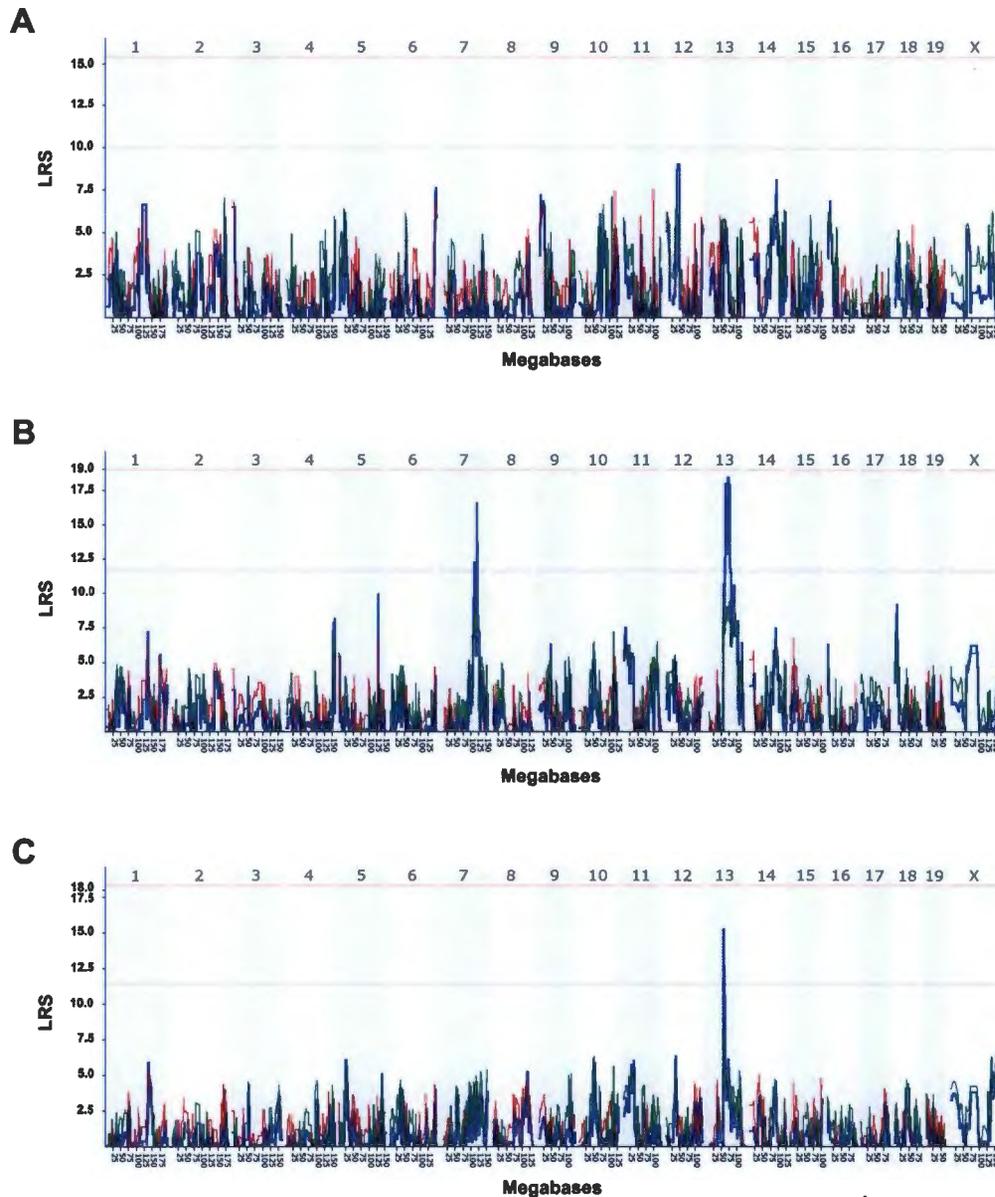
Figure 21. Preliminary QTL mapping.

Preliminary QTLs were mapped based on BXD colonization data from day two- (A), three- (B), and four-(C) post infection. A total of 29 BXD strains and 321 mice were analyzed in WebQTL. LRS scores were computed from permutation tests, and the threshold score for suggestive (grey horizontal line) and significant (red horizontal line) QTLs were determined: (A) Suggestive: 9.94, Significant: 15.42; (B) Suggestive: 11.62, Significant: 18.99; (C) Suggestive: 11.37, Significant: 18.34. The chromosome numbers are annotated on top of the significant QTL line while the specific megabase location within each chromosome is denoted along the bottom. Two preliminary, suggestive QTLs (blue peaks) were identified. The first appeared on day 3 post infection only, located on chromosome 7 (B). The second suggestive QTL on chromosome 13 approached the significant threshold on day 3(B), and remained on day 4 (C)

139

DISCUSSION

Although the data in this Appendix are preliminary, we have presented evidence in support of a host factor that augments EHEC O157:H7 colonization levels in mice. The mosaic-like genetic complexity of the ARI BXD panel provided the diversity required to map a QTL that may predict if an individual animal will be susceptible or relatively resistant to O157:H7 infection. The long term goal of this project is to translate the QTL to human disease and identify a host factor responsible for the variable disease states observed during EHEC O157:H7 outbreaks.

We initially determined the colonization profiles of the founder strains after infection with both, 86-24, an Stx2a positive strain, and TUV86-2, an Stx negative strain. The statistical power provided by ARI BXD panel is great enough that a significant difference between the founder strains is not required; however, a difference increases the likelihood that a QTL exists. Therefore, we decided to only infect the BXD strains with TUV86-2 to have the greatest chance of identifying such a QTL. Stx has been reported to affect EHEC colonization levels in traditional mouse models (236). The decision to proceed with a toxin- negative strain enables us to identify host factors associated with colonization that may be masked by the effect of Stx. We believe this is physiologically relevant approach due to the varying degree of disease severity after infection with an Stx- positive EHEC strain.

Traditionally, the level of colonization in the ICF model on day one indicates whether infection with that inoculum was successfully established. This establishment of infection is critical for comparison of colonization levels across multiple experiments. However, initial low colonization levels of BXD strains may be inherent to the genetic diversity of the panel and may not indicate a poor infection "take". The

140

BXD founder strains were therefore included in every experiment as an internal control. Since the initial B6 and D2 colonization levels were consistently within the expected range (10^6-10^8), we are confident that the variation in BXD colonization levels is representative of the genotypic differences. The wide spread in colonization levels across BXD strains was consistent with the mosaic genotypes of the panel. Additionally, the cyclical colonization patterns observed with some of the BXD strains was a phenotype not observed with the founder strains. This observation was further evidence that the genotypic recombinations of the BXD strains were responsible for differences in colonization phenotypes. Although the analysis is preliminary, we are encouraged by the high LRS score of the potential QTL identified on chromosome 13. That the QTL was identified in the same location of the chromosome on two days increases our confidence in the presence of a QTL; however, additional experimental analysis is required to confirm or discount that link.

FUTURE DIRECTIONS

The potential QTL on chromosome 13 is located between megabases 55-85. A review of the BXD panel identified nine additional BXD strains that have not been tested in our model and have a recombination event within the identified region. The next step for this project is to test a subset of those strains to either narrow the chromosomal region of the QTL or refute the QTL. Once the colonization studies are complete, final analysis will be conducted in WebQTL. Due to the complexity of host response to infection, it is likely that multiple interrelated genes or gene systems are responsible. The BXD model may not have the power required to discern the QTL. If the chromosomal region is too large, it may not be possible to determine the gene(s)

141

responsible and further analysis may be conducted with newer murine panels, such as the collaborative cross (CC), that have increased statistical power due to an increased number of recombination events (53; 54; 235; 290; 311). The CC panel was initiated with eight founder strains, 5 inbred (A/J, C57BL/6 J, 129S1/SvImJ, NOD/LtJ, and NZO/H1LtJ) and 3 outbred (CAST/EiJ, PWK/PhJ, and WSB/EiJ)), instead of the two inbred founder strains for the BXD panel (235). The increased genetic diversity of the panel has resulted in increased coverage and increased cross-over events. CC mice with genetic recombinations of smaller lengths in the region of the identified QTL could be tested in the ICF model to further define the region of interest (54; 115).

Finally, we also plan to infect some of the BXD strains that exhibited lower colonization numbers with the Stx2 positive 86-24 strain. We found that B6 mice maintained colonization after infection with 86-24, however colonization began to resolve after infection with TUV86-2. Therefore, we concluded that B6 mice are "relatively resistant" to infection by O157:H7 as Stx was critical to that infection. We want to determine whether the BXD strains are similar to B6 mice and maintain colonization levels when Stx is present or if an additional colonization phenotype is identified.

ACKNOWLEDGEMENTS.

REFERENCES

1. Abdeltawab NF, Aziz RK, Kansal R, Rowe SL, Su Y, *et al.* 2008. An unbiased systems genetics approach to mapping genetic loci modulating susceptibility to severe streptococcal sepsis. *PLoS pathogens* 4:e1000042

2. Abdul-Raouf UM, Beuchat LR, Ammar MS. 1993. Survival and growth of *Escherichia coli* O157:H7 in ground, roasted beef as affected by pH, acidulants, and temperature. *Appl.Environ.Microbiol.* 59:2364-8

3. Abdul-Raouf UM, Beuchat LR, Ammar MS. 1993. Survival and growth of *Escherichia coli* O157:H7 on salad vegetables. *Appl. Environ. Microbiol.* 59:1999-2006

4. Abiola O, Angel JM, Avner P, Bachmanov AA, Belknap JK, *et al.* 2003. The nature and identification of quantitative trait loci: a community's view. *Nature reviews. Genetics* 4:911-6

5. Acheson DW, Moore R, De Breucker S, Lincicome L, Jacewicz M, *et al.* 1996. Translocation of Shiga toxin across polarized intestinal cells in tissue culture. *Infect Immun.* 64:3294-300

6. Ake JA, Jelacic S, Ciol MA, Watkins SL, Murray KF, *et al.* 2005. Relative nephroprotection during *Escherichia coli* O157:H7 infections: association with intravenous volume expansion. *Pediatrics* 115:e673-e80

7. Ali S, Brockman HL, Brown RE. 1991. Structural determinants of miscibility in surface films of galactosylceramide and phosphatidylcholine: effect of unsaturation in the galactosylceramide acyl chain. *Biochemistry* 30:11198-205

8. Arab S, Lingwood CA. 1998. Intracellular targeting of the endoplasmic reticulum/nuclear envelope by retrograde transport may determine cell hypersensitivity to verotoxin via globotriaosyl ceramide fatty acid isoform traffic. *J Cell Physiol* 177:646-60

9. Argyle JC, Hogg RJ, Pysher TJ, Silva FG, Siegler RL. 1990. A clinicopathological study of 24 children with hemolytic uremic syndrome. A report of the Southwest Pediatric Nephrology Study Group. *Pediatric nephrology* 4:52-8

10. Armstrong GD, Fodor E, Vanmaele R. 1991. Investigation of Shiga-like toxin binding to chemically synthesized oligosaccharide sequences. *J Infect.Dis.* 164:1160-7

11. Armstrong GD, Rowe PC, Goodyer P, Orrbine E, Klassen TP, *et al.* 1995. A phase I study of chemically synthesized verotoxin (Shiga-like toxin) Pk-trisaccharide receptors attached to chromosorb for preventing hemolytic-uremic syndrome. *J Infect.Dis.* 171:1042-5

12. Armstrong GL, Hollingsworth J, Morris JG, Jr. 1996. Emerging foodborne pathogens: *Escherichia coli* O157:H7 as a model of entry of a new pathogen into the food supply of the developed world. *Epidemiol.Rev.* 18:29-51

13. Aslam M, Nattress F, Greer G, Yost C, Gill C, McMullen L. 2003. Origin of contamination and genetic diversity of *Escherichia coli* in beef cattle. *Applied and environmental microbiology* 69:2794-9

14. Austin PR, Jablonski PE, Bohach GA, Dunker AK, Hovde CJ. 1994. Evidence that the A2 fragment of Shiga-like toxin type I is required for holotoxin integrity. *Infect.Immun.* 62:1768-75

15. Aziz RK, Kansal R, Abdeltawab NF, Rowe SL, Su Y, *et al.* 2007. Susceptibility to severe Streptococcal sepsis: use of a large set of isogenic mouse lines to study genetic and environmental factors. *Genes and immunity* 8:404-15

16. Barlow RS, Gobius KS, Desmarchelier PM. 2006. Shiga toxin-producing *Escherichia coli* in ground beef and lamb cuts: results of a one-year study. *International journal of food microbiology* 111:1-5

17. Barrett TJ, Potter ME, Wachsmuth IK. 1989. Continuous peritoneal infusion of Shiga-like toxin II (SLT II) as a model for SLT II-induced diseases. *J Infect.Dis.* 159:774-7

18. Barton BC, Jones TF, Vugia DJ, Long C, Marcus R, *et al.* 2011. Deaths associated with bacterial pathogens transmitted commonly through food: foodborne diseases active surveillance network (FoodNet), 1996-2005. *J.Infect.Dis.* 204:263-7

19. Bauwens A, Betz J, Meisen I, Kemper B, Karch H, Muthing J. 2013. Facing glycosphingolipid-Shiga toxin interaction: dire straits for endothelial cells of the human vasculature. *Cellular and molecular life sciences : CMLS* 70:425-57

20. Bauwens A, Bielaszewska M, Kemper B, Langehanenberg P, von BG, *et al.* 2011. Differential cytotoxic actions of Shiga toxin 1 and Shiga toxin 2 on microvascular and macrovascular endothelial cells. *Thromb.Haemost.* 105

21. Bavaro MF. 2012. *E. coli* O157:H7 and other toxigenic strains: the curse of global food distribution. *Current gastroenterology reports* 14:317-23

22. Bergan J, Dyve Lingelem AB, Simm R, Skotland T, Sandvig K. 2012. Shiga toxins. *Toxicon* 60:1085-107

23. Bettelheim KA. 2007. The non-O157 shiga-toxigenic (verocytotoxigenic) *Escherichia coli*; under-rated pathogens. *Critical reviews in microbiology* 33:67-87

24. Betz J, Bauwens A, Kunsmann L, Bielaszewska M, Mormann M, *et al.* 2012. Uncommon membrane distribution of Shiga toxin glycosphingolipid receptors in toxin-sensitive human glomerular microvascular endothelial cells. *Biological chemistry* 393:133-47

25. Betz J, Bielaszewska M, Thies A, Humpf HU, Dreisewerd K, *et al.* 2011. Shiga toxin glycosphingolipid receptors in microvascular and macrovascular endothelial cells: differential association with membrane lipid raft microdomains. *J.Lipid Res.* 52:618-34

26. Bielaszewska M, Clarke I, Karmali MA, Petric M. 1997. Localization of intravenously administered verocytotoxins (Shiga-toxins) 1 and 2 in rabbits immunized against homologous and heterologous toxins and toxin subunits. #V164. *3rd International Symposium and Workshop on Shiga Toxin (verocytotoxin)-producing Escherichia coli Infections.*:p.76

27. Bielaszewska M, Friedrich AW, Aldick T, Schurk-Bulgrin R, Karch H. 2006. Shiga toxin activatable by intestinal mucus in *Escherichia coli* isolated from humans: predictor for a severe clinical outcome. *Clin.Infect Dis.* 43:1160-7

28. Bielaszewska M, Karch H. 2005. Consequences of enterohaemorrhagic *Escherichia coli* infection for the vascular endothelium. *Thrombosis and haemostasis* 94:312-8

29. Bielaszewska M, Prager R, Kock R, Mellmann A, Zhang W, *et al.* 2007. Shiga toxin gene loss and transfer *in vitro* and *in vivo* during enterohemorrhagic *Escherichia coli* O26 infection in humans. *Applied and environmental microbiology* 73:3144-50

30. Bitzan M, Moebius E, Ludwig K, M ller-Wiefel DE, Heesemann J, Karch H. 1991. High incidence of serum antibodies to *Escherichia coli* O157 lipopolysaccharide in children with hemolytic-uremic syndrome. *J.Pediatr.* 119:380-5

31. Bitzan M, Poole R, Mehran M, Sicard E, Brockus C, *et al.* 2009. Safety and pharmacokinetics of chimeric anti-Shiga toxin 1 and anti-Shiga toxin 2 monoclonal antibodies in healthy volunteers. *Antimicrob.Agents Chemother.* 53:3081-7

32. Boerlin P, McEwen SA, Boerlin-Petzold F, Wilson JB, Johnson RP, Gyles CL. 1999. Associations between virulence factors of Shiga toxin-producing *Escherichia coli* and disease in humans. *J Clin.Microbiol.* 37:497-503

33. Boon AC, deBeauchamp J, Hollmann A, Luke J, Kotb M, *et al.* 2009. Host genetic variation affects resistance to infection with a highly pathogenic H5N1 influenza A virus in mice. *Journal of virology* 83:10417-26

34. Boone EM, Hawks BW, Li W, Garlow SJ. 2008. Genetic regulation of hypothalamic cocaine and amphetamine-regulated transcript (CART) in BxD inbred mice. *Brain research* 1194:1-7

35. Boyce TG, Swerdlow DL, Griffin PM. 1995. *Escherichia coli* O157:H7 and the hemolytic-uremic syndrome. *N.Engl.J Med.* 333:364-8

36. Boyd B, Lingwood C. 1989. Verotoxin receptor glycolipid in human renal tissue. *Nephron* 51:207-10

37. Boyd B, Magnusson G, Zhiuyan Z, Lingwood CA. 1994. Lipid modulation of glycolipid receptor function. Availability of Gal(alpha 1-4)Gal disaccharide for verotoxin binding in natural and synthetic glycolipids. *Eur.J Biochem.* 223:873-8

38. Boyd B, Richardson S, Gariepy J. 1991. Serological responses to the B subunit of Shiga-like toxin 1 and its peptide fragments indicate that the B subunit is a vaccine candidate to counter action of the toxin. *Infect.Immun.* 59:750-7

39. Boyd B, Tyrrell G, Maloney M, Gyles C, Brunton J, Lingwood C. 1993. Alteration of the glycolipid binding specificity of the pig edema toxin from globotetraosyl to globotriaosyl ceramide alters *in vivo* tissue targetting and results in a verotoxin 1-like disease in pigs. *J Exp.Med.* 177:1745-53

40. Brandt ML, O'Regan S, Rousseau E, Yazbeck S. 1990. Surgical complications of the hemolytic-uremic syndrome. *Journal of pediatric surgery* 25:1109-12

41. Breuer T, Benkel DH, Shapiro RL, Hall WN, Winnett MM, *et al.* 2001. A multistate outbreak of *Escherichia coli* O157:H7 infections linked to alfalfa sprouts grown from contaminated seeds. *Emerg.Infect.Dis.* 7:977-82

42. Brigotti M, Carnicelli D, Alvergna P, Mazzaracchio R, Sperti S, Montanaro L. 1997. The RNA-N-glycosidase activity of Shiga-like toxin I: kinetic parameters of the native and activated toxin. *Toxicon* 35:1431-7

43. Brooks JT, Sowers EG, Wells JG, Greene KD, Griffin PM, *et al.* 2005. Non-O157 Shiga Toxin-Producing *Escherichia coli* Infections in the United States, 1983-2002. *J.Infect.Dis.* 192:1422-9

44. Calderwood SB, Acheson DWK, Keusch GT, Barrett TJ, Griffin PM, *et al.* 1996. Proposed new nomenclature for SLT (VT) family. Letter. *Amer.Soc.for.Microbiol.NEWS* 62:118-9

45. Calderwood SB, Mekalanos JJ. 1987. Iron regulation of Shiga-like toxin expression in *Escherichia coli* is mediated by the *fur* locus. *J Bacteriol* 169:4759-64

46. Callaway TR, Anderson RC, Edrington TS, Genovese KJ, Bischoff KM, *et al.* 2004. What are we doing about *Escherichia coli* O157:H7 in cattle? *Journal of animal science* 82 E-Suppl:E93-9

47. Celera. 2001. Celera Completes Assembly of Mouse Genome, CELERA, Rockville, MD

48. Chaisri U, Nagata M, Kurazono H, Horie H, Tongtawe P, *et al.* 2001. Localization of Shiga toxins of enterohaemorrhagic *Escherichia coli* in kidneys of paediatric and geriatric patients with fatal haemolytic uraemic syndrome. *Microb.Pathog.* 31:59-67

49. Chark D, Nutikka A, Trusevych N, Kuzmina J, Lingwood C. 2004. Differential carbohydrate epitope recognition of globotriaosyl ceramide by verotoxins and a monoclonal antibody. *Eur.J Biochem.* 271:405-17

50. Chart H, Scotland SM, Smith HR, Rowe B. 1989. Antibodies to *Escherichia coli* O157 in patients with haemorrhagic colitis and haemolytic uraemic syndrome. *J Clin.Pathol.* 42:973-6

51. Cheng LW, Stanker LH, Henderson TD, 2nd, Lou J, Marks JD. 2009. Antibody protection against botulinum neurotoxin intoxication in mice. *Infect Immun* 77:4305-13

52. Chesler EJ, Lu L, Shou S, Qu Y, Gu J, *et al.* 2005. Complex trait analysis of gene expression uncovers polygenic and pleiotropic networks that modulate nervous system function. *Nature genetics* 37:233-42

53. Chesler EJ, Miller DR, Branstetter LR, Galloway LD, Jackson BL, *et al.* 2008. The Collaborative Cross at Oak Ridge National Laboratory: developing a powerful resource for systems genetics. *Mammalian genome : official journal of the International Mammalian Genome Society* 19:382-9

54. Churchill GA, Airey DC, Allayee H, Angel JM, Attie AD, *et al.* 2004. The Collaborative Cross, a community resource for the genetic analysis of complex traits. *Nature genetics* 36:1133-7

55. Churchill GA, Doerge RW. 1994. Empirical threshold values for quantitative trait mapping. *Genetics* 138:963-71

56. Cilmi SA, Karalius BJ, Choy W, Smith RN, Butterton JR. 2006. Fabry Disease in Mice Protects against Lethal Disease Caused by Shiga Toxin-Expressing Enterohemorrhagic *Escherichia coli. J Infect Dis.* 194:1135-40

148

57.   Cimolai N, Morrison BJ, Carter JE. 1992. Risk factors for the central nervous system manifestations of gastroenteritis-associated hemolytic-uremic syndrome. *Pediatrics* 90:616-21

58.   Cody SH, Glynn MK, Farrar JA, Cairns KL, Griffin PM, *et al.* 1999. An outbreak of *Escherichia coli* O157:H7 infection from unpasteurized commercial apple juice. *Ann Intern Med* 130:202-9

59.   Conrady DG, Flagler MJ, Friedmann DR, Vander Wielen BD, Kovall RA, *et al.* 2010. Molecular basis of differential B-pentamer stability of shiga toxins 1 and 2. *PLoS.ONE.* 5:e15153

60.   Crabbe JC, Belknap JK, Buck KJ, Metten P. 1994. Use of recombinant inbred strains for studying genetic determinants of responses to alcohol. *Alcohol and alcoholism* 2:67-71

61.   Creydt VP, Silberstein C, Zotta E, Ibarra C. 2006. Cytotoxic effect of Shiga toxin-2 holotoxin and its B subunit on human renal tubular epithelial cells. *Microbes.Infect* 8:410-9

62.   DeGrandis S, Law H, Brunton J, Gyles C, Lingwood CA. 1989. Globotetraosylceramide is recognized by the pig edema disease toxin. *J Biol Chem* 264:12520-5

63.   Dowling TC, Chavaillaz PA, Young DG, Melton-Celsa A, O'Brien A, *et al.* 2005. Phase 1 safety and pharmacokinetic study of chimeric murine-human monoclonal antibody càStx2 administered intravenously to healthy adult volunteers. *Antimicrob.Agents Chemother.* 49:1808-12

64.   Downes FP, Barrett TJ, Green JH, Aloisio CH, Spika JS, *et al.* 1988. Affinity purification and characterization of Shiga-like toxin II and production of toxin-specific monoclonal antibodies. *Infect.Immun.* 56:1926-33

65.   Doyle MP, Schoeni JL. 1987. Isolation of *Escherichia coli* O157:H7 from retail fresh meats and poultry. *Appl.Environ.Microbiol.* 53:2394-6

66.   Edwards AC, Melton-Celsa AR, Arbuthnott K, Stinson JR, Schmitt CK, *et al.* 1998. Vero cell neutralization and mouse protective efficacy of humanized monoclonal antibodies against *Escherichia coli* toxins Stx1 and Stx2. In *Escherichia coli O157:H7 and other Shiga toxin-producing E. coli strains*, ed. JB Kaper, AD O'Brien:388-92. Washington, DC: ASM Press. Number of 388-92 pp.

67.   Eklund M, Scheutz F, Siitonen A. 2001. Clinical isolates of non-O157 Shiga toxin-producing *Escherichia coli*: serotypes, virulence characteristics, and molecular profiles of strains of the same serotype. *J Clin Microbiol* 39:2829-34

68. Elder RO, Keen JE, Siragusa GR, Barkocy-Gallagher GA, Koohmaraie M, Laegreid WW. 2000. Correlation of enterohemorrhagic *Escherichia coli* O157 prevalence in feces, hides, and carcasses of beef cattle during processing. *Proc.Natl.Acad.Sci.U.S.A* 97:2999-3003

69. Endo Y, Tsurugi K, Yutsudo T, Takeda Y, Ogasawara T, Igarashi K. 1988. Site of action of a Vero toxin (VT2) from *Escherichia coli* O157:H7 and of Shiga toxin on eukaryotic ribosomes. RNA N-glycosidase activity of the toxins. *Eur.J Biochem.* 171:45-50

70. Etcheverria AI, Padola NL, Sanz ME, Polifroni R, Kruger A, *et al.* 2010. Occurrence of Shiga toxin-producing *E. coli* (STEC) on carcasses and retail beef cuts in the marketing chain of beef in Argentina. *Meat science* 86:418-21

71. Falguieres T, Romer W, Amessou M, Afonso C, Wolf C, *et al.* 2006. Functionally different pools of Shiga toxin receptor, globotriaosyl ceramide, in HeLa cells. *FEBS J*

72. Farfan MJ, Torres AG. 2012. Molecular mechanisms that mediate colonization of Shiga toxin-producing *Escherichia coli* strains. *Infect Immun* 80:903-13

73. Feng P, Lampel KA, Karch H, Whittam TS. 1998. Genotypic and phenotypic changes in the emergence of *Escherichia coli* O157:H7. *J Infect.Dis.* 177:1750-3

74. Feng P, Weagant SD, Monday SR. 2001. Genetic analysis for virulence factors in *Escherichia coli* O104:H21 that was implicated in an outbreak of hemorrhagic colitis. *J Clin Microbiol* 39:24-8

75. Fenwick BW, Cowan LA. 1998. Canine model of the hemolytic uremic syndrome. In *Escherichia coli O157:H7 and Other Shiga Toxin-Producing E. coli* ed. JB Kaper, AD O'Brien:268-77. Washington, DC: ASM Press. Number of 268-77 pp.

76. Flagler MJ, Mahajan SS, Kulkarni AA, Iyer SS, Weiss AA. 2010. Comparison of binding platforms yields insights into receptor binding differences between shiga toxins 1 and 2. *Biochemistry* 49:1649-57

77. Fracheboud Y, Ribaut JM, Vargas M, Messmer R, Stamp P. 2002. Identification of quantitative trait loci for cold-tolerance of photosynthesis in maize (Zea mays L.). *Journal of experimental botany* 53:1967-77

78. Frank C, Werber D, Cramer JP, Askar M, Faber M, *et al.* 2011. Epidemic Profile of Shiga-Toxin-Producing *Escherichia coli* O104:H4 Outbreak in Germany - Preliminary Report. *N.Engl.J.Med.*

79. Frankel G, Phillips AD, Rosenshine I, Dougan G, Kaper JB, Knutton S. 1998. Enteropathogenic and enterohaemorrhagic *Escherichia coli* : more subversive elements. *Mol.Microbiol.* 30:911-21

80. Fraser ME, Chernaia MM, Kozlov YV, James MN. 1994. Crystal structure of the holotoxin from Shigella dysenteriae at 2.5 resolution. *Nat.Struct.Biol.* 1:59-64

81. Fraser ME, Fujinaga M, Cherney MM, Melton-Celsa AR, Twiddy EM, *et al.* 2004. Structure of Shiga toxin type 2 (Stx2) from *Escherichia coli* O157:H7. *J Biol Chem* 279:27511-7

82. Friedrich AW, Borell J, Bielaszewska M, Fruth A, Tschape H, Karch H. 2003. Shiga toxin 1c-producing *Escherichia coli* strains: phenotypic and genetic characterization and association with human disease. *J Clin Microbiol* 41:2448-53

83. Friesema I, Sigmundsdottir G, van der Zwaluw K, Heuvelink A, Schimmer B, *et al.* 2008. An international outbreak of Shiga toxin-producing *Escherichia coli* O157 infection due to lettuce, September-October 2007. *Euro surveillance : bulletin Europeen sur les maladies transmissibles = European communicable disease bulletin* 13

84. Fujii J, Kinoshita Y, Yutsudo T, Taniguchi H, Obrig T, Yoshida SI. 2001. Toxicity of Shiga toxin 1 in the central nervous system of rabbits. *Infect Immun* 69:6545-8

85. Fujii Y, Numata S, Nakamura Y, Honda T, Furukawa K, *et al.* 2005. Murine glycosyltransferases responsible for the expression of globo-series glycolipids: cDNA structures, mRNA expression, and distribution of their products. *Glycobiology* 15:1257-67

86. Fuller CA, Pellino CA, Flagler MJ, Strasser JE, Weiss AA. 2011. Shiga toxin subtypes display dramatic differences in potency. *Infect.Immun.* 79:1329-37

87. Fulton RJ, Uhr JW, Vitetta ES. 1986. The effect of antibody valency and lysosomotropic amines on the synergy between ricin A chain- and ricin B chain-containing immunotoxins. *J Immunol* 136:3103-9

88. Gallegos KM, Conrady DG, Karve SS, Gunasekera TS, Herr AB, Weiss AA. 2012. Shiga toxin binding to glycolipids and glycans. *PLoS.ONE.* 7:e30368

89. Garg AX, Suri RS, Barrowman N, Rehman F, Matsell D, *et al.* 2003. Long-term renal prognosis of diarrhea-associated hemolytic uremic syndrome: a systematic review, meta-analysis, and meta-regression. *JAMA* 290:1360-70

90. Garred O, van Deurs B, Sandvig K. 1995. Furin-induced cleavage and activation of Shiga toxin. *J Biol.Chem.* 270:10817-21

91. Gentry MK, Dalrymple JM. 1980. Quantitative microtiter cytotoxicity assay for Shigella toxin. *J Clin.Microbiol.* 12:361-6

92. Gerber A, Karch H, Allerberger F, Verweyen HM, Zimmerhackl LB. 2002. Clinical course and the role of shiga toxin-producing *Escherichia coli* infection in the hemolytic-uremic syndrome in pediatric patients, 1997- 2000, in Germany and Austria: a prospective study. *J Infect.Dis.* 186:493-500

93. Grif K, Dierich MP, Karch H, Allerberger F. 1998. Strain-specific differences in the amount of Shiga toxin released from enterohemorrhagic *Escherichia coli* O157 following exposure to subinhibitory concentrations of antimicrobial agents. *European journal of clinical microbiology & infectious diseases : official publication of the European Society of Clinical Microbiology* 17:761-6

94. Griffin PM, Ostroff SM, Tauxe RV, Greene KD, Wells JG, *et al.* 1988. Illnesses associated with *Escherichia coli* O157:H7 infections. A broad clinical spectrum. *Annals of Internal Medicine* 109:705-12

95. Griffin PM, Tauxe RV. 1991. The epidemiology of infections caused by *Escherichia coli* O157:H7, other enterohemorrhagic *E. coli* , and the associated hemolytic uremic syndrome. *Epidemiol.Rev.* 13:60-98

96. Grisel JE, Belknap JK, O'Toole LA, Helms ML, Wenger CD, Crabbe JC. 1997. Quantitative trait loci affecting methamphetamine responses in BXD recombinant inbred mouse strains. *The Journal of neuroscience : the official journal of the Society for Neuroscience* 17:745-54

97. Gunzer F, Bohn U, Fuchs S, Muhldorfer I, Hacker J, *et al.* 1998. Construction and characterization of an isogenic slt-ii deletion mutant of enterohemorrhagic *Escherichia coli Infect.Immun.* 66:2337-41

98. Gyles CL. 2007. Shiga toxin-producing *Escherichia coli* : An overview. *J Anim Sci.* 85:E45-E62

99. Hain HS, Crabbe JC, Bergeson SE, Belknap JK. 2000. Cocaine-induced seizure thresholds: quantitative trait loci detection and mapping in two populations derived from the C57BL/6 and DBA/2 mouse strains. *The Journal of pharmacology and experimental therapeutics* 293:180-7

100. Haley CS, Knott SA. 1992. A simple regression method for mapping quantitative trait loci in line crosses using flanking markers. *Heredity* 69:315-24

101. Hamer HM, Jonkers D, Venema K, Vanhoutvin S, Troost FJ, Brummer RJ. 2008. Review article: the role of butyrate on colonic function. *Alimentary pharmacology & therapeutics* 27:104-19

102. Hancock DD, Besser TE, Rice DH, Tarr PI. 1998. Ecology of *Escherichia coli* O157:H7 in cattle and impact of management practices. In *Escherichia coli*

O157:H7 and other Shiga toxin-producing E. coli strains, ed. JB Kaper, AD O'Brien:85-91. Washington, D.C.: American Society for Microbiology. Number of 85-91 pp.

103. Harris SM, Yue WF, Olsen SA, Hu J, Means WJ, *et al.* 2012. Salt at concentrations relevant to meat processing enhances Shiga toxin 2 production in *Escherichia coli* O157:H7. *International journal of food microbiology* 159:186-92

104. Head SC, Karmali MA, Lingwood CA. 1991. Preparation of VT1 and VT2 hybrid toxins from their purified dissociated subunits. Evidence for B subunit modulation of a subunit function. *J Biol.Chem.* 266:3617-21

105. Head SC, Karmali MA, Lingwood CA. 1991. Preparation of VT1 and VT2 hybrid toxins from their purified dissociated subunits. Evidence for B subunit modulation of a subunit function. *J Biol Chem* 266:3617-21

106. Hosler GA, Cusumano AM, Hutchins GM. 2003. Thrombotic thrombocytopenic purpura and hemolytic uremic syndrome are distinct pathologic entities. A review of 56 autopsy cases. *Archives of pathology & laboratory medicine* 127:834-9

107. Hovde CJ, Calderwood SB, Mekalanos JJ, Collier RJ. 1988. Evidence that glutamic acid 167 is an active-site residue of Shiga-like toxin I. *Proc.Natl.Acad.Sci.U.S.A* 85:2568-72

108. Hughes AK, Stricklett PK, Kohan DE. 1998. Cytotoxic effect of Shiga toxin-1 on human proximal tubule cells. *Kidney Int* 54:426-37

109. Hughes AK, Stricklett PK, Kohan DE. 2001. Shiga toxin-1 regulation of cytokine production by human glomerular epithelial cells. *Nephron* 88:14-23

110. Hurley BP, Jacewicz M, Thorpe CM, Lincicome LL, King AJ, *et al.* 1999. Shiga toxins 1 and 2 translocate differently across polarized intestinal epithelial cells. *Infect.Immun.* 67:6670-7

111. Hurley BP, Thorpe CM, Acheson DW. 2001. Shiga toxin translocation across intestinal epithelial cells is enhanced by neutrophil transmigration. *Infect Immun* 69:6148-55

112. Ikeda K, Ida O, Kimoto K, Takatorige T, Nakanishi N, Tatara K. 1999. Effect of early fosfomycin treatment on prevention of hemolytic uremic syndrome accompanying *Escherichia coli* O157:H7 infection. *Clin.Nephrol.* 52:357-62

113. Ikeda M, Ito S, Honda M. 2004. Hemolytic uremic syndrome induced by lipopolysaccharide and Shiga-like toxin. *Pediatric nephrology* 19:485-9

114.   Inward CD, Howie AJ, Fitzpatrick MM, Rafaat F, Milford DV, Taylor CM. 1997. Renal histopathology in fatal cases of diarrhoea-associated haemolytic uraemic syndrome. British Association for Paediatric Nephrology. *Pediatric nephrology* 11:556-9

115.   Iraqi FA, Churchill G, Mott R. 2008. The Collaborative Cross, developing a resource for mammalian systems genetics: a status report of the Wellcome Trust cohort. *Mammalian genome : official journal of the International Mammalian Genome Society* 19:379-81

116.   Ito H, Terai A, Kurazono H, Takeda Y, Nishibuchi M. 1990. Cloning and nucleotide sequencing of Vero toxin 2 variant genes from *Escherichia coli* O91:H21 isolated from a patient with the hemolytic uremic syndrome. *Microb.Pathog.* 8:47-60

117.   Ito H, Yutsudo T, Hirayama T, Takeda Y. 1988. Isolation and some properties of A and B subunits of Vero toxin 2 and *in vitro* formation of hybrid toxins between subunits of Vero toxin 1 and Vero toxin 2 from *Escherichia coli* O157:H7. *Microb.Pathog.* 5:189-95

118.   Jacewicz MS, Acheson DW, Binion DG, West GA, Lincicome LL, *et al.* 1999. Responses of human intestinal microvascular endothelial cells to Shiga toxins 1 and 2 and pathogenesis of hemorrhagic colitis. *Infect.Immun.* 67:1439-44

119.   Jacewicz MS, Mobassaleh M, Gross SK, Balasubramanian KA, Daniel PF, *et al.* 1994. Pathogenesis of Shigella diarrhea: XVII. A mammalian cell membrane glycolipid, Gb3, is required but not sufficient to confer sensitivity to Shiga toxin. *J Infect Dis* 169:538-46

120.   Jelacic S, Wobbe CL, Boster DR, Ciol MA, Watkins SL, *et al.* 2002. ABO and P1 blood group antigen expression and stx genotype and outcome of childhood *Escherichia coli* O157:H7 infections. *J Infect Dis* 185 214-9

121.   Jemal C, Haddad JE, Begum D, Jackson MP. 1995. Analysis of Shiga toxin subunit association by using hybrid A polypeptides and site-specific mutagenesis. *J Bacteriol* 177:3128-32

122.   Johnson KE, Thorpe CM, Sears CL. 2006. The Emerging Clinical Importance of Non-O157 Shiga Toxin-Producing *Escherichia coli Clin.Infect Dis.* 43:1587-95

123.   Johnson S, Waters A. 2012. Is complement a culprit in infection-induced forms of haemolytic uraemic syndrome? *Immunobiology* 217:235-43

124.   Kaplan BS, Cleary TG, Obrig TG. 1990. Recent advances in understanding the pathogenesis of the hemolytic uremic syndromes. *Pediatr.Nephrol.* 4:276-83

125. Karch H, Tarr PI, Bielaszewska M. 2005. Enterohaemorrhagic *Escherichia coli* in human medicine. *Int.J Med.Microbiol* 295:405-18

126. Karmali MA. 1989. Infection by verocytotoxin-producing *Escherichia coli* *Clin.Microbiol.Rev.* 2:15-38

127. Karmali MA, Petric M, Lim C, Fleming PC, Arbus GS, Lior H. 1985. The association between idiopathic hemolytic uremic syndrome and infection by verotoxin-producing *Escherichia coli J Infect.Dis.* 151:775-82

128. Karmali MA, Steele BT, Petric M, Lim C. 1983. Sporadic cases of haemolytic-uraemic syndrome associated with faecal cytotoxin and cytotoxin-producing *Escherichia coli* in stools. *Lancet* 1:619-20

129. Karpman D, Hakansson A, Perez MT, Isaksson C, Carlemalm E, *et al.* 1998. Apoptosis of renal cortical cells in the hemolytic-uremic syndrome: *in vivo* and *in vitro* studies. *Infect.Immun.* 66:636-44

130. Kashiwamura M, Kurohane K, Tanikawa T, Deguchi A, Miyamoto D, Imai Y. 2009. Shiga toxin kills epithelial cells isolated from distal but not proximal part of mouse colon. *Biol.Pharm.Bull.* 32:1614-7

131. Keepers TR, Psotka MA, Gross LK, Obrig TG. 2006. A murine model of HUS: Shiga toxin with lipopolysaccharide mimics the renal damage and physiologic response of human disease. *J Am.Soc.Nephrol.* 17:3404-14

132. Kenny B, DeVinney R, Stein M, Reinscheid DJ, Frey EA, Finlay BB. 1997. Enteropathogenic *E. coli* (EPEC) transfers its receptor for intimate adherence into mammalian cells. *Cell* 91:511-20

133. Kiarash A, Boyd B, Lingwood CA. 1994. Glycosphingolipid receptor function is modified by fatty acid content. Verotoxin 1 and verotoxin 2c preferentially recognize different globotriaosyl ceramide fatty acid homologues. *J Biol.Chem.* 269:11138-46

134. Kimmitt PT, Harwood CR, Barer MR. 2000. Toxin gene expression by shiga toxin-producing *Escherichia coli*: the role of antibiotics and the bacterial SOS response. *Emerging infectious diseases* 6:458-65

135. Kimura T, Co MS, Vasquez M, Wei S, Xu H, *et al.* 2002. Development of humanized monoclonal antibody TMA-15 which neutralizes Shiga toxin 2. *Hybrid.Hybridomics.* 21:161-8

136. King LA, Nogareda F, Weill FX, Mariani-Kurkdjian P, Loukiadis E, *et al.* 2012. Outbreak of Shiga Toxin-Producing *Escherichia coli* O104:H4 Associated With Organic Fenugreek Sprouts, France, June 2011 *Clinical Infectious Diseases*

137. Kitova EN, Daneshfar R, Marcato P, Mulvey GL, Armstrong G, Klassen JS. 2005. Stability of the homopentameric B subunits of shiga toxins 1 and 2 in solution and the gas phase as revealed by nanoelectrospray fourier transform ion cyclotron resonance mass spectrometry. *J Am.Soc.Mass Spectrom.* 16:1957-68

138. Kitova EN, Kitov PI, Paszkiewicz E, Kim J, Mulvey GL, *et al.* 2007. Affinities of Shiga toxins 1 and 2 for univalent and oligovalent Pk-trisaccharide analogs measured by electrospray ionization mass spectrometry. *Glycobiology* 17:1127-37

139. Kitova EN, Mulvey GL, Dingle T, Sinelnikov I, Wee S, *et al.* 2009. Assembly and stability of the shiga toxins investigated by electrospray ionization mass spectrometry. *Biochemistry* 48:5365-74

140. Kleanthous H, Smith HR, Scotland SM, Gross RJ, Rowe B, *et al.* 1990. Haemolytic uraemic syndromes in the British Isles, 1985-8: association with verocytotoxin producing *Escherichia coli*. Part 2: Microbiological aspects. *Archives of disease in childhood* 65:722-7

141. Klein EJ, Stapp JR, Clausen CR, Boster DR, Wells JG, *et al.* 2002. Shiga toxin-producing *Escherichia coli* in children with diarrhea: a prospective point-of-care study. *J Pediatr.* 141:172-7

142. Klein RF. 2002. Genetic regulation of bone mineral density in mice. *Journal of musculoskeletal & neuronal interactions* 2:232-6

143. Kojima Y, Fukumoto S, Furukawa K, Okajima T, Wiels J, *et al.* 2000. Molecular cloning of globotriaosylceramide/CD77 synthase, a glycosyltransferase that initiates the synthesis of globo series glycosphingolipids. *J Biol.Chem.* 275:15152-6

144. Kokai-Kun JF, Melton-Celsa AR, O'Brien AD. 2000. Elastase in intestinal mucus enhances the cytotoxicity of Shiga toxin type 2d. *J Biol.Chem.* 275:3713-21

145. Konowalchuk J, Speirs JI, Stavric S. 1977. Vero response to a cytotoxin of *Escherichia coli. Infect.Immun.* 18:775-9

146. L¢pez EL, Contrini MM, Glatstein E, Gonz lez AS, Santoro R, *et al.* 2010. Safety and Pharmacokinetics of Urtoxazumab, a Humanized Monoclonal Antibody, against Shiga-Like Toxin 2 in Healthy Adults and in Pediatric Patients Infected with Shiga-Like Toxin-Producing *Escherichia coli Antimicrob.Agents Chemother.* 54:239-43

147. Lander E, Kruglyak L. 1995. Genetic dissection of complex traits: guidelines for interpreting and reporting linkage results. *Nature genetics* 11:241-7

148. Lapeyraque AL, Malina M, Fremeaux-Bacchi V, Boppel T, Kirschfink M, *et al.* 2011. Eculizumab in severe Shiga-toxin-associated HUS. *N.Engl.J.Med.* 364:2561-3

149. Lee BC, Mayer CL, Leibowitz CS, Stearns-Kurosawa DJ, Kurosawa S. 2013. Quiescent complement in nonhuman primates during E coli Shiga toxin-induced hemolytic uremic syndrome and thrombotic microangiopathy. *Blood* 122:803-6

150. Lentz EK, Leyva-Illades D, Lee MS, Cherla RP, Tesh VL. 2011. Differential response of the human renal proximal tubular epithelial cell line HK-2 to Shiga toxin types 1 and 2. *Infect.Immun.* 79:3527-40

151. Leung PH, Peiris JS, Ng WW, Robins-Browne RM, Bettelheim KA, Yam WC. 2003. A newly discovered verotoxin variant, VT2g, produced by bovine verocytotoxigenic *Escherichia coli Appl.Environ.Microbiol.* 69:7549-53

152. Limami AM, Rouillon C, Glevarec G, Gallais A, Hirel B. 2002. Genetic and physiological analysis of germination efficiency in maize in relation to nitrogen metabolism reveals the importance of cytosolic glutamine synthetase. *Plant Physiol* 130:1860-70

153. Lindgren SW, Melton AR, O'Brien AD. 1993. Virulence of enterohemorrhagic *Escherichia coli* O91:H21 clinical isolates in an orally infected mouse model. *Infect.Immun.* 61:3832-42

154. Lindgren SW, Samuel JE, Schmitt CK, O'Brien AD. 1994. The specific activities of Shiga-like toxin type II (SLT-II) and SLT-II-related toxins of enterohemorrhagic *Escherichia coli* differ when measured by Vero cell cytotoxicity but not by mouse lethality. *Infect.Immun.* 62:623-31

155. Ling H, Boodhoo A, Hazes B, Cummings MD, Armstrong GD, *et al.* 1998. Structure of the shiga-like toxin I B-pentamer complexed with an analogue of its receptor Gb3. *Biochemistry* 37:1777-88

156. Lingwood CA. 1993. Verotoxins and their glycolipid receptors. *Adv.Lipid Res.* 25:189-211

157. Lingwood CA. 1994. Verotoxin-binding in human renal sections. *Nephron* 66:21-8

158. Lingwood CA. 1996. Role of verotoxin receptors in pathogenesis. *Trends Microbiol.* 4:147-53

159. Lingwood CA, Binnington B, Manis A, Branch DR. 2010. Globotriaosyl ceramide receptor function - where membrane structure and pathology intersect. *FEBS letters* 584:1879-86

160. Lingwood CA, Law H, Richardson S, Petric M, Brunton JL, *et al.* 1987. Glycolipid binding of purified and recombinant *Escherichia coli* produced verotoxin *in vitro J Biol.Chem.* 262:8834-9

161. Lingwood D, Binnington B, Rog T, Vattulainen I, Grzybek M, *et al.* 2011. Cholesterol modulates glycolipid conformation and receptor activity. *Nature chemical biology* 7:260-2

162. Liu YN, Wang SH, Li T, Wang Q, Tu W, *et al.* 2011. Shiga toxin type 2 (Stx2), a potential agent of bioterrorism, has a short distribution and a long elimination half-life, and induces kidney and thymus lesions in rats. *Archives of toxicology* 85:1133-40

163. Lopez-Novoa JM, Rodriguez-Pena AB, Ortiz A, Martinez-Salgado C, Lopez Hernandez FJ. 2011. Etiopathology of chronic tubular, glomerular and renovascular nephropathies: clinical implications. *Journal of translational medicine* 9:13

164. Loudet O, Chaillou S, Camilleri C, Bouchez D, Daniel-Vedele F. 2002. Bay-0 x Shahdara recombinant inbred line population: a powerful tool for the genetic dissection of complex traits in Arabidopsis. *TAG. Theoretical and applied genetics. Theoretische und angewandte Genetik* 104:1173-84

165. Louise CB, Obrig TG. 1995. Specific interaction of *Escherichia coli* O157:H7-derived Shiga-like toxin II with human renal endothelial cells. *J Infect.Dis.* 172:1397-401

166. Lu L, Wei L, Peirce JL, Wang X, Zhou J, *et al.* 2008. Using gene expression databases for classical trait QTL candidate gene discovery in the BXD recombinant inbred genetic reference population: mouse forebrain weight. *BMC genomics* 9:444

167. Mahfoud R, Manis A, Binnington B, Ackerley C, Lingwood CA. 2010. A major fraction of glycosphingolipids in model and cellular cholesterol-containing membranes is undetectable by their binding proteins. *J.Biol.Chem.* 285:36049-59

168. Marcato P, Vander HK, Mulvey GL, Armstrong GD. 2003. Serum amyloid P component binding to Shiga toxin 2 requires both a subunit and B pentamer. *Infect Immun* 71:6075-8

169. Marques LRM, Peiris JSM, Cryz SJ, O'Brien AD. 1987. *Escherichia coli* strains isolated from pigs with edema disease produce a variant of Shiga-like toxin II. *FEMS Microbiol.Lett.* 44:33-8

170. Martensson E. 1966. Neutral glycolipids of human kidney isolation, identification, and fatty acid composition. *Biochimica et biophysica acta* 116:296-308

171. Mayer CL, Leibowitz CS, Kurosawa S, Stearns-Kurosawa DJ. 2012. Shiga toxins and the pathophysiology of hemolytic uremic syndrome in humans and animals. *Toxins* 4:1261-87

172. Melton-Celsa A, Mohawk K, Teel L, O'Brien A. 2012. Pathogenesis of Shiga-Toxin Producing *Escherichia coli Curr.Top.Microbiol.Immunol.* 357:67-103

173. Melton-Celsa AR. *In press*. Shiga toxin (Stx) classification, structure, and function. In *Enterohemorrhagic Escherichia coli*, ed. V Sperandio, CJ hovde:XXX-XXX: ASM Press. Number of XXX-XXX pp.

174. Melton-Celsa AR, Darnell SC, O'Brien AD. 1996. Activation of Shiga-like toxins by mouse and human intestinal mucus correlates with virulence of enterohemorrhagic *Escherichia coli* O91:H21 isolates in orally infected, streptomycin-treated mice. *Infect.Immun.* 64:1569-76

175. Melton-Celsa AR, O'Brien AD. 1998. Structure, biology, and relative toxicity of Shiga toxin family members for cells and animals. In *Escherichia coli O157:H7 and other Shiga toxin-producing E. coli strains*, ed. JB Kaper, AD O'Brien:121-8. Washington DC: ASM Press. Number of 121-8 pp.

176. Melton-Celsa AR, O'Brien AD. 1998. Toxin activation by intestinal mucus correlates with the virulence of Shiga toxin-producing *Escherichia coli* in orally-infected mice. *Zent.bl.Bakteriol.Suppl.* 29:192-9

177. Melton-Celsa AR, O'Brien AD. 2003. Animal models for STEC-mediated disease. *Methods Mol.Med.* 73:291-305

178. Melton-Celsa AR, O'Brien AD. *In Press*. New Therapeutic Developments Against Shiga Toxin-Producing *Escherichia coli*. In *Enterohemorrhagic Escherichia coli*, ed. V Sperandio, CJ Hovde:XXX-XXX: ASM Press. Number of XXX-XXX pp.

179. Melton-Celsa AR, Smith MJ, O'Brien AD. 2005. Shiga toxins: potent poisons, pathogenicity determinants, and pharmacological agents. In *EcoSal-Escherichia coli and Salmonella : Cellular and Molecular Biology [Online]*, ed. RC In, III, 2. Washington, D.C.: ASM Press. Number of.

180. Menne J, Nitschke M, Stingele R, Abu-Tair M, Beneke J, *et al.* 2012. Validation of treatment strategies for enterohaemorrhagic *Escherichia coli* O104:H4 induced haemolytic uraemic syndrome: case-control study. *BMJ* 345:e4565

181. Michino H, Araki K, Minami S, Takaya S, Sakai N, *et al.* 1999. Massive outbreak of *Escherichia coli* O157:H7 infection in schoolchildren in Sakai City, Japan, associated with consumption of white radish sprouts. *Am.J Epidemiol.* 150:787-96

182. Miyairi I, Laxton JD, Wang X, Obert CA, Arva Tatireddigari VR, *et al.* 2011. Chlamydia psittaci genetic variants differ in virulence by modulation of host immunity. *J Infect Dis* 204:654-63

183. Mohawk KL, Melton-Celsa AR, Robinson CM, O'Brien AD. 2010. Neutralizing antibodies to Shiga toxin type 2 (Stx2) reduce colonization of mice by Stx2-expressing *Escherichia coli* O157:H7. *Vaccine* 28:4777-85

184. Mohawk KL, Melton-Celsa AR, Zangari T, Carroll EE, O'Brien AD. 2010. Pathogenesis of *Escherichia coli* O157:H7 strain 86-24 following oral infection of BALB/c mice with an intact commensal flora. *Microb.Pathog.* 48:131-42

185. Mohawk KL, O'Brien AD. 2011. Mouse models of *Escherichia coli* O157:H7 infection and Shiga toxin injection. *J.Biomed.Biotechnol.* 2011:258185

186. Morigi M, Galbusera M, Gastoldi S, Locatelli M, Buelli S, *et al.* 2011. Alternative pathway activation of complement by shiga toxin promotes exuberant c3a formation that triggers microvascular thrombosis. *J.Immunol.* 187:172-80

187. Moxley RA, Francis DH. 1998. Overview of animal models. In *Escherichia coli O157:H7 and Other Shiga Toxin-Producing E.coli Strains*, ed. JB Kaper, AD O'Brien:249-60. Washington DC: ASM Press. Number of 249-60 pp.

188. Moxley RA, Smith DR, Luebbe M, Erickson GE, Klopfenstein TJ, Rogan D. 2009. *Escherichia coli* O157:H7 vaccine dose-effect in feedlot cattle. *Foodborne pathogens and disease* 6:879-84

189. Mukherjee J, Chios K, Fishwild D, Hudson D, O'Donnell S, *et al.* 2002. Human Stx2-specific monoclonal antibodies prevent systemic complications of *Escherichia coli* O157:H7 infection. *Infect.Immun.* 70:612-9

190. Mukherjee J, Chios K, Fishwild D, Hudson D, O'Donnell S, *et al.* 2002. Production and Characterization of Protective Human Antibodies against Shiga Toxin 1. *Infect Immun.* 70:5896-9

191. Mural RJ, Adams MD, Myers EW, Smith HO, Miklos GL, *et al.* 2002. A comparison of whole-genome shotgun-derived mouse chromosome 16 and the human genome. *Science* 296:1661-71

192. Muthing J, Schweppe CH, Karch H, Friedrich AW. 2009. Shiga toxins, glycosphingolipid diversity, and endothelial cell injury. *Thrombosis and haemostasis* 101:252-64

193. Nakao H, Kataoka C, Kiyokawa N, Fujimoto J, Yamasaki S, Takeda T. 2002. Monoclonal antibody to shiga toxin 1, which blocks receptor binding and neutralizes cytotoxicity. *Microbiol Immunol.* 46:777-80

194. Nakao H, Kiyokawa N, Fujimoto J, Yamasaki S, Takeda T. 1999. Monoclonal antibody to Shiga toxin 2 which blocks receptor binding and neutralizes cytotoxicity. *Infect.Immun.* 67:5717-22

195. Nataro JP, Kaper JB. 1998. Diarrheagenic *Escherichia coli Clin.Microbiol.Rev.* 11:142-201

196. Naylor SW, Low JC, Besser TE, Mahajan A, Gunn GJ, *et al.* 2003. Lymphoid follicle-dense mucosa at the terminal rectum is the principal site of colonization of enterohemorrhagic *Escherichia coli* O157:H7 in the bovine host. *Infect.Immun.* 71:1505-12

197. Neupane M, Abu-Ali GS, Mitra A, Lacher DW, Manning SD, Riordan JT. 2011. Shiga toxin 2 overexpression in *Escherichia coli* O157:H7 strains associated with severe human disease. *Microb.Pathog.* 51:466-70

198. Nuzhdin SV, Pasyukova EG, Dilda CL, Zeng ZB, Mackay TF. 1997. Sex-specific quantitative trait loci affecting longevity in Drosophila melanogaster. *Proceedings of the National Academy of Sciences of the United States of America* 94:9734-9

199. Nyholm PG, Magnusson G, Zheng Z, Norel R, Binnington-Boyd B, Lingwood CA. 1996. Two distinct binding sites for globotriaosyl ceramide on verotoxins: identification by molecular modelling and confirmation using deoxy analogues and a new glycolipid receptor for all verotoxins. *Chem.Biol.* 3:263-75

200. O'Brien AD, Holmes RK. 1987. Shiga and Shiga-like toxins. *Microbiol.Rev.* 51:206-20

201. O'Brien AD, Karmali M, Scotland SM. A proposal for rationalization of the *Escherichia coli* cytotoxins, *Amsterdam, Netherlands, 1994*:147-9: Elsevier Science

202. O'Brien AD, Lively TA, Chang TW, Gorbach SL. 1983. Purification of Shigella dysenteriae 1 (Shiga)-like toxin from *Escherichia coli* O157:H7 strain associated with haemorrhagic colitis. *Lancet* 2:573

203. O'Brien AD, Lively TA, Chen ME, Rothman SW, Formal SB. 1983. *Escherichia coli* O157:H7 strains associated with haemorrhagic colitis in the United States produce a Shigella dysenteriae 1 (Shiga) like cytotoxin. *Lancet* 1:702

204. O'Brien AD, Tesh VL, Donohue-Rolfe A, Jackson MP, Olsnes S, *et al.* 1992. Shiga toxin: biochemistry, genetics, mode of action, and role in pathogenesis. In *Pathogenesis of shigellosis*, ed. PJ Sansonetti, 180:66-94. Berlin-Heidelberg: Springer-Verlag. Number of 66-94 pp.

205. Obata F, Tohyama K, Bonev AD, Kolling GL, Keepers TR, *et al.* 2008. Shiga toxin 2 affects the central nervous system through receptor globotriaosylceramide localized to neurons. *J Infect Dis* 198:1398-406

206. Obrig TG. 1997. Shiga toxin mode of action in *E. coli* O157:H7 disease. *Frontiers in bioscience : a journal and virtual library* 2:d635-42

207. Obrig TG, Louise CB, Lingwood CA, Boyd B, Barley-Maloney L, Daniel TO. 1993. Endothelial heterogeneity in Shiga toxin receptors and responses. *J Biol.Chem.* 268:15484-8

208. Obrig TG, Moran TP, Brown JE. 1987. The mode of action of Shiga toxin on peptide elongation of eukaryotic protein synthesis. *The Biochemical journal* 244:287-94

209. Ogasawara T, Ito K, Igarashi K, Yutsudo T, Nakabayashi N, Takeda Y. 1988. Inhibition of protein synthesis by a Vero toxin (VT2 or Shiga-like toxin II) produced by *Escherichia coli* O157:H7 at the level of elongation factor 1-dependent aminoacyl-tRNA binding to ribosomes. *Microb.Pathog.* 4:127-35

210. Ohmura-Hoshino M, Ho ST, Kurazono H, Igarashi K, Yamasaki S, Takeda Y. 2003. Genetic and immunological analysis of a novel variant of Shiga toxin 1 from bovine *Escherichia coli* strains and development of bead-ELISA to detect the variant toxin. *Microbiol Immunol* 47:717-25

211. Okuda T, Tokuda N, Numata S, Ito M, Ohta M, *et al.* 2006. Targeted disruption of Gb3/CD77 synthase gene resulted in the complete deletion of globo-series glycosphingolipids and loss of sensitivity to verotoxins. *J Biol Chem* 281:10230-5

212. Orth D, Grif K, Khan AB, Naim A, Dierich MP, Wurzner R. 2007. The Shiga toxin genotype rather than the amount of Shiga toxin or the cytotoxicity of Shiga toxin *in vitro* correlates with the appearance of the hemolytic uremic syndrome. *Diagnostic microbiology and infectious disease* 59:235-42

213. Ostroff SM, Tarr PI, Neill MA, Lewis JH, Hargrett-Bean N, Kobayashi JM. 1989. Toxin genotypes and plasmid profiles as determinants of systemic sequelae in *Escherichia coli* O157:H7 infections. *J Infect.Dis.* 160:994-8

214. Pai CH, Kelly JK, Meyers GL. 1986. Experimental infection of infant rabbits with verotoxin-producing *Escherichia coli Infect.Immun.* 51:16-23

215. Painter JA, Hoekstra RM, Ayers T, Tauxe RV, Braden CR, *et al.* 2013. Attribution of foodborne illnesses, hospitalizations, and deaths to food commodities by using outbreak data, United States, 1998-2008. *Emerging infectious diseases* 19:407-15

216. Palermo M, Alves-Rosa F, Rubel C, Fernandez GC, Fernandez-Alonso G, *et al.* 2000. Pretreatment of mice with lipopolysaccharide (LPS) or IL-1beta exerts dose-dependent opposite effects on Shiga toxin-2 lethality. *Clin Exp Immunol* 119:77-83

217. Paton AW, Woodrow MC, Doyle RM, Lanser JA, Paton JC. 1999. Molecular characterization of a Shiga toxigenic *Escherichia coli* O113:H21 strain lacking eae responsible for a cluster of cases of hemolytic-uremic syndrome. *J Clin Microbiol* 37:3357-61

218. Peirce JL, Lu L, Gu J, Silver LM, Williams RW. 2004. A new set of BXD recombinant inbred lines from advanced intercross populations in mice. *BMC.Genet.* 5:7

219. Pellizzari A, Pang H, Lingwood CA. 1992. Binding of Verocytotoxin 1 to its receptor is influenced by differences in receptor fatty acid content. *Biochemistry* 31:1363-70

220. Perera LP, Marques LR, O'Brien AD. 1988. Isolation and characterization of monoclonal antibodies to Shiga-like toxin II of enterohemorrhagic *Escherichia coli* and use of the monoclonal antibodies in a colony enzyme-linked immunosorbent assay. *J Clin.Microbiol.* 26:2127-31

221. Petruzziello TN, Mawji IA, Khan M, Marsden PA. 2009. Verotoxin biology: molecular events in vascular endothelial injury. *Kidney Int.Suppl*:S17-S9

222. Philpott DJ, Ackerley CA, Kiliaan AJ, Karmali MA, Perdue MH, Sherman PM. 1997. Translocation of verotoxin-1 across T84 monolayers: mechanism of bacterial toxin penetration of epithelium. *Am.J Physiol* 273:G1349-G58

223. Pierard D, Muyldermans G, Moriau L, Stevens D, Lauwers S. 1998. Identification of new verocytotoxin type 2 variant B-subunit genes in human and animal *Escherichia coli* isolates. *J Clin.Microbiol.* 36:3317-22

224. Proesmans W. 1996. Typical and atypical hemolytic uremic syndrome. *Kidney Blood Press Res.* 19:205-8

225. Pruimboom-Brees IM, Morgan TW, Ackermann MR, Nystrom ED, Samuel JE, *et al.* 2000. Cattle lack vascular receptors for *Escherichia coli* O157:H7 Shiga toxins. *Proceedings of the National Academy of Sciences of the United States of America* 97:10325-9

226. Psotka MA, Obata F, Kolling GL, Gross LK, Saleem MA, *et al.* 2009. Shiga toxin 2 targets the murine renal collecting duct epithelium. *Infect.Immun.* 77:959-69

227. Raa H, Grimmer S, Schwudke D, Bergan J, W,,lchli S, *et al.* 2009. Glycosphingolipid requirements for endosome-to-golgi transport of shiga toxin. *Traffic.* 10:868-82

228. Rangel JM, Sparling PH, Crowe C, Griffin PM, Swerdlow DL. 2005. Epidemiology of *Escherichia coli* O157:H7 outbreaks, United States, 1982-2002. *Emerg.Infect Dis.* 11:603-9

229. Rasooly R, Do PM. 2010. Shiga toxin Stx2 is heat-stable and not inactivated by pasteurization. *International journal of food microbiology* 136:290-4

230. Rasooly R, Do PM, Griffey SM, Vilches-Moure JG, Friedman M. 2010. Ingested Shiga toxin 2 (Stx2) causes histopathological changes in kidney, spleen, and thymus tissues and mortality in mice. *Journal of agricultural and food chemistry* 58:9281-6

231. Reiner DJ, Jan TA, Boughter JD, Jr., Li CX, Lu L, *et al.* 2008. Genetic analysis of tongue size and taste papillae number and size in recombinant inbred strains of mice. *Chemical senses* 33:693-707

232. Richardson SE, Karmali MA, Becker LE, Smith CR. 1988. The histopathology of the hemolytic uremic syndrome associated with verocytotoxin-producing *Escherichia coli* infections. *Hum.Pathol.* 19:1102-8

233. Riley LW, Remis RS, Helgerson SD, McGee HB, Wells JG, *et al.* 1983. Hemorrhagic colitis associated with a rare *Escherichia coli* serotype. *N.Engl.J Med.* 308:681-5

234. Ritchie JM, Thorpe CM, Rogers AB, Waldor MK. 2003. Critical roles for stx2, eae, and tir in enterohemorrhagic *Escherichia coli* -induced diarrhea and intestinal inflammation in infant rabbits. *Infect Immun* 71:7129-39

235. Roberts A, Pardo-Manuel de Villena F, Wang W, McMillan L, Threadgill DW. 2007. The polymorphism architecture of mouse genetic resources elucidated using genome-wide resequencing data: implications for QTL discovery and systems genetics. *Mammalian genome : official journal of the International Mammalian Genome Society* 18:473-81

236. Robinson CM, Sinclair JF, Smith MJ, O'Brien AD. 2006. Shiga toxin of enterohemorrhagic *Escherichia coli* type O157:H7 promotes intestinal colonization. *Proc.Natl.Acad.Sci.U.S.A* 103:9667-72

237. Rosales A, Hofer J, Zimmerhackl LB, Jungraithmayr TC, Riedl M, *et al.* 2012. Need for Long-term Follow-up in Enterohemorrhagic *Escherichia coli* - Associated Hemolytic Uremic Syndrome Due to Late-Emerging Sequelae. *Clinical Infectious Diseases*

238. Rosenthal N, Brown S. 2007. The mouse ascending: perspectives for human-disease models. *Nature cell biology* 9:993-9

239. Russo LM, Melton-Celsa AR, Smith AJ, O'Brien AD. Analysis of chimeric shiga toxins (Stxs) to determine the contribution of individual Stx subunits to cytotoxicity and mouse lethality, abstr D2-3. *Proc. 8th Int. Symp. Shiga Toxin Producing E. coli Infect. VTEC 2012, Amsterdam, The Netherlands, 2012*:

240. Russo LM, Melton-Celsa AR, Smith MA, Smith MJ, O'Brien AD. 2014. Oral Intoxication of Mice with Shiga Toxin Type 2a (Stx2a) and Protection by Anti-Stx2a Monoclonal Antibody 11E10. *Infect Immun* 82:1213-21

241. Rutjes NW, Binnington BA, Smith CR, Maloney MD, Lingwood CA. 2002. Differential tissue targeting and pathogenesis of verotoxins 1 and 2 in the mouse animal model. *Kidney Int.* 62:832-45

242. Safdar N, Said A, Gangnon RE, Maki DG. 2002. Risk of hemolytic uremic syndrome after antibiotic treatment of *Escherichia coli* O157:H7 enteritis: a meta-analysis. *JAMA* 288:996-1001

243. Samuel JE, Perera LP, Ward S, O'Brien AD, Ginsburg V, Krivan HC. 1990. Comparison of the glycolipid receptor specificities of Shiga-like toxin type II and Shiga-like toxin type II variants. *Infect.Immun.* 58:611-8

244. Sandvig K, Garred O, Prydz K, Kozlov JV, Hansen SH, van Deurs B. 1992. Retrograde transport of endocytosed Shiga toxin to the endoplasmic reticulum. *Nature* 358:510-2

245. Sauter KA, Melton-Celsa AR, Larkin K, Troxell ML, O'Brien AD, Magun BE. 2008. Mouse model of hemolytic-uremic syndrome caused by endotoxin-free Shiga toxin 2 (Stx2) and protection from lethal outcome by anti-Stx2 antibody. *Infect.Immun.* 76:4469-78

246. Saxena SK, O'Brien AD, Ackerman EJ. 1989. Shiga toxin, Shiga-like toxin II variant, and ricin are all single-site RNA N-glycosidases of 28 S RNA when microinjected into Xenopus oocytes. *J Biol.Chem.* 264:596-601

247. Scallan E, Hoekstra RM, Angulo FJ, Tauxe RV, Widdowson MA, *et al.* 2011. Foodborne illness acquired in the United States--major pathogens. *Emerg.Infect.Dis.* 17:7-15

248. Scheutz F, Teel LD, Beutin L, Pierard D, Buvens G, *et al.* 2012. Multicenter evaluation of a sequence-based protocol for subtyping Shiga toxins and standardizing Stx nomenclature. *J Clin Microbiol* 50:2951-63

249. Schmidt H, Karch H, Beutin L. 1994. The large-sized plasmids of enterohemorrhagic *Escherichia coli* O157 strains encode hemolysins which are

presumably members of the *E. coli* à-hemolysin family. *FEMS Microbiol.Lett.* 117:189-96

250. Schmidt H, Scheef J, Morabito S, Caprioli A, Wieler LH, Karch H. 2000. A new Shiga toxin 2 variant (Stx2f) from *Escherichia coli* isolated from pigeons. *Appl.Environ.Microbiol.* 66:1205-8

251. Schmitt CK, McKee ML, O'Brien AD. 1991. Two copies of Shiga-like toxin II-related genes common in enterohemorrhagic *Escherichia coli* strains are responsible for the antigenic heterogeneity of the O157:H- strain E32511. *Infect.Immun.* 59:1065-73

252. Schweppe CH, Bielaszewska M, Pohlentz G, Friedrich AW, Buntemeyer H, *et al.* 2008. Glycosphingolipids in vascular endothelial cells: relationship of heterogeneity in Gb3Cer/CD77 receptor expression with differential Shiga toxin 1 cytotoxicity. *Glycoconj.J* 25:291-304

253. Scotland SM, Rowe B, Smith HR, Willshaw GA, Gross RJ. 1988. Vero cytotoxin-producing strains of *Escherichia coli* from children with haemolytic uraemic syndrome and their detection by specific DNA probes. *J Med.Microbiol.* 25:237-43

254. Scotland SM, Smith HR, Rowe B. 1985. Two distinct toxins active on Vero cells from *Escherichia coli* O157. *Lancet* 2:885-6

255. Scotland SM, Willshaw GA, Smith HR, Rowe B. 1987. Properties of strains of *Escherichia coli* belonging to serogroup O157 with special reference to production of Vero cytotoxins VT1 and VT2. *Epidemiol.Infect.* 99:613-24

256. Shifman S, Bell JT, Copley RR, Taylor MS, Williams RW, *et al.* 2006. A high-resolution single nucleotide polymorphism genetic map of the mouse genome. *PLoS biology* 4:e395

257. Shiga K. 1898. Ueber den Dysenterie-bacillus (Bacillus dysenteriae). *Zbl.Bakt.Orig.* 24:913-8

258. Shimizu H, Field RA, Homans SW, Donohue-Rolfe A. 1998. Solution structure of the complex between the B-subunit homopentamer of verotoxin VT-1 from *Escherichia coli* and the trisaccharide moiety of globotriaosylceramide. *Biochemistry* 37:11078-82

259. Shimizu T, Sato T, Kawakami S, Ohta T, Noda M, Hamabata T. 2007. Receptor affinity, stability and binding mode of Shiga toxins are determinants of toxicity. *Microb.Pathog.* 43:88-95

260. Sieberts SK, Schadt EE. 2007. Moving toward a system genetics view of disease. *Mammalian genome : official journal of the International Mammalian Genome Society* 18:389-401

261. Siegler RL, Obrig TG, Pysher TJ, Tesh VL, Denkers ND, Taylor FB. 2003. Response to Shiga toxin 1 and 2 in a baboon model of hemolytic uremic syndrome. *Pediatr.Nephrol.* 18:92-6

262. Siegler RL, Pysher TJ, Lou R, Tesh VL, Taylor FB, Jr. 2001. Response to Shiga toxin-1, with and without lipopolysaccharide, in a primate model of hemolytic uremic syndrome. *Am.J Nephrol.* 21:420-5

263. Sinclair JF, O'Brien AD. 2002. Cell surface-localized nucleolin is a eukaryotic receptor for the adhesin intimin-gamma of enterohemorrhagic *Escherichia coli* O157:H7. *J Biol.Chem.* 277:2876-85

264. Slutsker L, Ries AA, Greene KD, Wells JG, Hutwagner L, Griffin PM. 1997. *Escherichia coli* O157:H7 diarrhea in the United States: clinical and epidemiologic features. *Annals of Internal Medicine* 126:505-13

265. Smith DR, Moxley RA, Peterson RE, Klopfenstein TJ, Erickson GE, *et al.* 2009. A two-dose regimen of a vaccine against type III secreted proteins reduced *Escherichia coli* O157:H7 colonization of the terminal rectum in beef cattle in commercial feedlots. *Foodborne.Pathog.Dis.* 6:155-61

266. Smith MJ, Carvalho HM, Melton-Celsa AR, O'Brien AD. 2006. The 13C4 monoclonal antibody that neutralizes Shiga toxin Type 1 (Stx1) recognizes three regions on the Stx1 B subunit and prevents Stx1 from binding to its eukaryotic receptor globotriaosylceramide. *Infect.Immun.* 74:6992-8

267. Smith MJ, Melton-Celsa AR, Sinclair JF, Carvalho HM, Robinson CM, O'Brien AD. 2009. Monoclonal Antibody 11E10, Which Neutralizes Shiga Toxin Type 2 (Stx2), Recognizes Three Regions on the Stx2 A Subunit, Blocks the Enzymatic Action of the Toxin *In vitro*, and Alters the Overall Cellular Distribution of the Toxin. *Infect.Immun.* 77:2730-40

268. Smith MJ, Teel LD, Carvalho HM, Melton-Celsa AR, O'Brien AD. 2006. Development of a hybrid Shiga holotoxoid vaccine to elicit heterologous protection against Shiga toxins types 1 and 2. *Vaccine* 24:4122-9

269. Stahl AL, Sartz L, Karpman D. 2011. Complement activation on platelet-leukocyte complexes and microparticles in enterohemorrhagic *Escherichia coli* -induced hemolytic uremic syndrome. *Blood* 117:5503-13

270. Staples M, Jennison AV, Graham RM, Smith HV. 2012. Evaluation of the Meridian Premier EHEC assay as an indicator of Shiga toxin presence in direct faecal specimens *Diagn.Microbiol.Infect.Dis.*

271. Stearns-Kurosawa DJ, Collins V, Freeman S, Debord D, Nishikawa K, *et al.* 2011. Rescue from lethal Shiga toxin 2-induced renal failure with a cell-permeable peptide. *Pediatr.Nephrol.* 26:2031-9

272. Stearns-Kurosawa DJ, Collins V, Freeman S, Tesh VL, Kurosawa S. 2010. Distinct physiologic and inflammatory responses elicited in baboons after challenge with Shiga toxin type 1 or 2 from enterohemorrhagic *Escherichia coli Infect.Immun.* 78:2497-504

273. Stephan R, Hoelzle LE. 2000. Characterization of shiga toxin type 2 variant B-subunit in *Escherichia coli* strains from asymptomatic human carriers by PCR-RFLP. *Letters in applied microbiology* 31:139-42

274. Strockbine NA, Marques LR, Holmes RK, O'Brien AD. 1985. Characterization of monoclonal antibodies against Shiga-like toxin from *Escherichia coli Infect Immun* 50:695-700

275. Strockbine NA, Marques LR, Newland JW, Smith HW, Holmes RK, O'Brien AD. 1986. Two toxin-converting phages from *Escherichia coli* O157:H7 strain 933 encode antigenically distinct toxins with similar biologic activities. *Infect.Immun.* 53:135-40

276. Suzuki K, Tateda K, Matsumoto T, Gondaira F, Tsujimoto S, Yamaguchi K. 2000. Effects of interaction between *Escherichia coli* verotoxin and lipopolysaccharide on cytokine induction and lethality in mice. *Journal of medical microbiology* 49:905-10

277. Takeda T, Yoshino K, Adachi E, Sato Y, Yamagata K. 1999. *In vitro* assessment of a chemically synthesized Shiga toxin receptor analog attached to chromosorb P (Synsorb Pk) as a specific absorbing agent of Shiga toxin 1 and 2. *Microbiol Immunol* 43:331-7

278. Tam P, Mahfoud R, Nutikka A, Khine AA, Binnington B, *et al.* 2008. Differential intracellular transport and binding of verotoxin 1 and verotoxin 2 to globotriaosylceramide-containing lipid assemblies. *J Cell Physiol* 216:750-63

279. Tam PJ, Lingwood CA. 2007. Membrane cytosolic translocation of verotoxin A 1 subunit in target cells. *Microbiology* 153:2700-10

280. Tarr PI, Gordon CA, Chandler WL. 2005. Shiga-toxin-producing *Escherichia coli* and haemolytic uraemic syndrome. *Lancet* 365:1073-86

281. Taylor BA. 1978. Recombinant inbred strains: use in gene mapping. In *Origins of Inbred Mice*, ed. H Morse, III:423-38: New York: Academic Press. Number of 423-38 pp.

282. Taylor BA, Wnek C, Kotlus BS, Roemer N, MacTaggart T, Phillips SJ. 1999. Genotyping new BXD recombinant inbred mouse strains and comparison of BXD and consensus maps. *Mammalian genome : official journal of the International Mammalian Genome Society* 10:335-48

283. Taylor FB, Jr., Tesh VL, DeBault L, Li A, Chang AC, *et al.* 1999. Characterization of the baboon responses to Shiga-like toxin: descriptive study of a new primate model of toxic responses to Stx-1. *Am.J Pathol.* 154:1285-99

284. Tazzari PL, Ricci F, Carnicelli D, Caprioli A, Tozzi AE, *et al.* 2004. Flow cytometry detection of Shiga toxins in the blood from children with hemolytic uremic syndrome. *Cytometry* 61B:40-4

285. Tesh VL. 2010. Induction of apoptosis by Shiga toxins. *Future.Microbiol.* 5:431-53

286. Tesh VL. 2012. Activation of cell stress response pathways by Shiga toxins. *Cell Microbiol* 14:1-9

287. Tesh VL, Burris JA, Owens JW, Gordon VM, Wadolkowski EA, *et al.* 1993. Comparison of the relative toxicities of Shiga-like toxins type I and type II for mice. *Infect.Immun.* 61:3392-402

288. Tesh VL, Samuel JE, Perera LP, Sharefkin JB, O'Brien AD. 1991. Evaluation of the role of Shiga and Shiga-like toxins in mediating direct damage to human vascular endothelial cells. *J Infect.Dis.* 164:344-52

289. Thomson DU, Loneragan GH, Thornton AB, Lechtenberg KF, Emery DA, *et al.* 2009. Use of a siderophore receptor and porin proteins-based vaccine to control the burden of *Escherichia coli* O157:H7 in feedlot cattle. *Foodborne.Pathog.Dis.* 6:871-7

290. Threadgill DW, Churchill GA. 2012. Ten years of the collaborative cross. *G3* 2:153-6

291. Tilden J, Jr., Young W, McNamara AM, Custer C, Boesel B, *et al.* 1996. A new route of transmission for *Escherichia coli* : infection from dry fermented salami. *Am.J Public Health* 86:1142-5

292. Tironi-Farinati C, Loidl CF, Boccoli J, Parma Y, Fernandez-Miyakawa ME, Goldstein J. 2010. Intracerebroventricular Shiga toxin 2 increases the expression of its receptor globotriaosylceramide and causes dendritic abnormalities. *J.Neuroimmunol.* 222:48-61

293. Trachtman H, Austin C, Lewinski M, Stahl RA. 2012. Renal and neurological involvement in typical Shiga toxin-associated HUS. *Nat.Rev.Nephrol.* 8:658-69

294. Trachtman H, Cnaan A, Christen E, Gibbs K, Zhao S, *et al.* 2003. Effect of an oral Shiga toxin-binding agent on diarrhea-associated hemolytic uremic syndrome in children: a randomized controlled trial. *JAMA* 290:1337-44

295. Tyrrell GJ, Ramotar K, Toye B, Boyd B, Lingwood CA, Brunton JL. 1992. Alteration of the carbohydrate binding specificity of verotoxins from Gal alpha

1-4Gal to GalNAc beta 1-3Gal alpha 1-4Gal and vice versa by site-directed mutagenesis of the binding subunit. *Proc.Natl.Acad.Sci.U.S.A* 89:524-8

296.   U.S. National Research Council CftUotGftCaUoLA, Institute for Laboratory Animal Research. 2011. *Guide for the care and use of laboratory animals.* Washington, DC: National Academies Press

297.   Uchida H, Kiyokawa N, Horie H, Fujimoto J, Takeda T. 1999. The detection of Shiga toxins in the kidney of a patient with hemolytic uremic syndrome. *Pediatr.Res.* 45:133-7

298.   Uchida H, Kiyokawa N, Taguchi T, Horie H, Fujimoto J, Takeda T. 1999. Shiga toxins induce apoptosis in pulmonary epithelium-derived cells. *J Infect Dis* 180:1902-11

299.   Van Setten PA, van Hinsbergh VW, Van den Heuvel LP, van der Velden TJ, van de Kar NC, *et al.* 1997. Verocytotoxin inhibits mitogenesis and protein synthesis in purified human glomerular mesangial cells without affecting cell viability: evidence for two distinct mechanisms. *Journal of the American Society of Nephrology : JASN* 8:1877-88

300.   Waddell T, Cohen A, Lingwood CA. 1990. Induction of verotoxin sensitivity in receptor-deficient cell lines using the receptor glycolipid globotriosylceramide. *Proceedings of the National Academy of Sciences of the United States of America* 87:7898-901

301.   Waddell T, Head S, Petric M, Cohen A, Lingwood C. 1988. Globotriosyl ceramide is specifically recognized by the *Escherichia coli* verocytotoxin 2. *Biochem.Biophys.Res.Commun.* 152:674-9

302.   Wadolkowski EA, Sung LM, Burris JA, Samuel JE, O'Brien AD. 1990. Acute renal tubular necrosis and death of mice orally infected with *Escherichia coli* strains that produce Shiga-like toxin type II. *Infect.Immun.* 58:3959-65

303.   Wagner PL, Livny J, Neely MN, Acheson DW, Friedman DI, Waldor MK. 2002. Bacteriophage control of Shiga toxin 1 production and release by *Escherichia coli Mol.Microbiol.* 44:957-70

304.   Wahl E, Vold L, Lindstedt BA, Bruheim T, Afset JE. 2011. Investigation of an *Escherichia coli* O145 outbreak in a child day-care centre--extensive sampling and characterization of eae- and stx1-positive *E. coli* yields epidemiological and socioeconomic insight. *BMC infectious diseases* 11:238

305.   Wang J, Williams RW, Manly KF. 2003. WebQTL: web-based complex trait analysis. *Neuroinformatics* 1:299-308

306.   Wang LS, Jiao Y, Huang Y, Liu XY, Gibson G, *et al.* 2013. Critical evaluation of transcription factor Atf2 as a candidate modulator of alcohol preference in

mouse and human populations. *Genetics and molecular research : GMR* 12:5992-6005

307. Wang X, al. E. 2010. High-throughput sequencing of the DBA/2J mouse genome. *BMC.Bioinformatics.* 11:07

308. Waterston RH, Lindblad-Toh K, Birney E, Rogers J, Abril JF, *et al.* 2002. Initial sequencing and comparative analysis of the mouse genome. *Nature* 420:520-62

309. Weeratna RD, Doyle MP. 1991. Detection and production of verotoxin 1 of *Escherichia coli* O157:H7 in food. *Applied and environmental microbiology* 57:2951-5

310. Weinstein DL, Jackson MP, Perera LP, Holmes RK, O'Brien AD. 1989. *In vivo* formation of hybrid toxins comprising Shiga toxin and the Shiga- like toxins and role of the B subunit in localization and cytotoxic activity. *Infect.Immun.* 57:3743-50

311. Welsh CE, Miller DR, Manly KF, Wang J, McMillan L, *et al.* 2012. Status and access to the Collaborative Cross population. *Mamm.Genome* 23:706-12

312. Wen SX, Teel LD, Judge NA, O'Brien AD. 2006. Genetic toxoids of Shiga toxin types 1 and 2 protect mice against homologous but not heterologous toxin challenge. *Vaccine* 24:1142-8

313. Whittam TS. 1998. Evolution of *Escherichia coli* O157:H7 and other Shiga toxin-producing *E. coli* strains. In *Escherichia coli O157:H7 and other Shiga toxin-producing E. coli strains*, ed. JB Kaper, AD O'Brien:195-209. Washington, DC: American Society for Microbiology. Number of 195-209 pp.

314. Whittam TS, Wolfe ML, Wachsmuth IK, Orskov F, Orskov I, Wilson RA. 1993. Clonal relationships among *Escherichia coli* strains that cause hemorrhagic colitis and infantile diarrhea. *Infect.Immun.* 61:1619-29

315. Williams RW, Gu J, Qi S, Lu L. 2001. The genetic structure of recombinant inbred mice: high-resolution consensus maps for complex trait analysis. *Genome biology* 2:RESEARCH0046

316. Windschiegl B, Orth A, Romer W, Berland L, Stechmann B, *et al.* 2009. Lipid reorganization induced by Shiga toxin clustering on planar membranes. *PLoS.ONE.* 4:e6238

317. Wong CS, Jelacic S, Habeeb RL, Watkins SL, Tarr PI. 2000. The risk of the hemolytic-uremic syndrome after antibiotic treatment of *Escherichia coli* O157:H7 infections. *N.Engl.J.Med.* 342:1930-6

318. Wong CS, Mooney JC, Brandt JR, Staples AO, Jelacic S, *et al.* 2012. Risk Factors for the Hemolytic Uremic Syndrome in Children Infected With *Escherichia coli* O157:H7: A Multivariable Analysis. *Clinical Infectious Diseases* 55:33-41

319. Yamagami S, Motoki M, Kimura T, Izumi H, Takeda T, *et al.* 2001. Efficacy of postinfection treatment with anti-Shiga toxin (Stx) 2 humanized monoclonal antibody TMA-15 in mice lethally challenged with Stx-producing *Escherichia coli J.Infect.Dis.* 184:738-42

320. Zhang W, Bielaszewska M, Kuczius T, Karch H. 2002. Identification, characterization, and distribution of a Shiga toxin 1 gene variant (stx 1c) in *Escherichia coli* strains isolated from humans. *J Clin.Microbiol* 40:1441-6

321. Zoja C, Buelli S, Morigi M. 2010. Shiga toxin-associated hemolytic uremic syndrome: pathophysiology of endothelial dysfunction. *Pediatr.Nephrol.* 25:2231-40

322. Zoja C, Morigi M, Remuzzi G. 2001. The role of the endothelium in hemolytic uremic syndrome. *J Nephrol.* 14 Suppl 4:S58-S62

323. Zumbrun EE, Abdeltawab NF, Bloomfield HA, Chance TB, Nichols DK, *et al.* 2012. Development of a murine model for aerosolized ebolavirus infection using a panel of recombinant inbred mice. *Viruses* 4:3468-93

324. Zumbrun SD, Hanson L, Sinclair JF, Freedy J, Melton-Celsa AR, *et al.* 2010. Human Intestinal Tissue and Cultured Colonic Cells Contain Globotriaosylceramide Synthase mRNA and the Alternate Shiga Toxin Receptor, Globotetraosylceramide. *Infect.Immun.* 78:4488-99